USING DISTRIBUTED TEMPERATURE SENSING FIBER-OPTICS AND *HEAT SOURCE* MODELING TO CHARACTERIZE A NORTHERN CALIFORNIA STREAM'S THERMAL REGIME

By

Rosealea Mae Bond

A Thesis Presented to

The Faculty of Humboldt State University

In Partial Fulfillment of the Requirements for the Degree

Master of Science in Natural Resources: Forest, Watershed, and Wildland Sciences

Committee Membership

Dr. Andrew Stubblefield, Committee Chair

Dr. Rob Van Kirk, Committee Member

Dr. Darren Ward, Committee Member

Dr. Alison O'Dowd, Graduate Coordinator

December 2013

ABSTRACT

USING DISTRIBUTED TEMPERATURE SENSING FIBER-OPTICS AND *HEAT SOURCE* MODELING TO CHARACTERIZE A NORTHERN CALIFORNIA STREAM'S THERMAL REGIME

Rosealea Mae Bond

This study employed Distributed Temperature Sensing (DTS) and *Heat Source* modeling to quantify the thermal regime of a one-kilometer section of the North Fork of the Salmon River, a tributary of the Klamath River, northern California, USA. The study collected eight days of temperature data using DTS at one-meter, 15-minute intervals during July 2012. The research aimed to: 1) investigate the geomorphic and thermal conditions of the study reach and their impact on native Salmonids. 2) identify and quantify groundwater seeps; and 3) employ and calibrate *Heat Source* to predict effects of riparian management, channel geometry, and climate change on stream temperature over the study reach. DTS observations revealed nearly uniform warming over the study reach, a diel heating cycle of 5 °C, a small groundwater spring (7 % of mainstem flow), and a Maximum Weekly Maximum Temperature (MWMT) of 23.00 °C. Statistical modeling of salmonid distribution field observations with AICc found that depth was the most explanatory parameter. Habitat inventory of the study reach indicated poor salmonid habitat quality with low habitat complexity with no large woody debris or instream cover. *Heat Source* model performance (Bias, RMSE, MARE, and NSE), compared to DTS

observations, were all within the range of previous *Heat Source* applications. *Heat Source* modeling of reforestation of denuded legacy gravel bars from historic gold mining and areas of low vegetation in the study reach indicated that reforestation buffered daily maximum stream temperatures. Modeled channel restoration scenarios reduced the rate of heating (ºC /90 m) in the treatment area by a maximum of 34 %. Climate change scenarios were simulated with a uniform increase of air temperature by 2 °C, 4 °C, and 6 °C which warmed stream temperatures by 0.09 ºC / km per 2 ºC air temperature increase. Warming predicted by climate change was ameliorated with reforestation (0.11 ºC /km and 0.26 ºC per 2 ºC /km air temperature increase for partial and fully forested respectively).

ACKNOWLEDGEMENTS

I would first like to acknowledge that this project was a tremendous group effort. I am truly grateful to everyone who helped me in my personal and scientific growth during this time. While I cannot name everyone who helped along the way I will try: First, I would like to thank my advisor Andy for his kindness in time, effort, and finding funding for this project. Funding was provided by the USDA McIntire Stennis Program. Second, thank you to my committee Rob, Darren, and Dr. Ken Fulgham who gave his support while Andy was on sabbatical. I thank the great HSU faculty and staff especially: George Pease, Sarah Hannah, and the late and often missed Gayleen Smith. Thank you to the Center for Transformative Environmental Monitoring Programs: Dr. Scott Tyler, Dr. John Selker, Chris Sladek, Mark Hausner, and staff who made the DTS technology and research accessible. My thanks to Julia Crown, Ryan Michie, and staff at Oregon Department of Environmental Quality who helped with *Heat Source* modeling. I thank the Salmon River Restoration Council; especially Lyra Cressey and Karuna Greenberg and Will Harling, Mid-Klamath Watershed Council, for lending their local knowledge and support in the Salmon River. Thank you Spencer Hitzeroth. Thank you scouting crew Cameron Bond and Joseph Cosentino aka the "Widgets of Science". I also thank my remarkable field crew: Christopher Henderson, Deidra Rodriguez, Scott Benson, Aidan Stephens, Brian Huggett, Robert Di Paolo, Phoenix Anthony, Al Geritz and Ryan Trent. Finally, thank you family, community, Earth, SLVHS's Doug Morris and Jane Orbuch and my many teachers who keep my life's journey vibrant and slight bumpy.

TABLE OF CONTENTS

LIST OF TABLES

LIST OF TABLES (CONT.)

LIST OF FIGURES

LIST OF FIGURES (CONT.)

LIST OF FIGURES (CONT.)

LIST OF FIGURES (CONT.)

LIST OF FIGURES (CONT.)

INTRODUCTION

Stream temperature plays a critical role in determining the overall structure and function of stream ecosystems. Temperature directly affects the distribution of fish (Meisner 1990, Berman and Quinn 1991, Eaton and Scheller 1995, Welsh *et al.* 2001), individual's metabolic and overall growth rates (Markarian 1980, Gregory *et al.* 2000), and the abiotic conditions - such as gas solubility and solute concentration - that surround them (Mathew and Berg 1997). Aquatic fauna are particularly vulnerable to changes in the magnitude and duration of elevated stream temperatures due to their limited mobility in the stream environment.

Previous research has shown that land management practices both directly and indirectly affect stream temperature. For example, regulated flows have changed the magnitude and extent of peak temperature downstream (Lowney 2000). Logging and livestock grazing have modified the quantity and quality of riparian vegetation, which buffer the stream from incoming solar radiation (Brown 1960, Brown 1970, Brown and Krygier 1970, Armour *et al.* 1991, Fleischner 1994). Land uses that modify stream channel structure and bank stability can also alter the mechanisms of heat transfer within the stream, typically increasing daily maximum temperatures (Poole and Berman 2001). To make matters worse, stream temperature is projected to increase with changes in global climate due to elevated air temperature and changes in precipitation patterns (Eaton and Scheller 1996, Mohseni *et al.* 2003, IPCC 2007, Battin *et al.* 2007).

Thermal modeling of current and future climate stream temperature conditions is a central are of research to help guide management actions to create and maintain resilient ecological communities. Stream temperature modeling has allowed land managers to predict the effectiveness of different management options such as reforestation and channel modification, and understand and plan for future climate conditions (Roth *et al.* 2010). Currently modeling techniques are needed at the reach and watershed scales to provide management tools for fish habitat protection (Caissie 2006).

This study investigated radiative and hydrologic processes that regulate stream temperatures and current thermal and physical habitat conditions for native salmon and trout species (*i.e.* salmonids). Species of interest included the federally listed coho salmon (*Oncorhynchus kisutch)* (Federal Register 1997), Chinook salmon (*O. tashawytsha*) and rainbow trout (*O. mykiss*) (*i.e.* steelhead). The study took place on the North Fork of the Salmon River, near Sawyers Bar, CA, USA, for fourteen days in July 2012. The one-kilometer study reach is upstream of the last (most upstream) identified major thermal refuge for migrating salmonids to natal tributaries on the North Fork (*i.e.* confluence with Little North Fork Creek) (Sutton and Soto 2010, Lyra Cressey, personal communication, November 9, 2011). The study reach has been dramatically impacted by previous land practices such as hydraulic gold mining and has been identified as an exceptionally warm reach whose thermal drivers were unknown (Watershed Sciences 2009).

A novel measurement approach, Distributed Temperature Sensing (DTS), was used to detect stream heating and cooling in a very precise longitudinal profile along a fiber-optic cable. The cable technology is capable of measuring temperature continuously at high spatial (1m) and temporal (seconds to minutes) resolution, allowing the detection of non-uniform fluctuations in stream temperature (Selker *et al*. 2006a). The fiber-optic cable technology, in conjunction with heat flux modeling in *Heat Source*, was used to quantify radiative and hydrologic processes to gain insight into influencing the stream's thermal regime and improve land managers' ability to address areas in need of thermal restoration.

The primary objective of this research was to quantify the thermal regime of a one-kilometer reach on the North Fork Salmon River and investigate sources of heat flux. The research aimed to: 1) investigate the geomorphic and thermal conditions of the study reach and their impact on native salmonids; 2) spatially identify groundwater seeps and quantify their contribution to the stream's thermal regime as potential thermal refugia; and 3) employ and calibrate a mechanistic stream heating model, *Heat Source*, to predict stream temperature regime resulting from land management strategies and climate change. Specific hypotheses are listed below:

1.1 Over-summering juvenile salmonids are experiencing physiologically stressful temperatures in the Salmon River.

1.2 Temperature is driving the distribution of juvenile and resident salmon and trout at the reach scale.

1.3 Channel geometry is outside the range of suggested literature values for providing salmonid habitat in the Salmon River.

2.1 Groundwater springs are detectable and quantifiable using Distributed Temperature Sensing fiber-optics.

3.1 The energy budget model *Heat Source* correctly predicts summer stream temperature for the study reach in the Salmon River.

3.2 Riparian reforestation can buffer daily maximum summer stream temperatures.

3.3 Reducing the channel bottom width of the most upstream run in the study reach (*i.e.* Run 1) will buffer current summer stream temperatures.

3.4 Increased air temperature from climate change will increase mean summer stream temperatures.

3.5 Riparian reforestation can ameliorate elevated stream temperature from climate change.

Thesis Structure

This thesis is organized into three focus areas: physical impacts on salmonids, quantifying a groundwater spring, and *Heat Source* modeling of thermal restoration and climate change scenarios. Subsequent sections (Results, Discussion, and Conclusions) are partitioned into these three focus areas.

Literature Review

This section reviews the impact of hydraulic gold mining, physical mechanisms of stream heating, the use of stream energy budgets such as *Heat Source* to investigate stream heating flux, and Distributed Temperature Sensing technology employed by the study.

Hydraulic Gold Mining and Channel Structure

Hydraulic mining was one of the most popular and widespread methods for extracting gold in northern California; mountains where blasted, hillsides where scraped off and rivers become both pressure engines and sluice boxes. Gold was "discovered" in northern California in the late 1840s, but it was the invention of hydraulic mining in 1853 that set in motion the lasting impacts seen today on the landscape (Kelley 1954). Streams have aggraded from the increased sediment load from mining tailings; pool habitat was filled in; and channel bottoms became armored from modified sediment transport processes. Mining also increased the lateral accumulation of sediment, with coarse material slowly moving as slugs (discrete sediment patches) and fines moving more quickly to the mouths of rivers (Knighton 1998).

It was first viewed that excess mining sediment in the Sierra Nevada mountains of California would quickly (*i.e.* within a half a century) flush out of the system as a sediment wave or pulse (Gilbert 1917). Later work was critical of the sediment-pulse model and emphasized that fluvial systems can retain sediment on a much larger time scale than previously predicted (James 1997). James (1993) found on the Bear River,

California, that sediment transport histories can differ between adjacent tributaries and by the number and distribution of sediment sources (*i.e.* mining operations). Further work by James *et al.* (2009) found that the lower Yuba and Feather Rivers, California, have mixed areas of channel aggradation and degradation that was related to the proximity to mining areas as well as to manmade levees used to alter channel morphology.

Most Californians have heard of the injunction ending hydraulic gold mining in 1884 due to major downstream flooding in the Sacramento Valley smothering agriculture and inhibiting upstream navigation (Woodruff v. Bloomfield 1884, Kelley 1954). What is less known is that this mandate applied only to rivers and tributaries connected to the Sacramento River. In northern California, hydraulic mining continued in the Salmon River through the 1940s and 50s, a half a century longer than in California's Sierra Nevadas. Most mining operations in the Salmon River had between three and ten men working around the clock scraping, sorting, and collecting (California 1916). Prospectors still hold claims along the river, actively looking for the once plentiful placer (*i.e.* gold-bearing sedimentary deposits).

Previous study has largely been limited to California's Sierra Nevada Range. Keen interest in sediment transport processes was the result of downstream flooding in the Sacramento Valley and instream navigation. Mining impacts in northern California outside of the Sierra Nevada has not been fully investigated. Few studies have investigated the legacy impacts of hydraulic mining with regards to altered temperature regimes. In this study, we speculate that the channel structure and geometry observed on

the North Fork Salmon is the result of historic hydraulic gold mining. This altered geometry, in turn, has changed the river's thermal regime, which is currently adversely affecting stream biota. I constructed a conceptual model of the channel responding to the changes in land use (Figure 1).

The conceptual model consists of three stages 1) Initial Condition, the historic, pre-disturbance condition, 2) Active Hydraulic Mining, when hydraulic mining as occurring, and 3) Current Condition, post-hydraulic mining activity and can currently be seen at the study site. During the mining period, hillsides were scoured by water cannons removing riparian vegetation (exposing the stream) and dumped tremendous amounts of sediment into the stream. The channel aggraded and widened from the excess sediment; converting the channel from a "V" shape to a "U" shape. When mining activity ended the sediment supply was stopped; fine sediments were flushed down stream, coarsening the remaining substrate. Channel incision began to take place until it hit the coarse substrate (*i.e.* armored) layer. The current channel showed a relatively shallow widened channel with exposed banks.

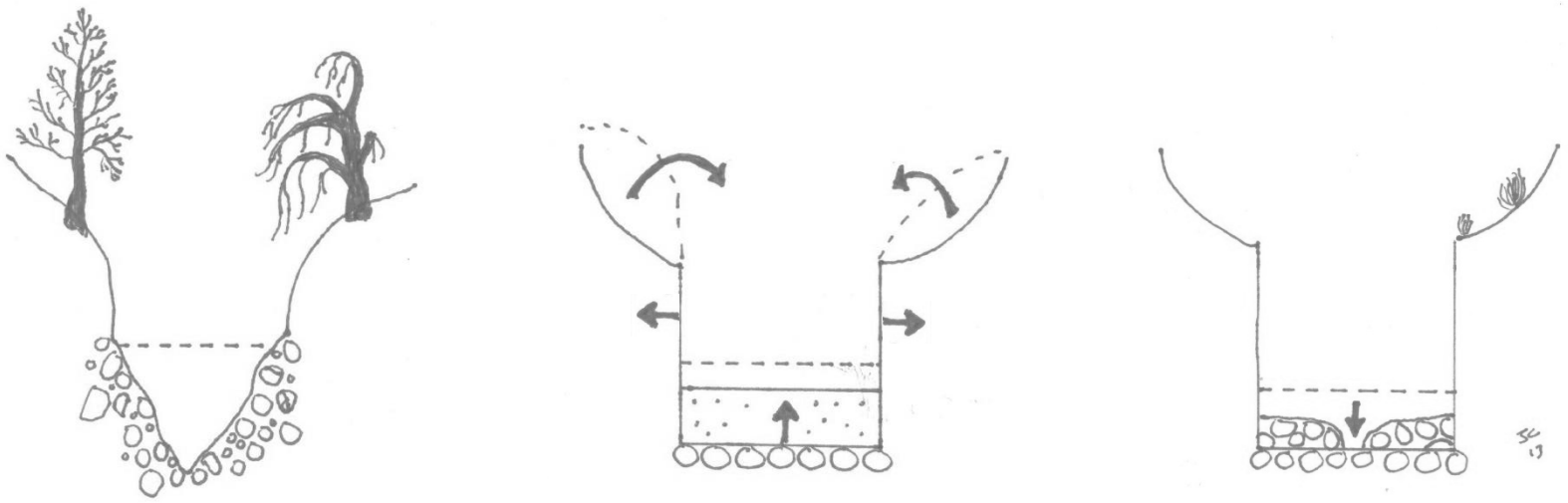

1 **2** **3**

	1. Initial Channel	2. Active Hydraulic Mining	3. Current Condition	Effect on Temperature
Shade along channel*	Shaded	Exposed	Exposed	+
Median particle size (D_{50})*	Mixed	Fines Dominated	Cobble Dominated	+/-
Boundary shear stress (*i.e.* internal friction) (τ)	Moderate		Higher	+
Width-to-depth ratio*	Small	Large	Large	+
Flow	Faster	--	Slower	+

Figure 1. Conceptual model of the changes to channel geometry from hydraulic mining which in turn affect stream temperature and each other. * = channel geometry parameters measured during the study period. Drawing courtesy of Joseph Cosentino.

Stream Temperature

Stream temperature is governed by atmospheric conditions, topography, stream geomorphology, and discharge (Caissie 2006). These factors in turn respond to each other, creating the setting for varying thermal regimes in dynamic equilibrium. Streams experience seasonal and diel temperature variability, tracking changes in solar radiation, climate, and air temperature (Evans McGregor and Petts 1998, Boyd and Kasper 2003). Also, stream heating differs across spatial scales (*i.e.* stream size) and longitudinally (*i.e.* stream order) (Smith 1972, Caissie *et al.* 2005, Caissie 2006).

Numerous studies have found solar radiation (net short- and long-wave radiation) to be the principal input of heat into the stream thermal system (Brown 1970, Mosley 1983, Sinokrot and Stefan 1994, Caissie *et al.* 2005). Researchers have used energy budget models to track thermal heat flux within the stream system (Boyd and Kasper 2003, Caissie 2006, Westhoff *et al.* 2007). During the development of fluvial energy models, researchers partition energy transfer into two interfaces: the air-water interface at the surface and the streambed-water interface on the stream substrate. Previous studies have found that net heat exchange primarily occurs at the air-water interface ($\geq$ 80 %), with little energy being transferred between the water and substrate ($\leq$ 20 %) (Brown 1969, Evans McGregor and Petts 1998).

Research has also shown that stream shading significantly reduced solar radiation and evaporative cooling, increasing the relative importance of streambed heat flux (Dong *et al.* 1998). "Effective" shade experienced by the stream is an interrelated process

between near-stream vegetation (*i.e.* height and density), channel morphology (*i.e.* width, entrenchment and sinuosity), local geology, and solar position (*i.e.* season and time of day) (Boyd and Kasper 2003). Furthermore, site - specific drivers such as evaporative fluxes, substrate type, hydraulic residence time, and flow pathway may govern maximum stream temperature magnitude and timing, whereas minimum and mean stream temperature may be more influenced by large-scale landscape drivers such as climate and topography (Johnson 2003). Internal heat exchanges, such as tributary inflow and groundwater seeps, are of current interest to managers for expanding cold-water habitat for salmonids (Loheide and Gorelick 2006, Neilson *et al.* 2009). Further investigation is needed to expand our understanding of thermal processes and modeling approaches to improve thermal habitat conditions for stream communities and shed light on riparian reforestation questions, which are currently in debate among land managers in California.

Stream Energy Budgets and the *Heat Source* model

Monitoring energy flux allows researchers to determine which types of heat energy are influencing stream temperature. Heat energy travels by advection, radiation, and conduction (Figure 2). Radiation is the sum of packets of electromagnetic energy moving between mediums (*i.e.* ultimately the sun to the earth as well as reflected radiation from plants/ topography). Advection is the transport of heat by the bulk movement of a fluid (*i.e.* downstream in a river). Conduction is the movement of heat from one fluid or surface to another via physical contact (*e.g.* heat moving from water to

cobble or air to water). Convection (*i.e.* convective heat transfer) is the combined processes of advection and conduction.

Net energy fluxes in the stream (Φ_{stream}) include: solar radiation (including shading effects) (Φ_{solar}); longwave radiation from reflective surfaces (primarily canopy cover) ($\Phi_{longwave}$); streambed conduction ($\Phi_{conduction}$); latent heat from evaporation ($\Phi_{evaporation}$); sensible heat from convection ($\Phi_{sensible}$); and lateral inflows such as tributaries and seeps (Φ_{Inflow}) (Boyd and Kasper 2003, Loheide and Gorelick 2006, Westhoff *et al.* 2007). Fluxes can be accounted for using the overarching equation:

$$\Phi_{stream} = \Phi_{solar} + \Phi_{longwave} + \Phi_{conduction} + \Phi_{evaporation} + \Phi_{sensible} + \Phi_{Inflow} \qquad \text{Equation 1}$$

Each heat flux transfer is further composed of additional energy transfer equations (the reader is referred to Boyd and Kasper 2003 for a full review of equations).

The "accounting" of heat fluxes has resulted in energy budget models similar to mass and sediment budgets. Stream temperature can be modeled using mechanistic or regression models. Stream energy budget models are typically use a mechanistic approach, where physical site specific measurements are used to model the stream thermal systems. Not only do these types of models keep track of energy fluxes at one point over time; they also spatially model an entire stream by integrating thermal changes as a series of fully mixed reservoirs (Westhoff et al 2007, Huff 2009).

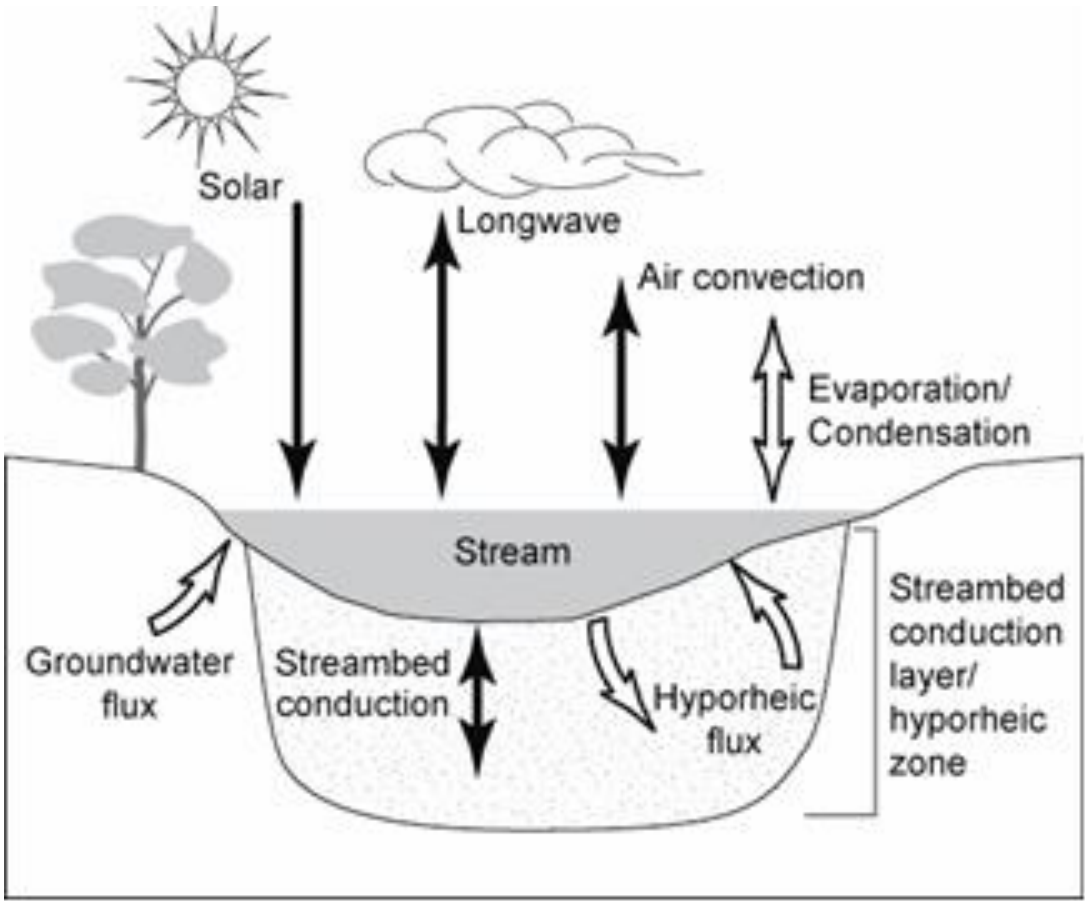

Figure 2. Schematic diagram of heat fluxes within a stream (Loheide and Gorelick 2006).

A common model used to simulate the complex nature of heat transfer in open-channels is *Heat Source* (Boyd and Kasper 2003). *Heat Source* was developed from the thesis of Boyd (1996) at Oregon State University and further refined by the Oregon Department of Environmental Quality (DEQ). DEQ has used *Heat Source* to investigate stream heating and establish criteria for TMDL compliance throughout Oregon. *Heat Source* includes multiple modules that simulate open channel hydraulics and flow routing, stream heat transfers, effective shade (topographic and vegetation) and the resulting stream temperature (Boyd and Kasper 2003). It was originally developed using Forward Looking Infrared (FLIR) measurements as the main thermal input. Recent studies have used Distributed Temperature Sensing (DTS) methods instead (Matheswaran *et al.* 2011).

DTS measurements have also been used in other stream energy budget models such as Westhoff *et al.* (2007). The high spatial resolution given by DTS has allowed researchers to address competing management options for stream thermal protection such as varying riparian forest cover (Roth *et al.* 2010). *Heat Source* applications have been limited to a narrow range of geographical locations (*i.e.* watersheds primarily in Oregon, USA and some small streams in Europe). The aim of this study is to use *Heat Source* and calibrate the model to a northern California stream so that the model can then be used by land managers to evaluate the stream temperature changes resulting from management actions such as reforestation, channel manipulation, and climate change.

Distributed Temperature Sensing Technology

Thermometers have been used for centuries to describe aquatic systems. As scientists began to measure a variety of environmental conditions, it became clear that stream temperature was not a fixed measurement. They realized that observations needed to be rooted in both temporal and spatial contexts. Numerous studies have attempted to bridge this "snap shot" gap by attaching multiple sensors together and/or recording a single measurement over a limited time scale. These studies have given hydrologists insight into stream temperature but their methodology also limited their ability to model stream heating dynamics. One way to expand temperature monitoring is with Distributed Temperature Sensing (DTS) equipment.

Distributed Temperature Sensing technology is a novel method that measures temperature continuously over a relatively long distance. DTS uses a glass fiber-optic cable to gather spatial temperature information over time. The fiber-optic cable can be up to tens of kilometers long and the temporal resolution is on the order of seconds to minutes extending over a series of weeks to months. The exact spatial and temporal resolution is based on the time sampling step decided upon by the observer. DTS measures Raman back scattering - the proportion of Stoke to anti-Stoke photon scattering through the cable - which change in frequency in varying thermal conditions (Tyler *et al.* 2009). Within the last decade, applications using DTS cables have improved environmental temperature modeling. Hydrologic applications of DTS include: hyporheic temperature modeling (Selker *et al.* 2006b, Huff 2009); hyporheic influence on a salt marsh (Moffett *et al.* 2008); soil moisture monitoring (Sayde *et al.* 2010, Steele-Dunne *et*

al. 2010); air-surface interactions (Boderie and Dardengo 2003), snow hydrology (Tyler *et al.* 2008); lacustrine surface and benthic temperature circulation; and temperature distribution along first-order streams (Selker *et al.* 2006a, Selker *et al.* 2006b, Westhoff *et al.* 2007, Roth *et al.* 2010, Westhoff *et al.* 2011).

This study identified spatial patterns of groundwater inflow and expands upon previous work to refine stream heating models. DTS was used to directly measure and model the "thermal context" (*i.e.* spatial and temporal thermal regime) experienced by fish and other aquatic organisms. The study continues the ongoing development of DTS technology as an indispensable tool for land managers to address stream heating issues on the reach and basin spatial scales.

METHODS

This section discusses the methods used throughout the study. I present the study site description, Distributed Temperature Sensing methodology, and then three sections related to the three areas of research: salmonid distribution, detection of groundwater spring, and *Heat Source* modeling.

Study Site Description

The Salmon River is the second largest tributary of the Klamath River in northern California. The Salmon flows east to west and consists of two major forks, North and South, joining at Forks of the Salmon, CA. The entire watershed drains an area of 1,945 km^2 with average annual discharge of 1.5 trillion cubic meters (1.2 million acre-ft.) (Elder *et al.* 2002). The Salmon River enters the Klamath River upstream of the Trinity River sub-basin. The bulk of the Salmon River's precipitation falls between November and May and varies between 203 centimeters (80 inches) in the headwaters to less than 100 centimeters (40 inches) at the South Fork (Elder *et al.* 2002). Elevation ranges from 2,609 m in the Trinity Alps to 139 m at its mouth. The Salmon River basin is within a tectonically active north-striking fault zone. It is primarily composed of uplifted mafic igneous and oceanic sedimentary deposits (Ando *et al.* 1983).

The Salmon River basin has a rich cultural heritage. It is part of the ancestral territories of Karuk, Shasta, and Konomihu first nations and is currently home to approximately 100 residents. Currently, the Klamath National Forest encompasses 90 %

of the Salmon River. In 1981, the Salmon River and its main tributary, Wooley Creek, were designated as National Wild and Scenic Rivers. The Klamath Basin as a whole has experienced widespread anthropogenic stress, primarily from logging, stream flow diversion, gravel mining, and hydraulic gold mining (National Research Council 2004). The Salmon River was extensively rearranged by hydraulic gold mining beginning in the 1850s and continuing through the 1990s (Elder *et al.* 2002). A historic estimate of sediment input from hydraulic mining was 12 million cubic meters (15.8 million cubic yards) of sediment between 1870 and 1950 (Elder *et al.* 2002).

Salmonid spawning and rearing habitat in Klamath tributaries was degraded by human activity resulting in lack of stream cover, sedimentation, and absence of large woody debris (LWD) (National Research Council 2004, National Marine Fisheries Service 2012).The National Research Council (2004) determined high summer temperatures in tributary waters of the Klamath was the greatest coho salmon impairment. The latest coho recovery plan for the area also echoed elevated summer temperatures as a limiting factor for coho in the Salmon River (National Marine Fisheries Service 2012). The Salmon River is listed as thermally impaired under California's List of Impaired Water Bodies 303(d), with mainstem temperature commonly exceeding salmonid temperature thresholds (CA Environmental Protection Agency 2002).

The North Coast Regional Water Quality Control Board (NCRWQCB), in collaboration with a variety of government, tribes, and nonprofits, developed a Total Maximum Daily Load (TMDL) for temperature in the Salmon River watershed. This plan indicated that salmonids were the most susceptible beneficial use in the watershed to

temperature impairment (NCRWQCB 2005). We conducted our study in July to further investigate summer stream temperatures and identify potential salmonid thermal and channel geomorphic impairment.

Current restoration efforts in the Salmon River have focused on reducing sediment runoff from logging roads created in the boom of the 1970s. The Salmon River is one of a few major drainages in the Klamath with no major diversions or dams, making it accessible to anadromous fish migrating from the Pacific (Hamilton *et al.* 2005). Anadromous salmon and trout in the Salmon River include Chinook (*Oncorhynchus tshawytscha*), coho (*O. kisutch*), and steelhead (*O. mykiss*). Previous fisheries work on the Salmon River has focused on spring Chinook and summer steelhead returns. The Salmon River Restoration Council and partners have identified peak summer stream temperature, in conjunction with low flow, as a limiting factor to the success of all life stages of spring Chinook (Salmon River Restoration Council 2004). Juvenile salmonids that over-summer in fresh water are the most at risk to adverse summer temperatures.

The study site consists of a one-kilometer reach of the North Fork (Figure 3). It is located one-kilometer upstream of Little North Fork Creek confluence, the last major thermal refuge for migrating adult salmonids (Sutton and Soto 2010, Lyra Cressey, personal communication, November 9 2011). It is also located downstream of Sawyers Bar, CA, the epicenter of gold mining activity on the North Fork Salmon River. The reach was broken into ten habitat units corresponding to runs, riffles, and pools (Figure 4). The following sections further outline the methods used in defining habitat units and field methods used in this study.

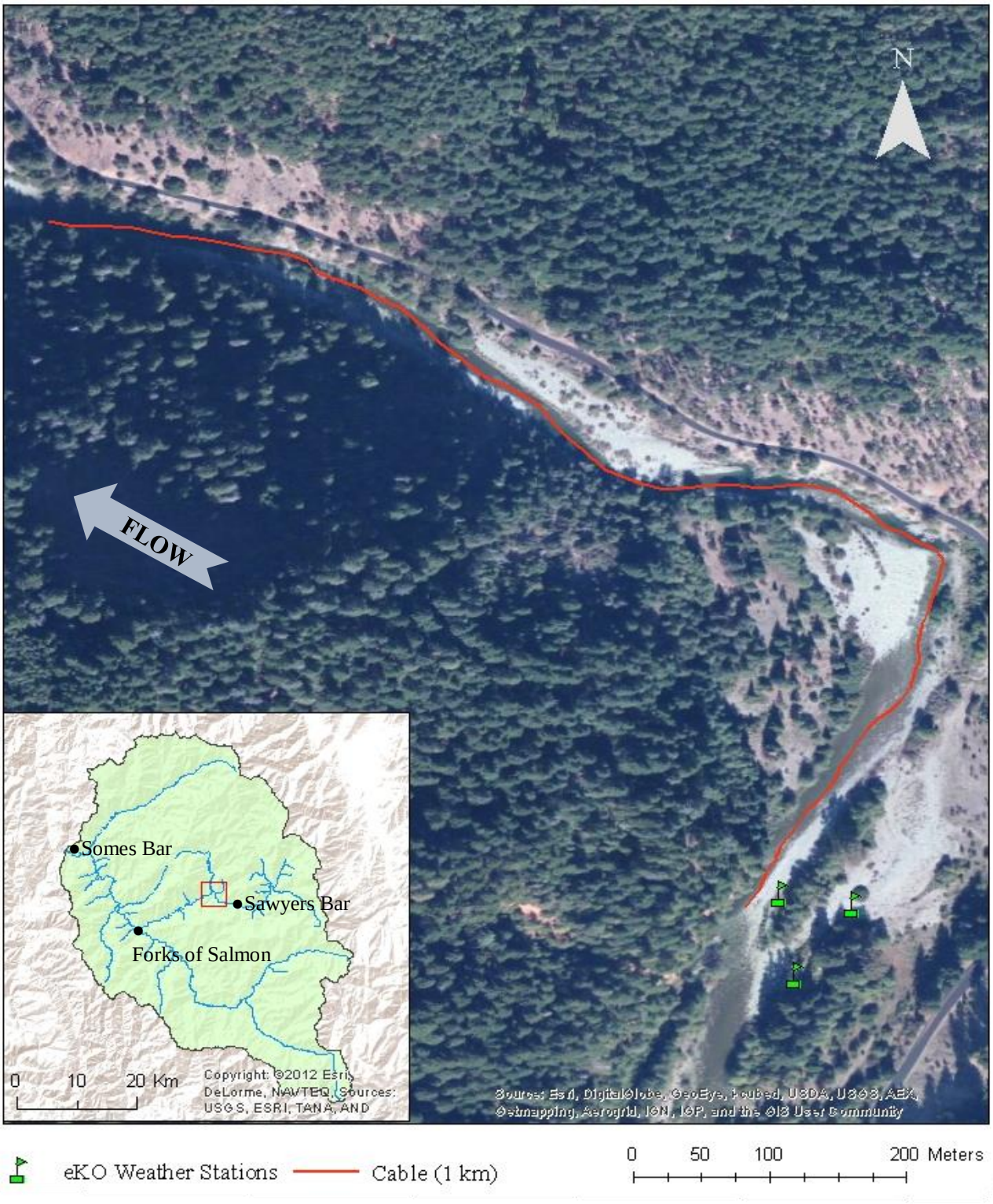

Figure 3. Map of one-kilometer study reach on the North Fork Salmon River, CA, USA, showing position of the fiber-optic cable and eKO weather stations. The river runs parallel to Salmon River Road (above red line). The inset map shows the Salmon River sub-basin with a red box to indicate the extent of the study area.

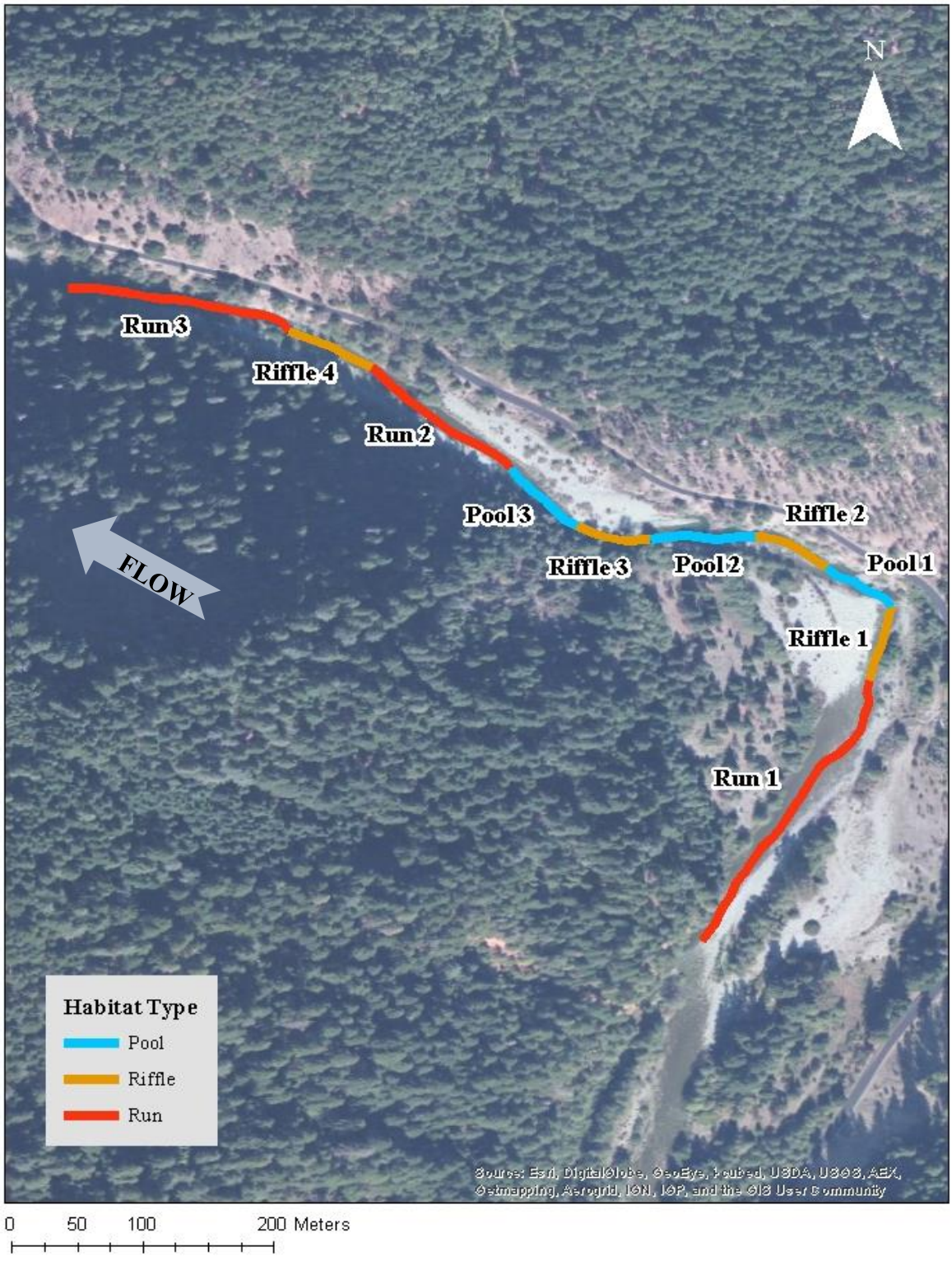

Figure 4. Map of one-kilometer study reach on the North Fork Salmon River, CA, USA, divided into ten habitat units. Pools were maintained by scour against Salmon River Road bedrock. Riffles were areas of greatest slope and Runs were the longest habitat units in the study.

Distributed Temperature Sensing Methodology

Site Setup

A four-channel Oryx remote logging unit (Sensornet LLC.) was used to quantify the Salmon River's thermal regime. The fiber-optic cable used in the study was a mini-flat drop cable (AFL Telecommunications). The cable is made from two singlemode optical filaments that are protected by a gel buffer coating and two dielectric rods to provide strength and rigidity (AFL Telecommunications 2007). The site layout consisted of the laser instrument and computer processor (labeled DTS in figure); the power source, three 70 amp-hour deep cycle marine batteries hooked up to two solar panels; two calibration baths, and the fiber-optic cable in the stream (Figure 5).

The cable was placed along the streambed thalweg (*i.e.* deepest point in channel ± 1 m) and was spliced at the downstream end, creating an internal loop in the cable. This configuration collects "double ended" measurements, which means that for each recording, the instrument recorded the entire stream length (to the end with the splice) and back. Two kilometers of information was collected on channel one. After 5 minutes of data collection the instrument collected an additional 5 minutes of data on the second channel. The instrument would then rest for 5 minutes to allow the data to be offloaded onto the computer processor and removable thumb drive.

The cable was anchored with cobbles to keep it firmly in place along the thalweg every couple of meters. On shore, two ice baths (in ice chests) with thermal couples housed two coils of cable, which helped calibrate the stream temperature data (discussed in further detail below) (Figure 5). Each ice chest had a guide to wrap the coils around

and to keep them from touching the sides of the ice chests. Small aquarium pumps with bubbler rocks ensured fully mixed baths reducing the risk of thermal stratification in the ics chest. A handheld Global Positioning Unit (Garmin Inc.) marked the cable's location in the stream for ArcGIS analysis. Additional observations such as geomorphic features and fish were recorded corresponding to cable length as described in the following sections.

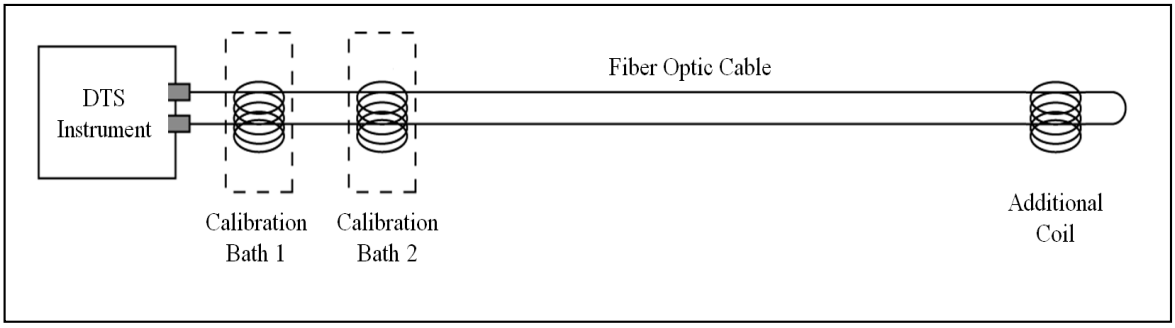

Figure 5. Schematic diagram of DTS and cable layout adapted from Hausner et. al (2011). The cable is attached to the DTS instrument then runs through two calibration baths. At the downstream end, the cable is wound into a third coil where an internal splice in the cable joins two optic filaments together creating an internal loop. The loop allows the DTS instrument to communicate on two separate channels through the cable.

In-field Calibration

This study employed the "dynamic calibration method" to calibrate DTS measurements in the field. This results in absolute temperature measurements rather than relative temperature measurements during the study period (Tyler *et al.* 2009). Two calibration baths in Igloo Ice Cube ™ ice chests housed two thermal couples and two 15-meter coils. The first bath was an ice-slush mixture which was placed in full shade and

the second bath a warm-water mixture where the ice chest was left fully exposed to the sun. Six temperature loggers (HOBO© Water Temperature Pro v2 Data Logger - U22-001) (Onset Computer Corporation, USA) were randomly installed along the cable in the stream and four loggers were attached to a 15-meter coiled section of cable at the downstream end to used to reference DTS temperature data (Selker *et al.* 2006a). No statistical tests were performed comparing the independent temperature loggers to the DTS measurements in the field.

Post Collection Processing

After downloading the data off the Oryx thumb drive, the data was processed in MATLAB (MathWorks Inc, USA) using a program provided by Center for Transformative Environmental Monitoring Programs (CTEMPs) based at the University of Nevada Reno and Oregon State University. The program calculated temperature from Stokes and anti-Stokes backscatter measurements recorded by the DTS. It also converted the data into a vector format to align the measurements with time and distance. The post-collection processing was completed on both channels using the single-ended method developed by Hausner *et. al* (2011). To remove noise, the processing requires three reference sections of known temperature with one reference being far away from the laser. Sections in both calibration baths were used with the cold bath used twice (near and far from the DTS). Furthermore, a section surrounding the cable splice (*i.e.* blunt downstream end of cable where optic filaments are joined to make a loop) was also used

to reduce noise caused by the splice. It is important to include a section around the splice because the physical fusion of optic filaments inherently introduces noise into the system which is accounted for by comparing measurements that are geographically in the same location but differ in signal path (*i.e.* how they intercept the splice). The Root Mean Square Error (RMSE), bias, and MARE (Mean Absolute Relative Error) for the processed data was calculated for both channels for the calibration and a validation test (Table 1). The validation test used a section of cable in the warm bath at the end of the cable and is independent of the data used for the calibration. Channel 2 has lower RMSE and bias values for both calibration and validation data sets and a similar MARE calibration value so it was used solely in the study analysis (*i.e.* Channel 1 data was not used).

Table 1. Post collection processing Root Mean Square Error and bias results for both channels in degrees Kelvin.

	Calibration			**Validation**		
Channel	**RMSE**	**Bias**	**MARE**	**RMSE**	**Bias**	**MARE**
1	0.032	3.7657 e-6	0.023	0.272	-0.267	0.017
2	0.025	2.3956 e-6	0.024	0.267	-0.263	0.020

Salmonid Methods

Salmonid Distribution

Intensive fish counts were conducted to quantify the relative abundance of salmon and trout species. Fish surveys overlapped in time and space with the DTS temperature

data collected in the previous section. The stream was divided into run, riffle, and pool habitat units. Surveys were randomly assigned day, time, and transect starting point. While randomly scheduling transects, units close together were excluded to reduce count bias. A minimum of a one-hour break was used to let fish resettle before sampling nearby units. Survey transects in run and riffle units were 42 meters long and approximately 12 minutes in duration. Pools were completely surveyed to take the entire habitat into account and were timed to standardize sampling effort (discussed further in Data Analysis of Salmonid Distribution below). Fish were identified as rainbow/steelhead, salmon (coho or Chinook) or unidentifiable. Recently emerged salmonids (less than 4 centimeters in fork length and located exclusively at the bank margins) were not included in the count because they do not use main channel habitat. Each habitat unit was sampled twice over the course of five days. Two divers started at the bottom of each unit and swam upstream counting fish. For each transect, a dominant bank was assigned based on greater habitat complexity (Dolloff *et al.* 1996). One observer counted along the dominant bank while the other observer counted fish from mid-channel to the non-dominant bank. In cases that had no dominant bank, the fiber-optic cable placed in the thalweg was used to divide the channel and observers zigzagged their respective halves to cover the entire channel. Fish were counted only as they passed the divers. In riffle units, divers briefly moved their masks above the water to help get upstream of large cobble.

Data Analysis of Salmonid Distribution

Linear regression models were constructed to investigate dependence of fish count on habitat predictors. Sampling effort was standardized by multiplying fish counts by a time factor (fraction of 8 minutes). This was especially important to standardize pool counts. Two sets of models were analyzed, one using total fish count (all species and unidentified individuals) as the response variable, and the other using count of only Salmon (coho and Chinook) as the response variable. Differences in results between the two model sets are presumed to be due to the effect of including rainbow trout in the counts. In both model sets, the habitat units served as the observational units for the analysis (n = 10). Counts were arithmetically averaged between the two transects within each habitat unit to obtain a single count for that unit and then each count was log-transformed. The temperature parameter was calculated as the average water temperature measured by DTS over the habitat unit during the middle of the observation time. Additional parameters included habitat type (labeled ctype) and log-transformed maximum depth for each unit (labeled lmaxdepth). For each of the two response variables, eight regression models were proposed:

H1: Fish count was a function of temperature.

H2: Fish count was a function of channel type.

H3: Fish count was a function of maximum depth.

H4: Fish count was a function of maximum depth and channel type.

H5: Fish count was a function of temperature and maximum depth.

H6: Fish count was a function of temperature and channel type.

H7: Fish count was a function of maximum depth, temperature, and channel type.

H8: Fish count was not dependent on any of the predictors (*i.e.* null model).

Models were ranked using Akaike's Information Criterion, adjusted for small sample size (AICc; Burnham and Anderson 2002). The AICc analysis balances increases in explanatory power against loss of precision introduced by over-parameterization (Anderson 2008); models with lower AICc values are optimal. The AICc values where used to calculate model weights, which can be interpreted as relative probabilities of evidence for or against the models in the candidate set (Anderson 2008, Bolker 2008). Analysis was conducted in R software (R Development Core Team). Dr. Robert Van Kirk and I co-wrote the R code for this analysis. In the ranking process ΔAICc and model "weight" were referred to in the discussion. ΔAICc is the difference in AICc value from the best model. The "weight" or measure of "informativeness" is included to highlight the differences in models. After the eight models were ranked, the best model summary for total count and salmon count were compared to investigate differences among fishes response.

Habitat Inventory

To assess the condition and available habitat in the stream, this study used the USDA Forest Service Region 6 Stream Habitat Inventory Level II Protocol (2006). The study reach was divided into ten habitat units (as outlined earlier). Units consisted of

runs, riffles, and pools as determined by generalized slope/velocity breaks. Pool units ended at the tail water control, the highest point of substrate at the thalweg at the downstream end of the pool before the channel bottom begins to slope downward. Units were measured starting at the upstream end of the study reach moving downstream, which is a deviation from the protocol. Measurements in each unit included total unit length, maximum longitudinal depth, wetted width, bankfull width, maximum bankfull depth, bankfull depths at 25 %, 50 %, and 75 % of the bankfull width, surface depths at 25 %, 50 %, and 75 % of the wetted width, and classification of riparian vegetation. All measurements were taken with a stadia rod and transect tape. Additionally, longitudinal average depth and floodprone width were measured for runs and riffle units, and pool crest depth was measured for pool units. Cross-section measurements were taken in three randomly selected locations in all runs and riffle units. Three cross-sections were also measured in pools: a random location at the beginning third of the unit, at the deepest point in the pool, and at the tail water control (*i.e.* pool tail crest depth). Riparian vegetation was classified as overstory and understory. The dominant vegetation species from a bird's eye view and average size class was recorded for each cross-section (*i.e.* three times for each unit). Understory vegetation was classified as forbs, grasses, sedge/rush, and bare earth/rock. Effective shade, Wolman Pebble Counts, and channel slope was also measured for each unit and are discussed further below.

Effective shade along the channel was measured using a Solar Pathfinder meter (Solar Pathfinder, USA). The meter was held one foot above the stream surface and oriented to the South (*i.e.* magnetic pole). The recorder identified areas of shade and

direct sun along the July path line. Riparian and total shade was recorded three times for run and riffle units and twice for pools. Pool depth was a limiting factor for taking a third shade measurement.

The stream's coarse substrate was quantified using the Wolman Pebble Count method (Wolman 1954, USDA Forest Service 2006), the most common method for quantifying the distribution of pebble size. The observer walked from bankfull to bankfull in a zig-zag fashion randomly sampling a minimum of 100 pebbles. The length along the intermediate axis of each pebble was measured using a gravelometer. Gravelometers quantify particles into standardized size classes. Counts were conducted in all units except one pool habitat which was primarily bedrock and would skew the particle results. After the count was completed, the D_{50} and D_{83} particle sizes were calculated for each unit.

Channel slope was measured using a theodolite and stadia rod on the channel bottom. Elevation measurements were taken at the beginning and end of each unit and were divided by the unit length (measured previously) to calculate channel slope for each habitat unit.

Habitat Condition Calculations

Fish habitat quality was assessed using the USDA Forest Service Region 6 Stream Habitat Inventory Level II Protocol (2006). Fast water habitat is defined as non-pool habitat (*i.e.* runs and riffles). Calculations included:

1. Percentage pools per study reach = sum of pool lengths / sum of all habitat lengths
2. Fast-water to slow-water ratio = sum of length of riffles and runs / sum pool lengths.
3. Percentage mean total shade = mean percent shade from the sum of riparian, conifer, and topographic sources.
4. Mean bankfull width: depth ratio = mean ratio of width-to-depth over all units.

Maximum Weekly Temperature Calculations

Maximum weekly maximum temperature (MWMT) and maximum weekly average temperature (MWAT) are two common measurements of peak stream temperature used by land managers (Welsh et al 2001, Madej *et al.* 2006). MWMT averages the *maximum* temperature recorded each day in the study reach over a seven day period while MWAT is the largest value of the daily *mean* temperature over the same period. MWAT has been used extensively to investigate thermal condition but bias exists due to the type of averaging. Cool evening temperatures reduce MWAT while MWMT is unaffected. For this study both were calculated over the eight day study period. Calculations were applied to the first seven whole study days and the second through 8th study days to see if there was any difference in the averaging.

Groundwater Spring Methods

Field Measurements

At the beginning of the study period, a spring was found along the side of the mainstem channel below Pool 2. A HOBO© Tidbit data logger (Onset Computer Corporation, USA) was placed in the spring, fully submerged, and covered by a rock to reduce direct solar heating. The logger recorded the spring's temperature continuously over 8 days at 15-minute intervals. To quantify the spring flow and identify if it was a hyporheic or groundwater seep, the period and daily maximum temperature was determined over the entire habitat units above (Pool 2) and below (Riffle 3) the spring using the DTS data. The spring temperature during this period, recorded by the temperature logger, and the average daily mainstem flow were used in a volumetric flow calculation (discussed below). Flow was calculated over the 8-day study period and averaged to find the mean spring volumetric flow and standard error. Originally, time series methods were proposed to help remove temporal autocorrelation (*i.e.* the correlation between the measurements and previous measurement), but the study period was not long enough for this method to be viable.

Mainstem Discharge

To measure stream discharge, the velocity-area procedure was used (Environmental Protection Agency 2006). Discharge and depth were measured at 15 one-meter increments to calculate stream discharge. The area chosen for the cross-section was

in Run 1 because it has a U-shaped channel with relatively uniform flow (Figure 4). Two stakes were secured along the stream to mark the cross-section and hold the transect tape steady. The cross-section was cleared of a few large cobbles before measurements were taken. Measurements were made twice a day, 9:00 and 16:00, for the entire study period. The sampler began on the left bank (looking downstream) and moved across the channel to the right bank. Velocity was measured with a Swoffer Velocity Meter© Model 2100 (Swoffer Instruments Inc. USA). The meter was placed at a distance beneath the water surface equal to 60 % of the water depth at each interval perpendicular to flow. An averaged measurement was taken for 30 seconds at each point.

Volumetric Inflow Calculation

Hyporheic or groundwater inflow can be calculated using the conservation of mass and energy (Arik 2011). Measuring the temperature of the mainstem upstream (T_{us}) and downstream (T_{ds}) of the spring, the temperature of the spring (T_{sp}), and the flow of the upstream mainstem channel (Q_{us}), the spring's volumetric flow (Q_{sp}) can be calculated:

$$Q_{us} + Q_{sp} = Q_{ds} \qquad \text{Equation 2}$$

$$T_{us} Q_{us} + T_{sp} Q_{sp} = T_{ds} Q_{ds} \qquad \text{Equation 3}$$

$$Q_{sp} = \frac{T_{us} - T_{ds}}{T_{us} - T_{sp}} Q_{us} \qquad \text{Equation 4}$$

Seep Source Determination

DTS has provided insight into groundwater and hyporheic flows in previous research. Groundwater seeps at a consistent temperature. If it is cooler then the mainstem temperature, a groundwater "signature" results in a dampening of daily maximum and minimum stream temperatures (Selker *et al.* 2006b, Huff 2009, Arik 2011). Hyporheic exchange acts as temporary heat storage of upstream mean annual air temperature without a net offset in temperature (Arrigoni *et al.* 2008). The hyporheic "signature" results in a cooling effect during the day (assuming the mainstem is very warm) and a warming effect during the night when streams are typically "cooling off." (Anderson 2005, Loheide and Gorelick 2006, Arrigoni et. al 2008, Collier 2008, Huff 2009, Westhoff *et al.* 2011). The subtle difference in warming trends of evening temperatures from hyporheic and groundwater has helped researchers to identify the origin of springs (Figure 6).

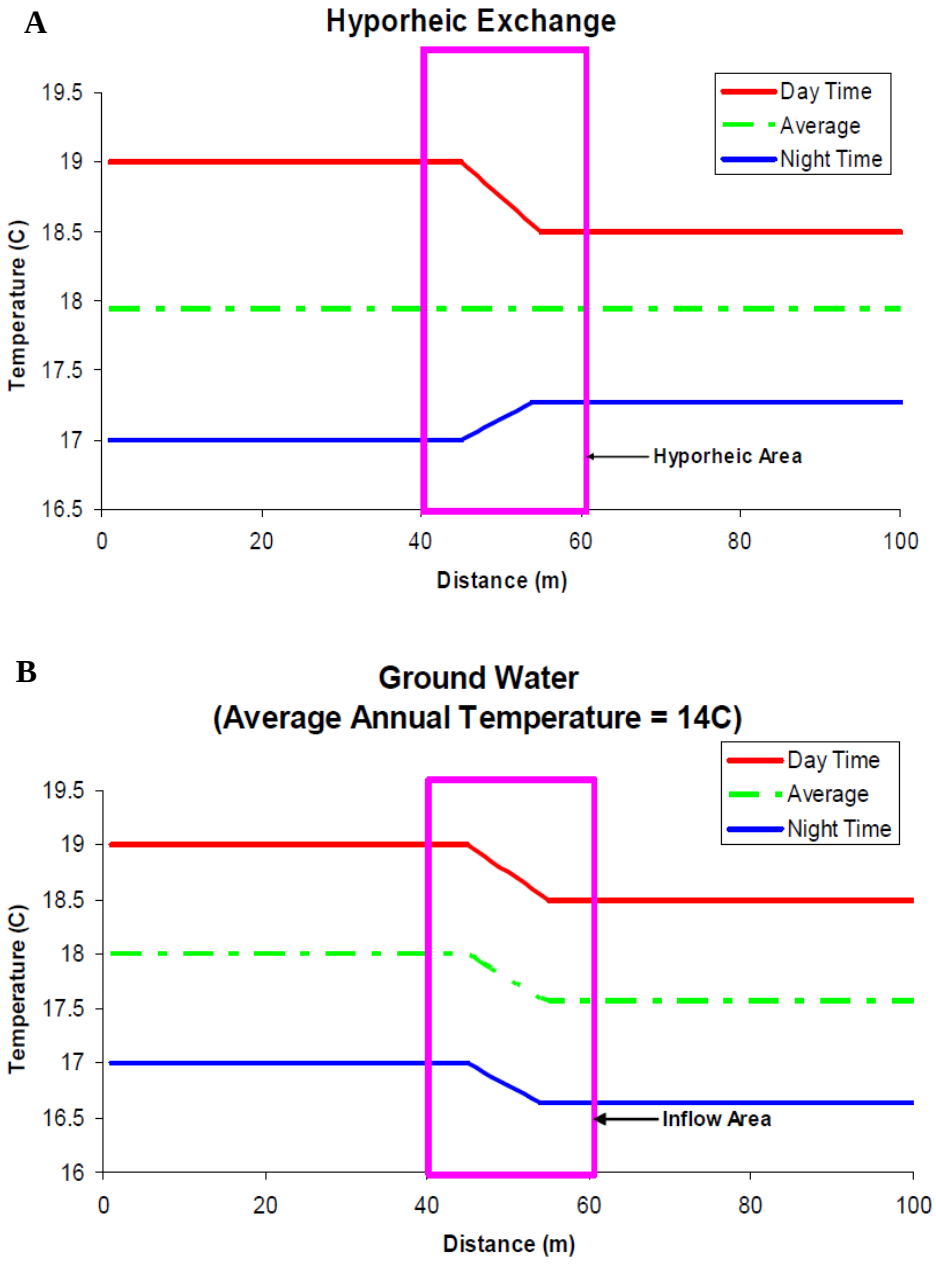

Figure 6. Comparison of temperature signatures of A) groundwater and B) hyporheic exchange (Collier 2008). Note the "warming trend" in the evening (blue line) for hyporheic exchange is different from the "downward shift" for groundwater

Heat Source Modeling Methods

Field Measurements

Three eKO Pro Series remote weather stations (Envco Environmental Equipment Suppliers, South Pacific) were deployed over the study period. Each station was equipped with an eS2000 eKo Weather Sensor which measured solar radiation, wind speed and direction, air temperature, humidity, barometric pressure, and precipitation with a tip bucket rain gauge. The stations were configured in a triangle around the DTS instrument site (Figure 3). One station was upstream of the cable close to the bank, one station was directly on the river bank along the cable buffered by riparian vegetation, and the third station was on top of an exposed gravel bar similar to the bars in the study site downstream. In addition to the meteorological conditions, mainstem flow and channel cross-sections were measured in the field and used to calculate several model parameters (discussed further below).

Spatial Analysis Using tTools

tTools is an ArcGIS extension that extracts geospatial data as input data for *Heat Source*. Data sources and their source years used for this analysis are defined below (Table 2). Before using tTools it was necessary to digitize the stream channel and vegetation features in the study site. Digitizing was completed in a map view between 1:500 and 1:600 (Boyd and Kasper 2003). First, the stream channel centerline and banks were digitized by hand using ESRI's World Imagery Basemap. In areas where channel

boundaries were difficult to distinguish (*e.g.* topographic shade), aerial photographs taken by Watershed Sciences (2009) were used. A section of Riffle 2 was used in stream bankfull calculations but not included in the stream outline digitization because the channel boundary was difficult to discern. Next, the stream centerline was broken into sixty points equally spaced 15 meters apart. Land cover was digitized by hand using ESRI's World Imagery Basemap (2011). Each vegetation polygon was assigned a vegetation code with associated height (m) and density (%) (Boyd and Kasper 2003) (Table 3). tTools then sampled the stream and vegetation layers and elevation used as input data for *Heat Source.* The input data was used to calculate total and effective vegetation and topographic shade.

Table 2. Data sets used in this study for tTool spatial analysis.

Data Set	**Year**	**Source**
World Imagery Basemap	2011	ESRI (2011)
Reference aerial photographs	2009	Watershed Sciences (2009)
National Elevation Dataset (NED) 10 m resolution	2009	U.S. Geologic Survey

Table 3. Land cover codes used in tTools to categorize land cover types from aerial photographs.

Land Cover Name	Code	Height (m)	Density (0 - 1)	Overhang (m)
Open Water	301	0.0	0 %	0.0
Bare Rock / Cobble	304	0.0	0 %	0.0
Paved Road	400	0.0	0 %	0.0
Large Mixed Stand	500	24.0	70 %	0.0
Small Mixed Stand	501	12.0	70 %	0.0
Large Conifer Stand	700	27.0	70 %	0.0
Small Conifer Stand	751	12.0	45 %	0.0
Willow / Shrub / Rock	850	2.0	30 %	0.0

The stream and vegetation digitized layers are included for ease of reference for the reader (Figure 7, Figure 8). Ground truthing of the digitized vegetation layer was performed by randomly choosing 24 points in the study reach and describing the substrate / vegetation and visually estimating canopy density. All but one point matched the digitized vegetation and may have been off due to GPS error (± 9 m). Then fixed area plots, 202 m^2 (1/20th acre) in area, were selected in the study reach to represent partial and full restoration scenarios. Two plots were fully described (vegetation type, density, and height) for each scenario. Tree height and density measurements were within 20 % of modeled restoration scenario estimates.

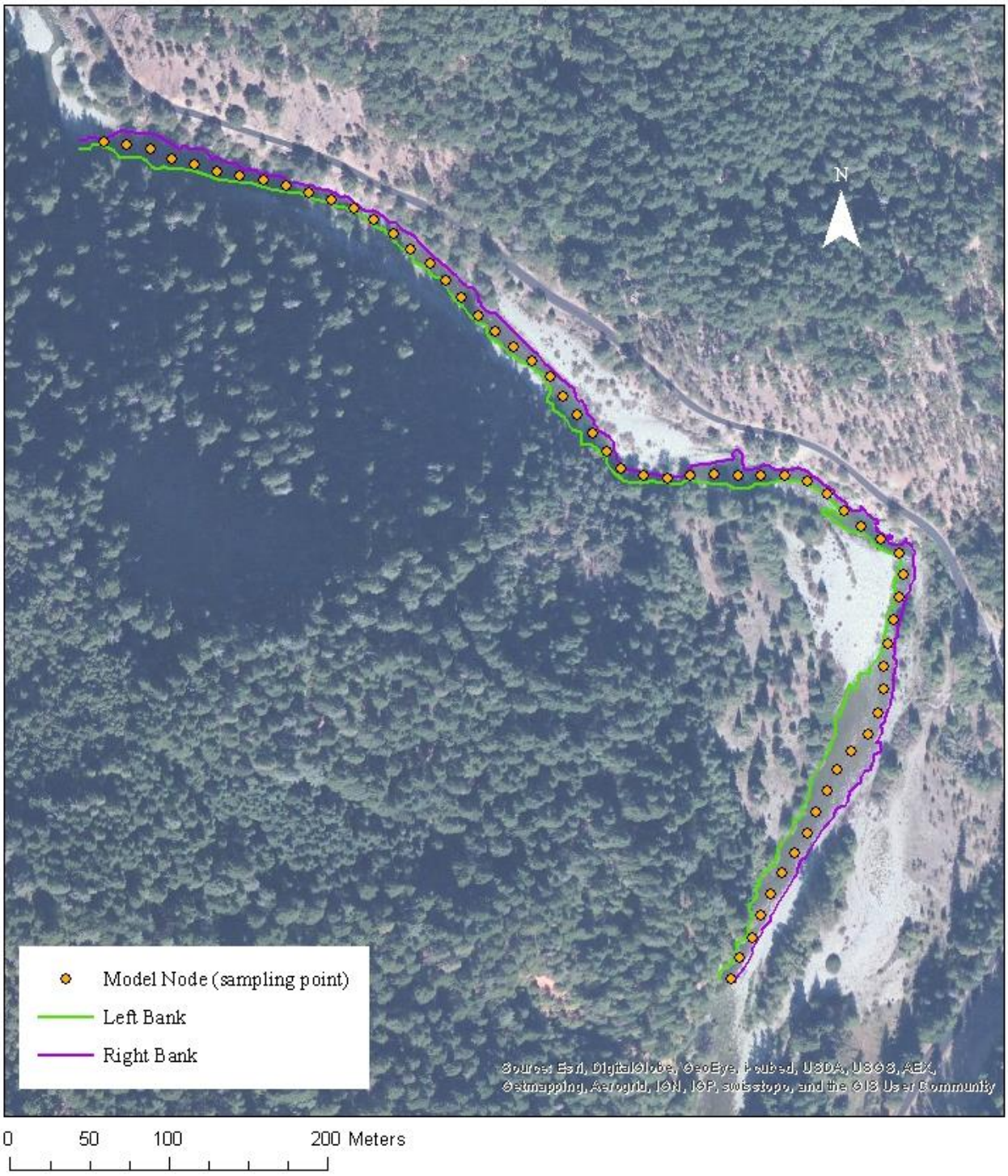

Figure 7. Map of one-kilometer study reach on the North Fork Salmon River, CA, USA, showing the model nodes - sampling locations - (orange circles) used in *Heat Source*. The digitized left and right banks are also highlighted (green and purple respectively).

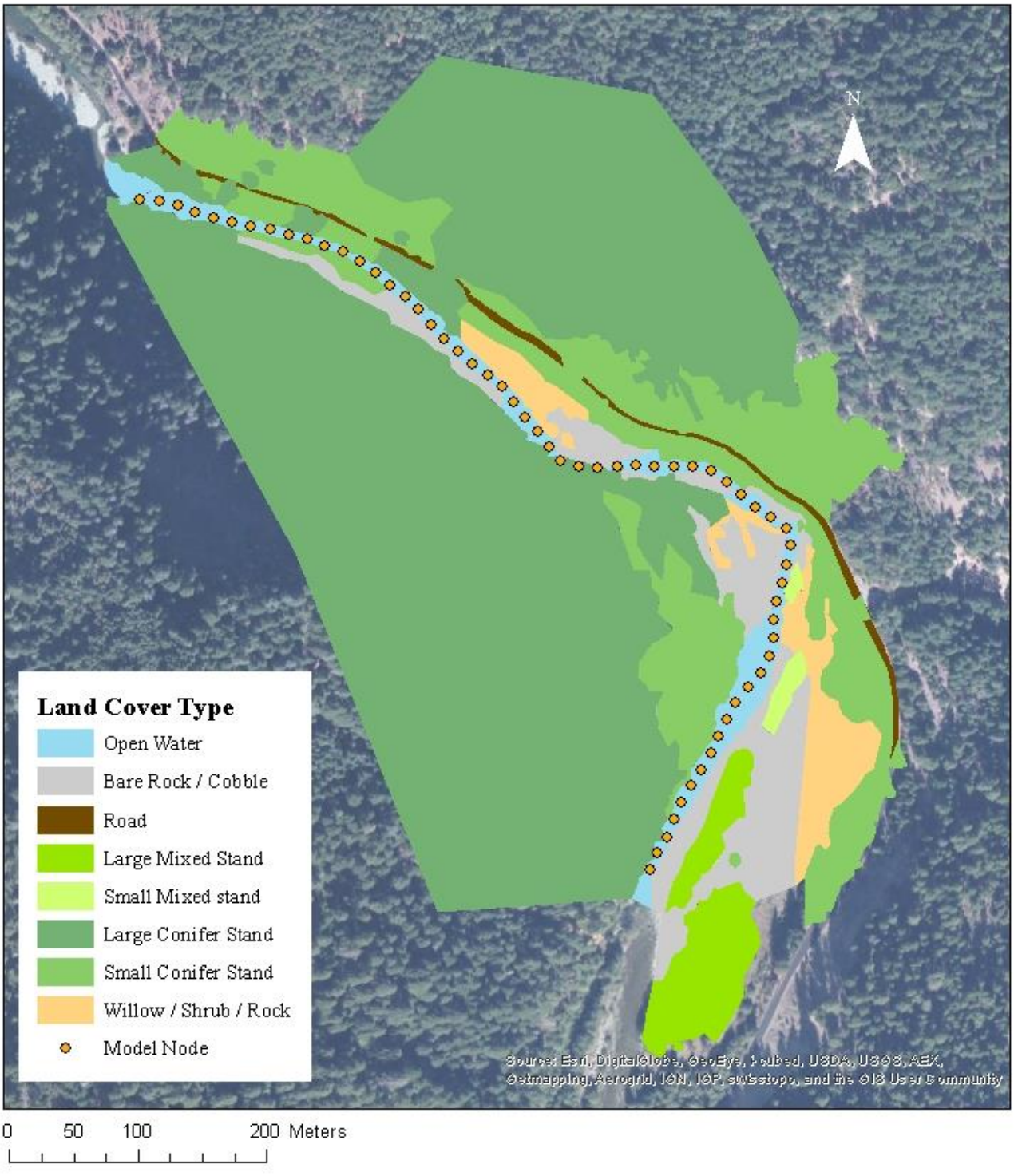

Figure 8. Map of one-kilometer study reach on the North Fork Salmon River, CA, USA, showing the digitized land cover types used in *Heat Source*. Model nodes (orange circles) are included for ease of reference between maps.

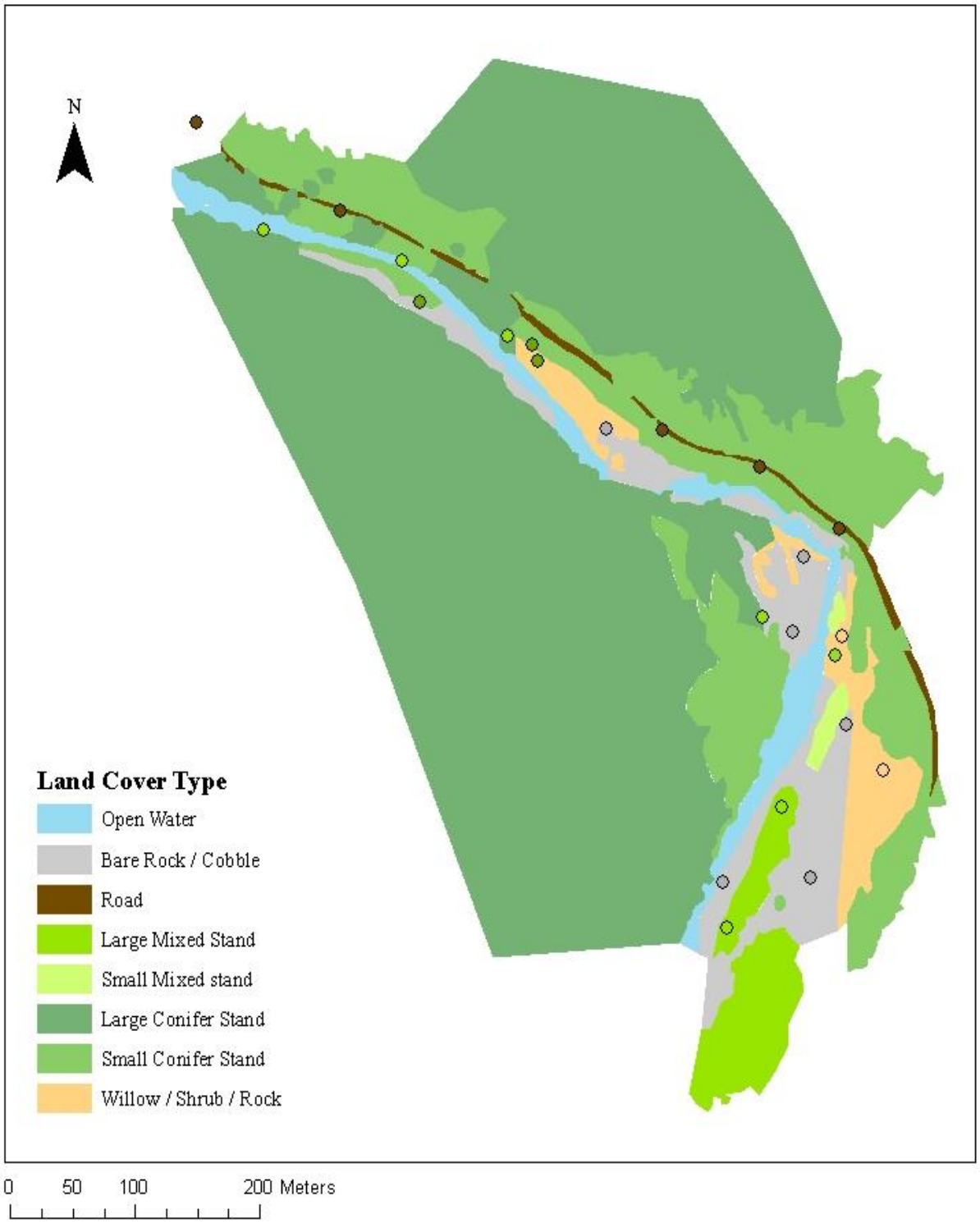

Figure 9. Map of ground truthing points whose color corresponds with the digitized vegetation layer, North Fork Salmon River, CA, USA. Note how most of the points match the digitized vegetation.

Model Initialization, Parameters, and Calibration

The model was initialized by setting boundary conditions at the upstream node to hourly stream temperature observations. Then *Heat Source* used the boundary condition of day one (beginning of simulation), at each time step, to simulated initial conditions for a five day period to "prime" the system (*e.g.* aid the simulated channel to reach an equilibrium state for flow and temperature) before the model was run with time-evolving boundary conditions. The time-evolving boundary conditions then produced the ultimate output where stream temperature varied both spatially and over time. Predicted values were calculated on an hourly basis at 90 m intervals (over one kilometer) over the simulation period. At the most upstream node, a single value served as both the initial and boundary condition. Hourly meteorological and flow conditions, at the most upstream node, served as model inputs, meaning they were used to determine the stream temperature response.

Heat Source employs a large number of parameters and constants to account for all internal and external thermal energy transfers to predict the stream temperature. The table below includes the parameters used in the model, the value, and the literature reference if applicable (Table 4). Parameters referenced as "measured" or "estimated" were directly measured in the field or estimated from field measurements whose calculations are described in further detail below. "Calibrated" parameters were chosen to minimize model bias and RMSE at the most downstream node in *Heat Source* and were not directly measured.

Deep alluvium temperature in previous modeling studies was 9 °C, which was included in this study (Westhoff *et al.* 2007, Roth *et al.* 2009). Freeze and Cherry (1979) estimated gravel porosity between 0.24 and 0.4. The larger value of the range was chosen because the channel sediment is a mix of gravel and cobble. Both sediment thermal diffusivity and thermal conductivity values of Pelletier *et al.* (2006) were recommended by the *Heat Source* interface to model gravel dominated substrate (Oregon Department of Environmental Quality 2012). Manning's roughness coefficient was assessed by matching reach descriptions to those in Arcement and Schneider (1989).

While most of the parameters used in *Heat Source* were directly measured or estimated, two parameters were used to improve model fitness. The thickness of hyporheic /substrate layer and percent hyporheic exchange were included in *Heat Source* simulations to improve predicted evening cooling rates. Parameter values were determined by minimizing model bias and RMSE at the most downstream node.

Table 4. Parameters and Constants used in *Heat Source*, value range shows minimum and maximum values measured over the study period, July 2012.

Constant	Description	Value	Reference
H [%]	Relative Humidity	20 - 100	Measured
T_{air} [°C]	Air temperature	10.2 – 35.8	Measured
v_{wind} [m s−1]	Wind velocity	0.0 – 3.6	Measured
C [%]	Cloudiness	0 - 100	Estimated
Z [dimensionless]	Mean channel side slope ratio	0.067 - 0.405	Estimated
W_b [m]	Channel bottom width	11.6 - 32.6	Estimated
d_{hyp} [m]	Thickness of hyporheic /substrate layer	0.30	Calibrated
Hyp. exchange [%]	Hyporheic exchange	1.00	Calibrated
T_{hyp} [°C]	Deep alluvium temperature	9.00	Westhoff *et al.* (2007), Roth *et al.* (2009)
η [unitless]	Porosity	0.40	Freeze and Cherry (1979)
κ_{sed} [cm^2sec^{-1}]	Sediment thermal diffusivity	0.0064	Pelletier *et al.* (2006)
K_{sed} [Wm^{-1} °C^{-1}]	Thermal conductivity of sediment	1.57	Pelletier *et al.* (2006)
n [dimensionless]	Manning's roughness coefficient	0.04	Arcement and Schneider (1989)

Calculated Parameters

Heat Source's flow model simulation partitions the stream into discrete reservoirs that fill from the bottom up. This means that channel bottom width is necessary to simulate flow conditions (Figure 10). While this study did not directly measure channel bottom width, it was calculated from measured bankfull widths assuming a trapezoidal channel shape using the equation:

$$W_b = W_{bf} - 2*Z* d_{bf} \quad \text{Equation 5}$$

Where W_b is the channel bottom width, W_{bf} is bankfull width, Z is the estimated channel slope ratio, and d_{bf} is the average bankfull depth. Bankfull width was measured once for each habitat unit. All model nodes within each habitat unit were assigned the calculated bottom width.

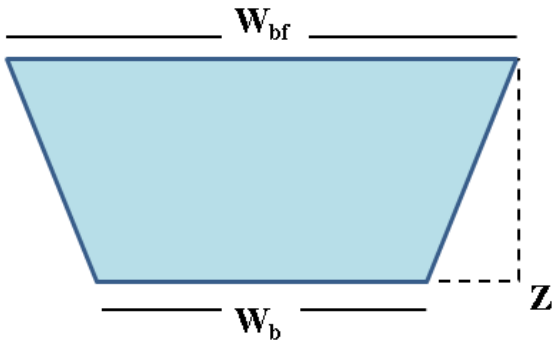

Figure 10. Theoretical trapezoidal channel shape used to calculate bottom width from bankfull width (adapted from *Heat Source 8.0.8*).

Channel side slope ratio (Z) was estimated using cross-sections measured in each habitat unit. Slope was calculated for the left and right bank to the thalweg / middle. The two slopes were then averaged. All model nodes within each habitat unit were assigned this averaged slope ratio.

Percent Cloudiness (C) was also estimated as a continuous meteorological input parameter in *Heat Source*. Cloudiness was estimated as a ratio of mean solar radiation (W/m^2) received by the eKO remote weather stations and potential (*i.e.* no interference including clouds) radiation (W/m^2) estimated by *Heat Source* using the equation:

$$C = SQRT(1.54*(1 - received / potential)) \quad \text{Equation 6}$$

Potential radiation was estimated by *Heat Source* by reducing all vegetation heights and densities and topology-related features to zero. Elevation was set to a constant value for all model nodes. Then "Shade-a-lator," a package within *Heat Source,* was used to calculate the potential solar radiation. In the past, cloudiness was directly measured and solar radiation was estimated from meteorlogic conditions (Boyd and Kasper 2003). The listed equation above solves for cloudiness by measured solar radiation. Assumptions of this calculation include an average vertical intensity of solar radiation from the sun, often referred to as the solar constant (Dingman 2002), constant air mass (*i.e.* atmospheric) thickness, and constant air mass transmissivity (*i.e.* optical path length to the Earth) (the reader is referred to Boyd and Kasper 2003 for the governing equations of solar radiation above topographic features).

Heat Source Accurately Predicts Stream Temperature

During the calibration phase of *Heat Source* it was identified that error systematically increased spatially with distance downstream but not in time. This is primarily due to *Heat Source* being driven by observed hourly meteorological conditions and not additional spatial observation downstream the beginning spatial node. This resulted in calculating four measures of model performance for each of the *Heat Source* spatial nodes (10 in total). The four measures included: bias, root mean square error (RMSE), mean absolute relative error (MARE) and Nash-Sutcliffe Modeling Efficiency (NSE). The four measures were calculated by the following equations:

$$Bias = mean(predicted - observed) \quad \text{Equation 7}$$

$$RMSE = \sqrt{(mean((predicted - observed)^2)} \quad \text{Equation 8}$$

$$MARE = mean(abs\left(\frac{(predicted-observed)}{observed}\right)) \quad \text{Equation 9}$$

$$NSE = 1 - (\frac{\sum((predicted-observed)^2)}{\sum(observed-mean(observed)^2)}) \quad \text{Equation 10}$$

The measures were calculated and plotted in R. Then potential autocorrelation between hourly observations was investigated using time series analysis. A periodicity component with a first-order autocorrelation was found in the data. A function to model sines and cosines was created to model the periodicity in the data. Six models were created with frequencies of one, two, three, four, six, and nine cycles per day. The six models and a null were ranked with AICc. The best model was presented to investigate the temporal errors and bias between *Heat Source* and DTS observations.

Riparian Reforestation

By varying forest canopy height and density in *Heat Source,* three scenarios were run to investigate the interactions between riparian vegetation and stream temperature. They included: 1) no forest, 2) partly forested, and 3) fully forested. The no forest condition was used to simulate a catastrophic wildfire, a worst case scenario, which burned both upland and riparian vegetation. All vegetation heights and densities were set to zero. The partly forested conditions increased areas classified as “rock” (no height and

no density) to small mixed stand conditions (12 m height, 70 % density) and "willow/shrub/rock" (2 m height, 45 % density) to small conifer stand conditions (12 m height and 45 % density). Fully forested increased "rock" and "willow/shrub/rock" areas to large mixed stand conditions (24 m height and 70 % density) and small conifer stand areas to large conifer stand conditions (27 m height, 70 % density). The fully forested condition was used to simulate stand conditions at the end of this century (*i.e.* 2099), where the partially forested stand and existing small conifers grow in height and density. All three models were compared to the "base model" which was calibrated to observed conditions over the study period (Figure 11). *Heat Source* energy flux output was compared between the base model and reforested scenarios to further investigate changes in heat flux within the system due to reforesting.

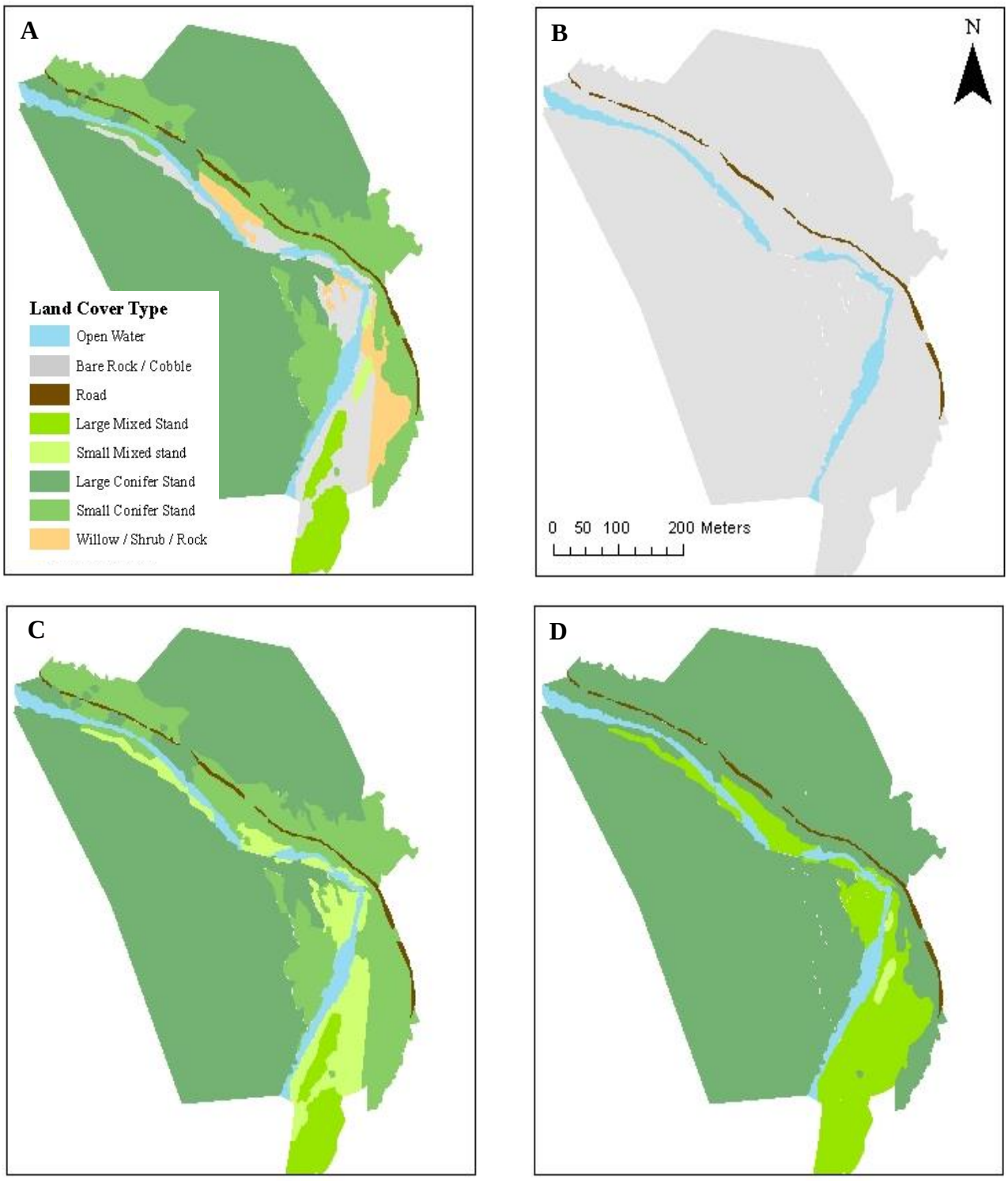

Figure 11. Vegetation maps of A) Base model, B) no forest, C) partly forested, and D) fully forested. Note how the bare cobble (grey area) and willow/brush/rock (light orange) varies.

Channel Geometry Restoration

Heat Source was used to investigate if changing the channel geometry of Run1, a particularly wide and shallow run, could reduce stream temperature downstream. By reducing channel bottom width (the primary channel measurement used in *Heat Source* hydraulic simulations) I hypothesize that stream surface area that receives solar radiation would also be reduced, thereby buffering stream temperatures. Reducing stream surface area increases channel depth, reducing how far solar radiation can penetrate the water column which in turn reduces streambed conduction. We explored two possible scenarios where the channel bottom width of Run 1 was reduced from 32.5 m to 27 m and 20 m respectively. The 27 m scenario reflects the widths of Riffles 1 and 2 in the study reach. The 20 meter scenario is similar to the most downstream habitat units. Again both scenarios were compared to the base model.

Predicting Thermal Impacts from Climate Change

Three climate change scenarios were simulated and compared to the base model (Table 5). Air temperature was increased uniformly (*i.e.* spatially and temporally) to reflect forecasted climate warming while all other parameters (*i.e.* meteorological and morphological parameters) remained unchanged (Null *et al.* 2013). It is important to note that, our study did not change *Heat Source*'s boundary stream temperature condition to reflect climate change rather we used current conditions used in the other modeling scenarios in this section. Climate warming of 2 °C, 4 °C, and 6 °C were within the range

forecasted by climate models for California and represent progressive warming through the end of the 21st century (Dettinger *et al.* 2004, Hayhoe *et al.* 2004). HadCM3 and PCM climate models have been used extensively to downscale climate change predictions to California. Both climate models have been important in investigating changes in precipitation and stream temperature in California's Sierra Nevada.

Table 5. Table of mean annual air temperature increase with associated climate models, emissions scenarios, and time horizons (Null *et al.* 2013).

Mean annual air temperature increase	Model	Emission Scenario	Time Horizon
+ 2 °C	HadCM3*	A1FI (higher emissions)	2020–2049
	PCM+	B1 (lower emissions)	2070–2099
+ 4 °C	PCM	A1FI (higher emissions)	2070–2099
+ 6 °C	HadCM3	A1FI (higher emissions)	2070–2099

*= HadCM3 is the medium-sensitivity U.K. Met Office Hadley Centre Climate Model version 3 (Hayhoe *et al.* 2004).

+= PCM is the low-sensitivity National Center for Atmospheric Research/Department of Energy Parallel Climate Model (Dettinger *et al.* 2004, Hayhoe *et al.* 2004).

Ameliorating Elevated Stream Temperature from Climate Change.

Previous ecological restoration strategies have emphasized the need to return to historical reference conditions. This has been complicated by the onset of climate change. Restoration practitioners need to restore ecosystem function as well as adapt to climate change and enhance ecological resilience (Millar *et al.* 2007, Heller and Zavaleta 2008). Ameliorating climate change through land management practices is an important area of research. By modeling climate and restoration scenarios, land managers can be more

informed about not only the magnitude of expected warming but also the magnitude of warming that might be offset by management actions (Seavy *et al.* 2009). Modeled scenarios included partial and fully forested conditions (described in Riparian Reforestation) with uniform increase of 2 °C, 4 °C, and 6 °C in air temperature. These scenarios were then compared to both the base model (2012 condition) and the climate change scenarios in the previous section.

A sensitivity analysis was run to investigate if initial boundary conditions constrained *Heat Source* predictions. Simulated boundary conditions for climate warming scenarios was unknown. A uniform increase by 2 ºC of stream temperature boundary condition was chosen. Climate warming and warming with reforestation scenarios were then compared as described above.

RESULTS

Physical Impacts on Salmonids

Study Site Thermal Regime

Water temperature over the study period ranged between 16 and 23 °C (Figure 12). The weather was mostly clear and sunny. The MWMT and MWAT over the study period were 23.00 ºC and 19.47 ºC respectively. No difference was found between averaging the first seven whole days versus averaging the second though 8th whole day. Mean channel daily maximum exceeded 21 ºC seven of the eight days monitored (Figure 13). The DTS profiled showed homogeneous temperature along the study reach with slightly higher daily maximum temperatures in the upstream half of the reach primarily along Run 1 (Figure 14). A spring was identified below Pool 2 (arrow in Figure 14) but no mainstem cooling, or a plume of cold-water was detected. The spring flow was quantified and is discussed in further detail in the following section (Quantifying a Groundwater Spring).

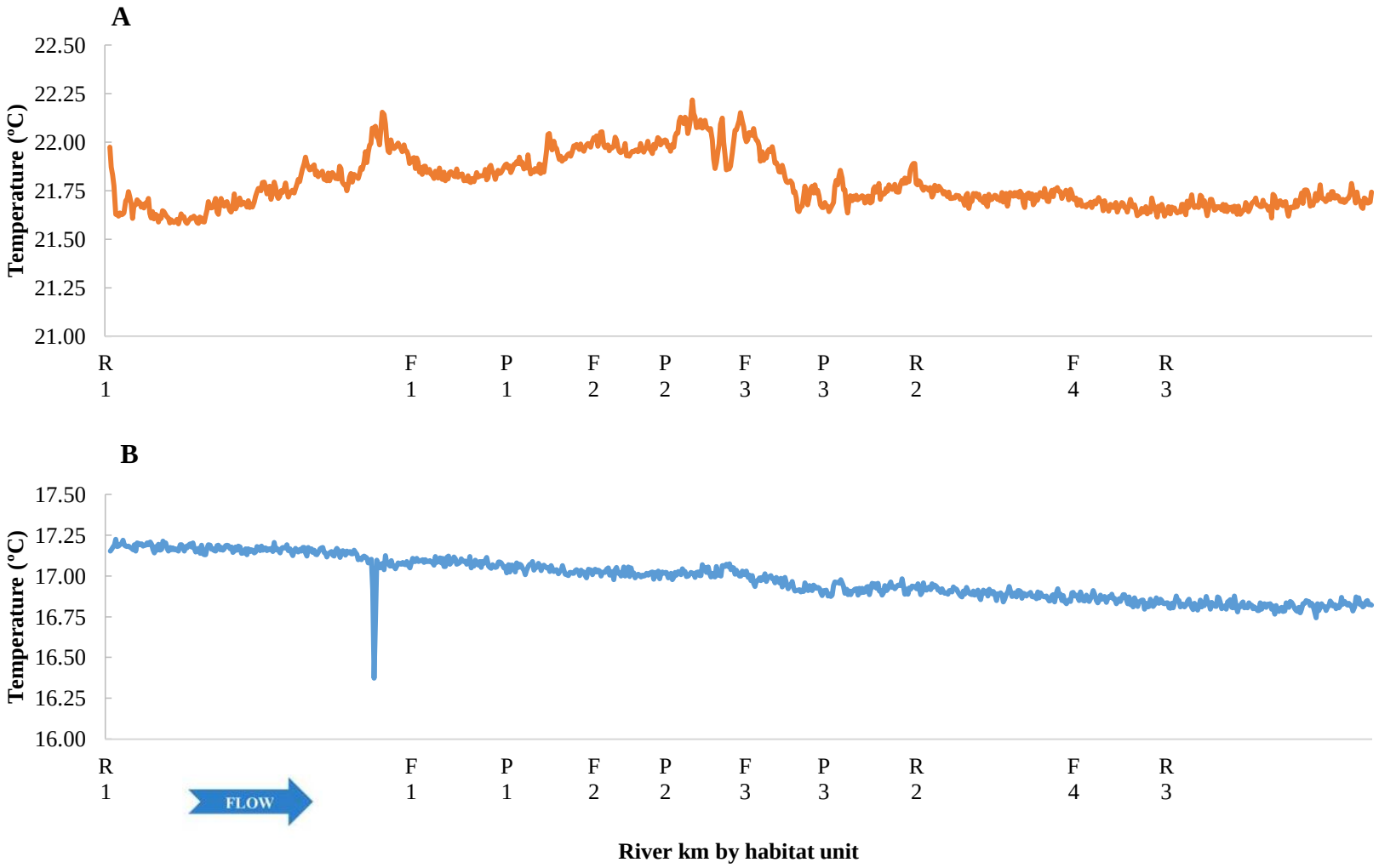

Figure 12. Temperature profile of A) daily maximum and B) daily minimum over the study reach for July 24, 2012, Salmon River, CA, USA. Habitat unit notation include R = run, F = riffle, and P = pool. The valley in the minimum temperature profile at the bottom of Run 1 is possibly an inflow from Kelley's Gulch, which was dry during the day and missing from the maximum profile.

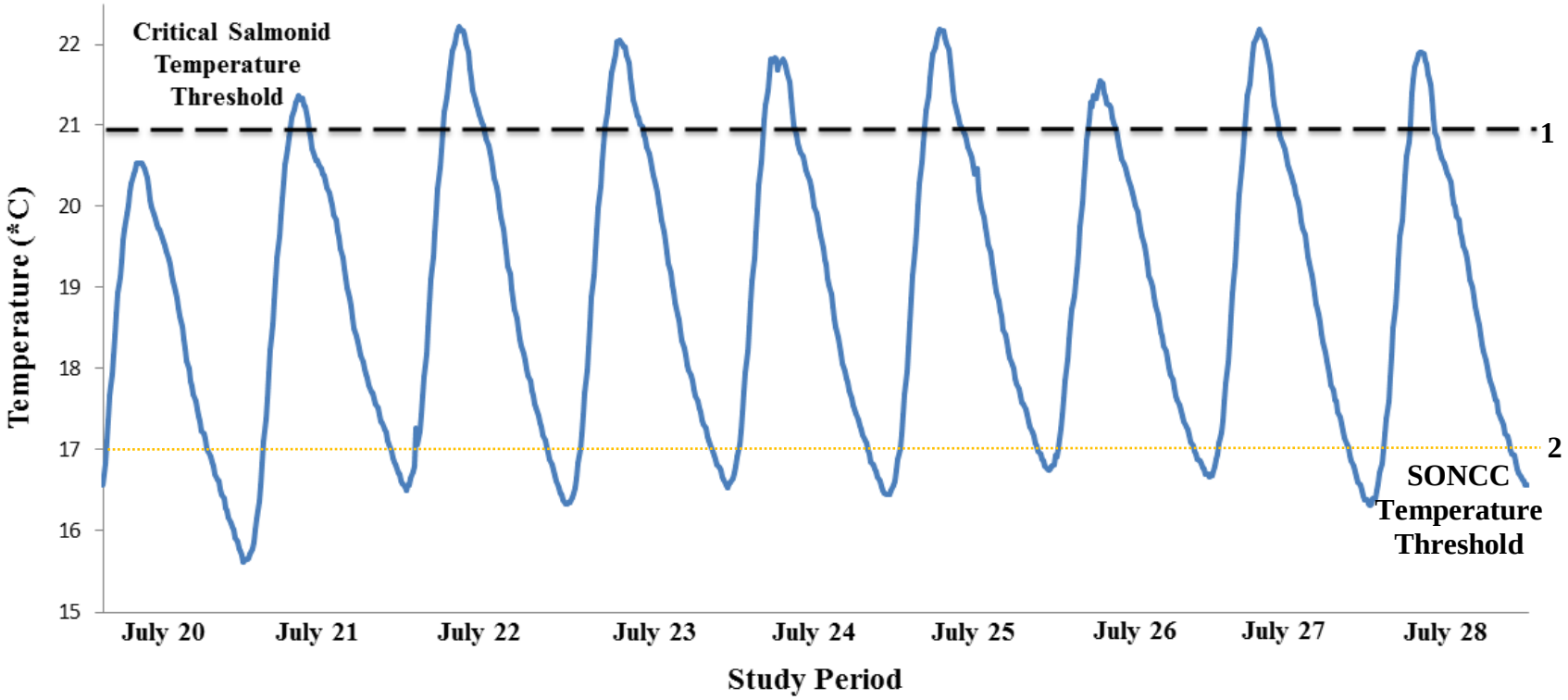

Figure 13. Mean reach temperature profile (solid line) over the study period, July 2012, Salmon River, CA, USA, with 1) the critical salmonid temperature threshold of 21 °C (large dashed line) and 2) National Marine Fisheries Service SONCC temperature threshold 17 °C (small dotted line) above which is considered detrimental to coho salmon (NMFS 2012).

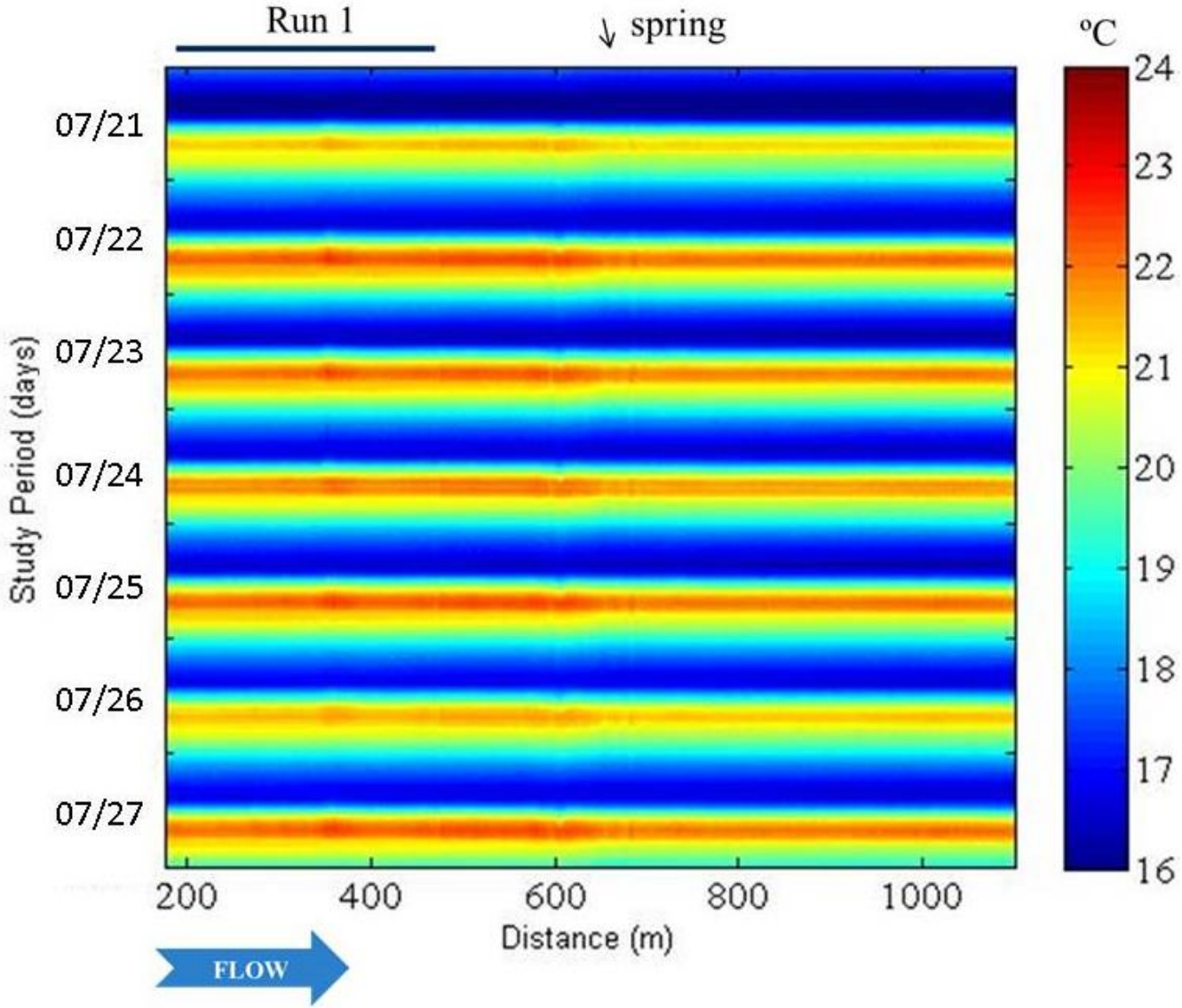

Figure 14. Temperature profile captured over study period Salmon River, CA, USA, July 2012. The first half of the graph shows daily maximum temperatures up to 23 ºC (red) corresponding with Run 1. A spring was also identified below Pool 2 (arrow) but it did not significantly cool the mainstem.

Salmonid Distribution

To investigate which stream parameters best described salmonid distribution, eight hypotheses were proposed. Hypotheses were ranked based on the lowest Log Likelihood values and corresponding Akaike Information Criterion (AICc) values. The AICc analysis provided strong evidence that depth was the single most important predictor of salmonid counts (Table 6, Table 7). However, the best model for total count included both temperature and depth, and this model carried over 74 % of the model weight. The best model for salmon count included depth as the only predictor, and this model carried over 63 % of the model weight. For both response variables, the coefficient on log-transformed depth was positive (Table 8, Table 9), indicating that higher counts occurred in units with greater depth. In the model explaining total count, the coefficient on temperature was positive, indicating higher counts in units with warmer water temperatures. Residual analysis of the AICc-best models showed reasonable adherence to model assumptions, given the small sample size (Figure 15).

The best models for mean fish counts were:

$$\text{Total Count} = e^{(-2.2553 + (0.3 * \text{Temp}))} \text{Depth}^{1.37} \quad \text{Equation 11}$$

$$\text{Salmon Count} = e^{2.5808} \text{Depth}^{1.92} \quad \text{Equation 12}$$

The relationship between count and depth is a power function because both variables were log-transformed (Figure 16).

Table 6. Ranking of hypotheses for Total Count using Akaike's Information Criterion.

Model Number	Description	Number Parameters	logL	AICc	ΔAICc	Weight
H5	Temp. & Depth	4	-0.3231	16.6461	0	0.7466
H3	Depth	3	-4.5663	19.1326	2.49	0.2154
H2	Channel type	4	-3.4368	22.8737	6.22	0.0332
H6	Temp. & C Type	5	-1.1646	27.3291	10.68	0.0036
H4	Depth & C Type	5	-2.7256	30.4512	13.805	0.0008
H8	Null	2	-13.0559	31.8261	15.18	0.0004
H1	Temperature	3	-12.3679	34.7357	18.09	0.0001
H7	Temp, Depth, & C Type	6	1.454	37.0921	20.44	0

Table 7. Ranking of hypotheses for Salmon Count using Akaike's Information Criterion.

Model Number	Description	Number Parameters	logL	AICc	ΔAICc	Weight
H3	Depth	3	-13.1062	36.2123	0	0.6352
H2	Channel Type	4	-11.3111	38.6222	2.41	0.1904
H6	Temp. & C Type	5	-7.8491	40.6983	4.49	0.0674
H8	Null	2	-17.7716	41.2576	5.05	0.051
H5	Temp. & Depth	4	-12.7241	41.4483	5.24	0.0463
H1	Temperature	3	-17.5669	45.1337	8.92	0.0073
H4	Depth & C Type	5	-11.2226	47.4452	11.23	0.0023
H7	Temp, Depth, & C Type	6	-6.8991	53.7983	17.59	0.0001

Table 8. Coefficient table for AICc best model for Total Count.

Coefficient	Estimate	Std. Error	t value	Pr(>|t|)
Intercept	-2.2553	2.0279	-1.112	0.3028
Temp [ºC]	0.3074	0.1005	3.059	0.0184
log(lmaxdepth) [m]	1.3715	0.1629	8.418	6.58E-05

Table 9. Coefficient table for AICc best model for Salmon Count.

Coefficient	Estimate	Std. Error	t value	Pr(>|t|)
Intercept	2.5808	0.3199	8.068	4.11E-05
log(lmaxdepth) [m]	1.9209	0.5468	3.513	0.00793

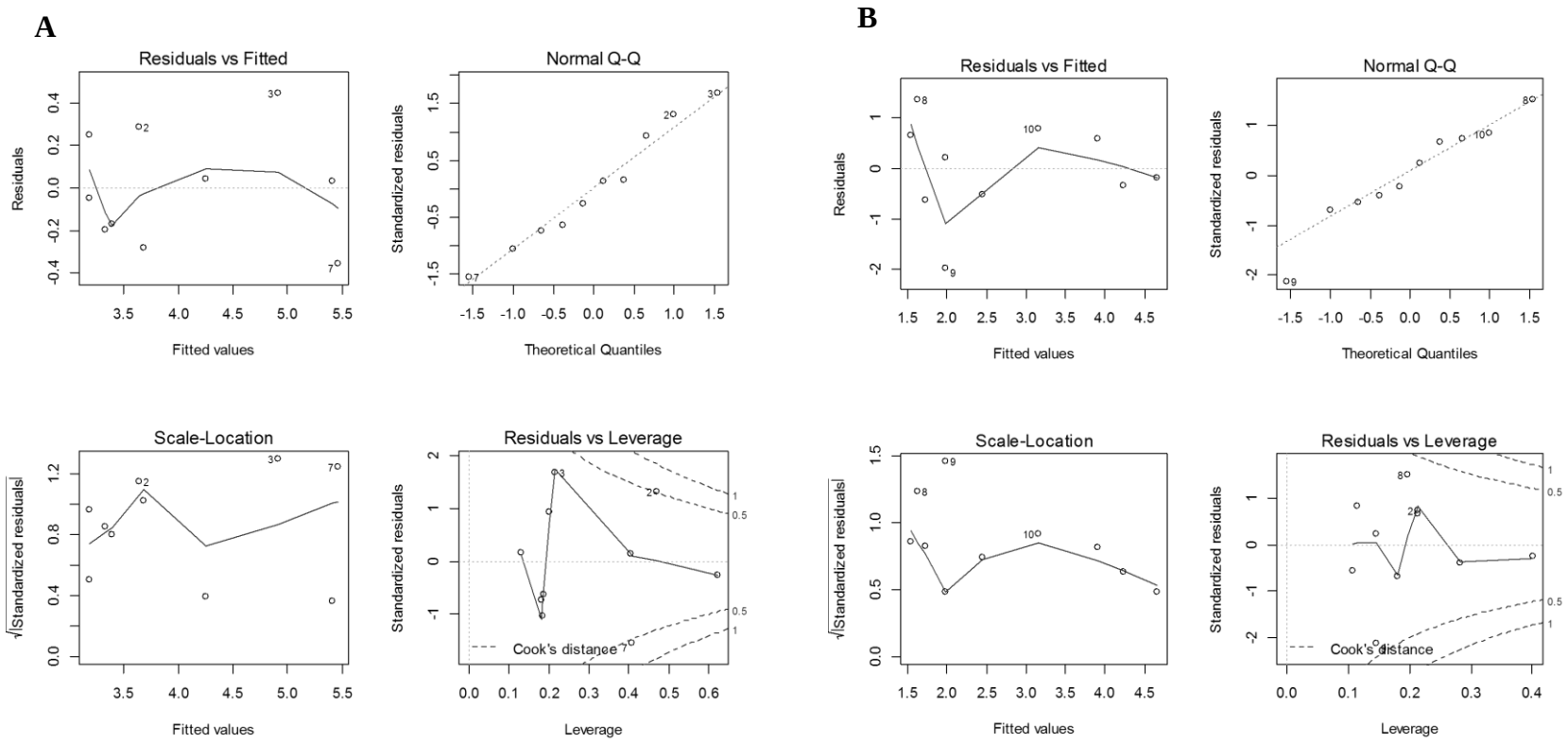

Figure 15. Residual plots of the AICc-best model for A) Total Count (H5: Fish count was a function of temperature and maximum depth) and B) Salmon Count (H3: Fish count was a function of maximum depth).

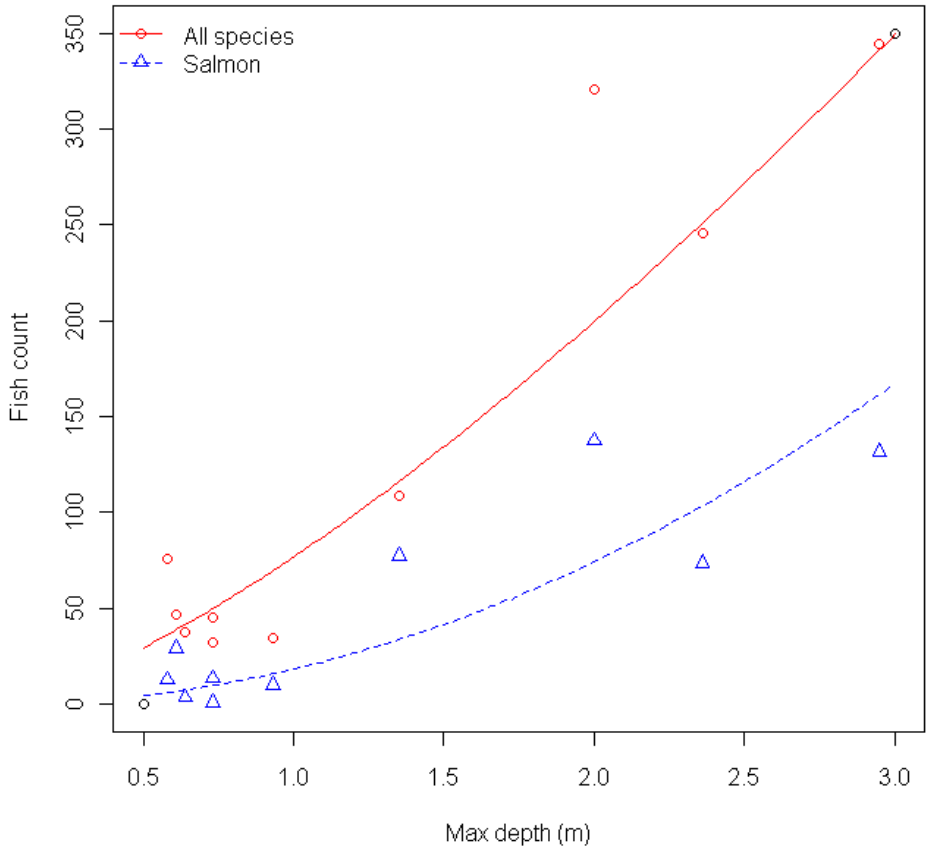

Figure 16. Salmonid count in response to max depth at mean survey temperature of 20.16 °C. The red line is the combined response of the three species and the blue dashed line is coho and Chinook count. The difference in the two lines is assumed to be rainbow trout.

Salmonid Habitat

Channel geometry measurements show that pools are deep and narrow, runs are wide and shallow and riffles are somewhere in between (Table 10, Figure 1). Habitat measures are presented with ± standard error. Overall, pools were the least common habitat type (18 % of reach). Riparian and total shade did not differ between habitat types (reach average 16 % ± 4 % and 22 % ± 5 % respectively). The study reach mean particle

size (D_{50}) was 72 ± 10 mm, and D_{83} was 160 ± 21 mm. Mean bankfull width and mean bankfull width-to-depth ratio did not differ between habitat units (26.34 ± 2.28 m and 24 ± 4 m respectively). Mean bankfull depth did vary between Riffles and Pools (1.09 ± 0.15 m and 1.79 ± 0.44 m respectively).

Pools had the greatest mean wetted and mean wetted maximum depths (1.02 ± 0.13 m and 2.44 ± 0.34 m respectively). Runs had the largest mean wetted width (20.08 ± 4.65 m) and shallowest mean wetted depth (0.54 ± 0.09 m). Riffle measurements were mostly between pools and runs and had the shallowest mean maximum depth (0.67 ± 0.04 m). The study reach mean wetted width-to-depth ratio was 41 ± 12.

Random cross-sections for each habitat type revealed that Run 1 was particularly wide and shallow whose length was about a fourth of the entire study site (Figure 16, Figure 3). Pools were generally v-shaped while riffles were difficult to profile due to the boulder/cobble bottom.

Most habitat characteristics in the study reach where dramatically different from optimal conditions cited in the literature (Table 11). The study reach was primarily fast water habitat. Pools were created and maintained by bedrock scour also known as "swing pools" (Lisle 1986) and comprised 18 % of the study reach. The fast water-to-slow water ratio was 6.3:1. The study reach had no large wood debris (LWD) in the channel. Pools had a bankfull width:depth ratio and standard error of 19 ± 9, while the study reach had a mean bankfull width:depth ratio of 24 ± 4. Pool mean wetted depth and standard error was 1.02 ± 0.13 m, and maximum wetted depth was 2.44 ± 0.34 m. Average wetted pool area and volume at the time of the study were 944.36 m^2 and 953.80 m^3 respectively.

Table 10. Summary of channel geomorphology over the study reach by habitat type with standard errors in parentheses, Salmon River, CA, USA, July 2012. Wetted width was based on flow conditions over the study period.

Stream Parameter	**Run**		**Riffle**		**Pool**		**Reach Ave.**	
n	3		4		3		10	
Habitat by length in reach [%]	53 %		29 %		18 %			
Mean Riparian Shade [%]	12 %	(6 %)	20 %	(6 %)	16 %	(13%)	16 %	(4 %)
Mean Total Shade [%]	18 %	(7 %)	21 %	(7 %)	27 %	(13%)	22 %	(5 %)
D_{50} [mm]							72	(10)
D_{83} [mm]							160	(21)
Mean Bankfull Width [m]	26.62	(4.39)	25.15	(4.85)	27.65	(3.06)	26.34	(2.28)
Mean Bankfull Depth [m]	0.97	(0.25)	1.09	(0.15)	1.79	(0.44)	1.26	(0.18)
Mean Bankfull Width-to-depth ratio	31	(10)	22	(4)	19	(9)	24	(4)
Mean Wetted Width [m]	20.10	(4.65)	12.84	(2.99)	14.38	(0.84)	16.52	(1.21)
Mean Wetted Depth [m]	0.54	(0.09)	0.34	(0.03)	1.02	(0.13)	0.603	(0.06)
Mean Max Wetted Depth [m]	0.96	(0.21)	0.67	(0.04)	2.44	(0.34)	1.29	(0.27)
Mean Wetted Width-to-depth ratio	56	(24)	48	(23)	18	(2)	41	(12)

Table 11. Summary of salmonid habitat conditions in study reach compared to optimal conditions in the literature, Salmon River, CA, USA, July 2012.

Salmonid Habitat Characteristics	**Study Reach**	**Optimal**	**Citation**
Percentage pools in reach [%]	18 %	30 % 40 – 60 %*	Flosi *et al.* (2010) McMahon (1983)
Fast-water to slow-water ratio	6.3:1	1:1	Reiser and Bjornn (1979)
LWD per kilometer	0	12	PACFISH/ INFISH RMO+
Mean Bankfull Width-to-depth ratio	24**	< 10	PACFISH/ INFISH RMO+
Mean Total Shade [%]	22 %**	50 – 75 %*	McMahon (1983)

*= denotes criteria specific to coho (*Oncorhynchus kisutch*).
+= Riparian Management Objective (RMO) criteria cited in Henderson *et al.* (2005).
**=Standard error for mean bankfull width/depth ratio, mean total shade, and mean pool depth was 4, 5 % and 0.13 m respectively.

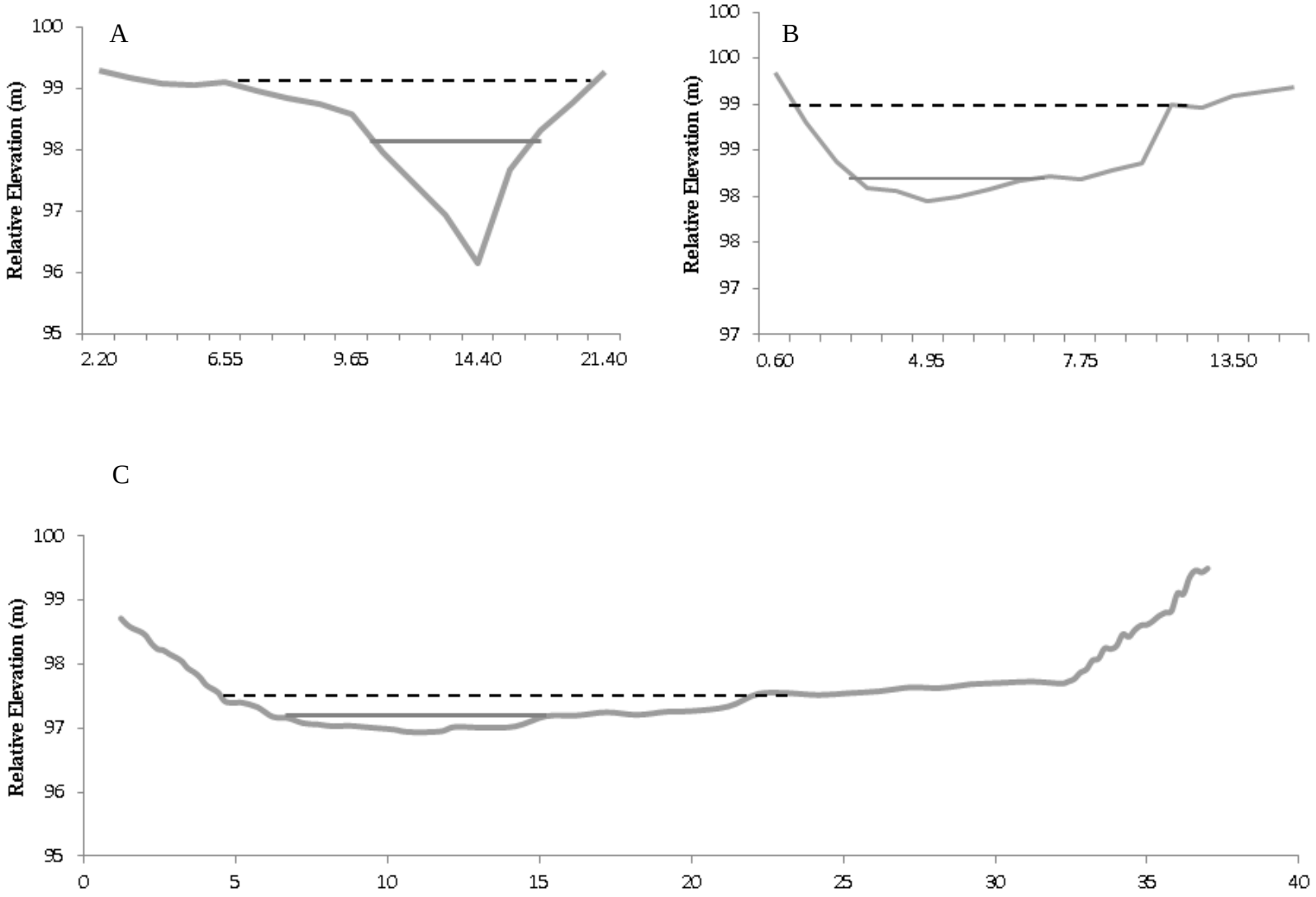

Figure 17. Characteristic habitat cross sections for A) pool and B) riffles and C) the largest run (Run 1), Salmon River, CA, USA, July 2012.

Quantifying a Groundwater Spring

During the study period, a spring was found at the tailwater of habitat unit Pool 2 (Figure 18). The spring temperature varied from 16 - 18 °C, while the peak mainstem temperature above the spring reached a maximum of 23 °C. The mean spring temperature was 17.21 ± 0.21 ºC and slowly warmed over the study period (Figure 19). The upstream and downstream sections of the mainstem were in phase with each other (*i.e.* minimum and maximums were at the same time), indicating that the spring was an inflow of groundwater and not hyporheic discharge (Collier 2008). The mainstem temperature downstream of the spring was slightly reduced, a difference of 0.35 ± 0.04 ºC compared to the upstream temperature (Table 12), which was difficult to discern from the DTS profile (Figure 14). The average mainstem flow was 1.05 ± 0.10 m^3s^{-1} (35.64 cfs) over the study period. Using equations 2 - 4, the spring's flow was calculated as 0.08 ± 0.01 m^3s^{-1} (2.63 cfs); 7.30% ± 1.16% of mainstem flow. Small scale effects from the spring were not detected by DTS because the cable was in the thalweg of the channel.

Figure 18. Photo of spring location (white oval) spilling into Pool 2, Salmon River, CA, USA. View is looking upstream.

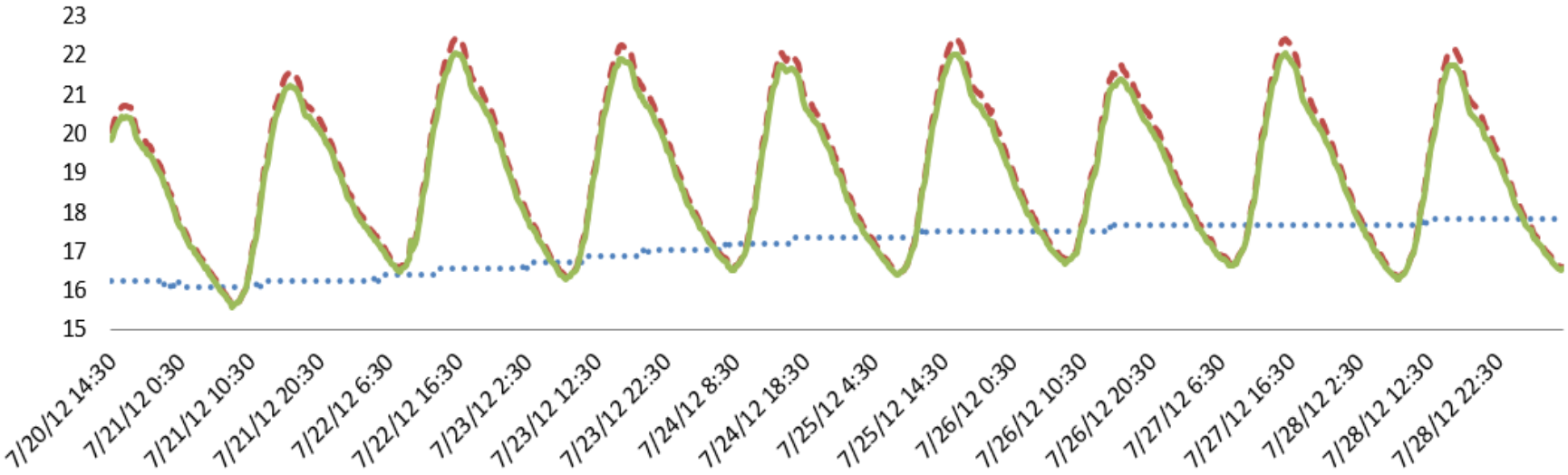

Figure 19. Mean temperature comparison between the mainstem upstream (red dashed line). Mainstem downstream (solid green line) and the spring (blue dotted line), Salmon River, CA, USA, July 2012.

Table 12. Spring inflow calculation over the study period Salmon River, CA, USA, July 2012.

Calculation Parameter	July 20	July 21	July 22	July 23	July 24	July 25	July 26	July 27	July 28	AVE	SE
Average Daily Maximum Temperature Upstream (°C)	20.72	21.52	22.38	22.18	22.03	22.31	21.54	22.21	22.04	22.03	(0.18)
Average Daily Maximum Temperature Downstream (°C)	20.43	21.19	22.02	22.83	21.67	21.92	21.26	21.83	21.66	21.67	(0.22)
Spring Temperature at Daily Maximum (°C)	16.24	16.24	16.56	16.88	17.35	17.51	17.67	17.67	17.83	17.21	(0.21)
Difference in temperature between Upstream and Downstream (°C)	0.29	0.33	0.36	0.35	0.37	0.39	0.28	0.38	0.38	0.35	(0.01)
Difference in temperature between Spring and Downstream (°C)	4.19	4.95	5.46	4.95	4.32	4.41	3.59	4.16	3.83	4.46	(0.20)
Average mainstem streamflow (m^3s^{-1})	1.24	1.04	1.17	1.07	1.06	0.94	0.97	0.95	1.01	1.05	(0.03)
Percent streamflow attributed to spring inflow	6.45 %	5.77 %	5.98 %	7.48 %	7.55 %	7.75 %	8.25 %	9.47 %	6.93 %	**7.30 %**	**(0.39%)**
Volumetric spring inflow (m^3s^{-1})	0.08	0.06	0.07	0.08	0.08	0.07	0.08	0.09	0.07	**0.08**	**(0.003)**

Heat Source Modeling

Heat Source had a spatial resolution of 90 m and an hourly temporal resolution. Channel geometry measurements and meteorological conditions were used in *Heat Source* to predict stream temperature over the study reach. Sampling nodes within each habitat unit were assigned the same channel morphology quantities (Table 13).

Heat Source requires hourly streamflow, water temperatures, and meteorological condition to be set at the upstream boundary. Flow was measured twice a day, so hourly estimates over the study period were interpolated. Stream flow fluctuated over the study period, influenced by snowmelt, and had a decreasing trend (Figure 20). Hourly DTS observations corresponding with the upstream node were used for the stream temperature boundary condition (Figure 21). Meteorological conditions used in *Heat Source* calculations were collected with three eKO remote weather stations (Figure 3). Hourly eKO measurements were arithmetically averaged. Wind speed and air temperature were greatest during midday while relative humidity was greatest during the evening hours (Figure 22). Note while meteorological conditions had diel variation, variance was low between days over the study period.

Table 13. Channel geometry quantities used in *Heat Source* to simulate hydraulics.

Habitat Unit	Model Node Range	Bankfull Width [m]	Z	Bottom Width [m]
1	0 – 15	32.60	0.06	32.51
2	16 – 19	27.30	0.14	27.00
3	20 – 22	27.76	0.40	26.05
4	23 – 26	27.00	0.18	26.42
5	27 – 30	32.90	0.40	32.14
6	31 – 33	34.70	0.18	34.27
7	34 – 37	22.30	0.40	20.30
8	38 – 45	29.20	0.12	28.97
9	16 – 48	11.60	0.18	11.28
10	49 - 60	18.05	0.18	17.51

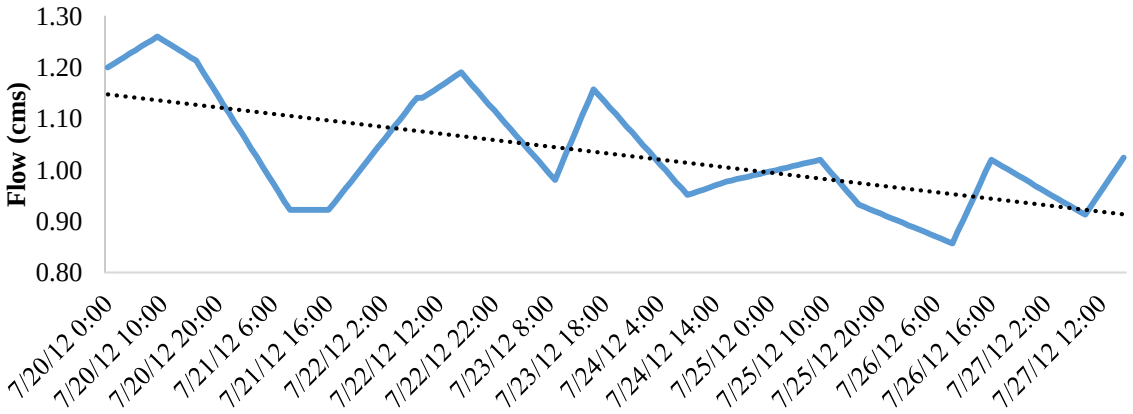

Figure 20. Mainstem flow in cubic meters per second (cms) (blue line) used in *Heat Source* to simulate hydrologic condition, July 2012, Salmon River, CA, USA. Note the diurnal fluctuation most likely from snow melt. The trend line (black dotted line) shows a decrease in mainstem flow over the study period.

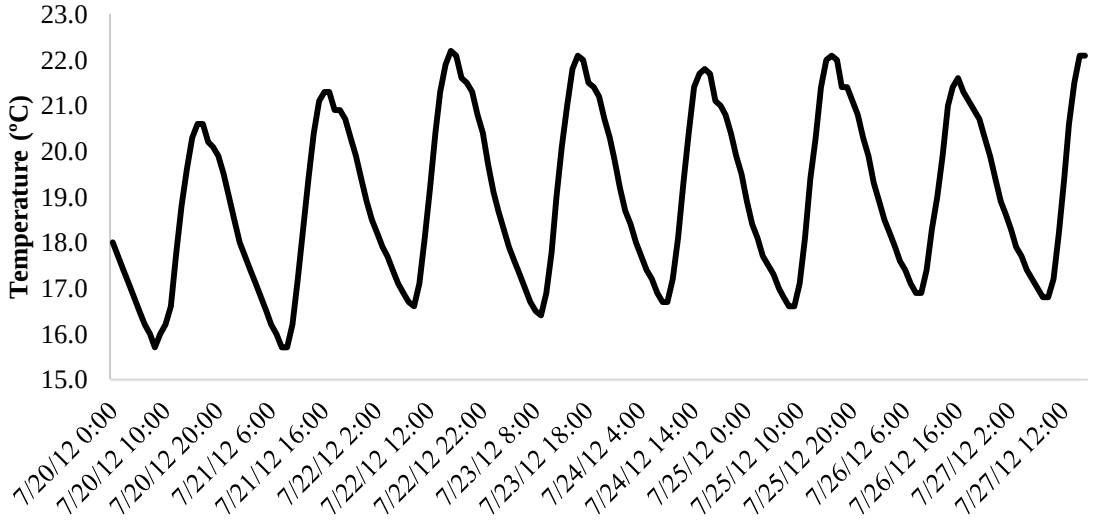

Figure 21. Profile of boundary stream temperature used in *Heat Source*, July 2012, Salmon River, CA, USA.

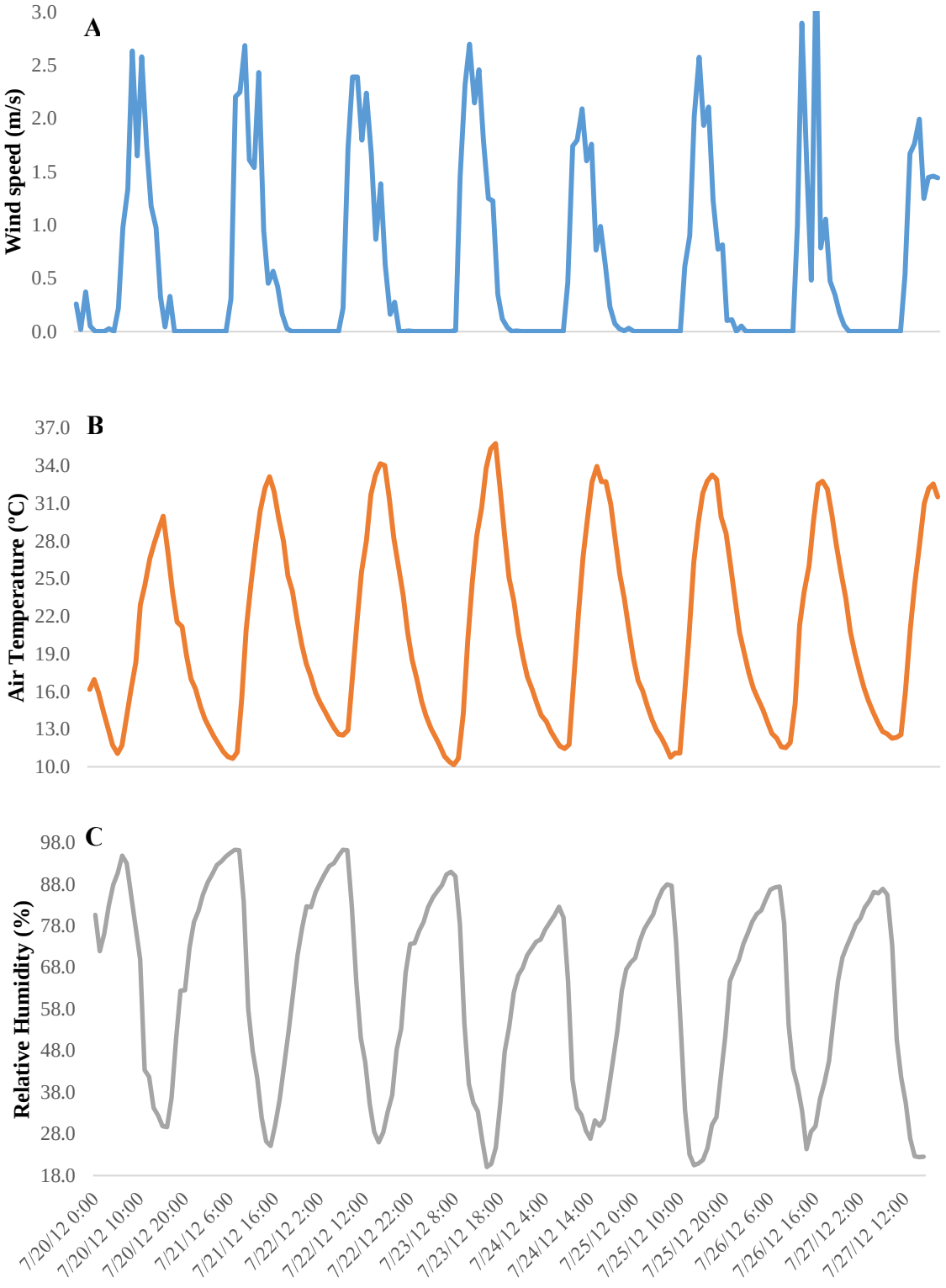

Figure 22. Mean meteorological conditions: A) wind speed, B) air temperature, and C) percent relative humidity, used in *Heat Source*, July 2012, Salmon River, CA, USA.

Heat Source Accurately Predicts Stream Temperature

Bias, root mean square error (RMSE), mean absolute relative error (MARE) and Nash-Sutcliffe Modeling Efficiency (NSE) were calculated over the four day modeled study period (Table 14). The four measures of model performance indicated a decrease in fit in a downstream direction (Figure 23).

Table 14: Mean and maximum estimates of *Heat Source* model performance.

Performance Measure	Study Mean	Study Maximum
Bias	0.032	0.099
RMSE	0.215	0.311
MARE	0.008	0.011
NSE	0.983	0.999

AICc ranking investigating the frequency of autocorrelation between temporal observations found that a model with nine cycles per day to be the best model. The best model had normal residuals with one large observation. Temporal bias was calculated as 0.075. The first-order autocorrelation coefficient was 0.693 meaning that when the model over predicted an observation it was likely to overpredict the next observation. A plot of the periodic component of the differences between *Heat Source* and DTS observations revealed that *Heat Source* over-predicted observations during midday and under-predicted observations at night (Figure 24).

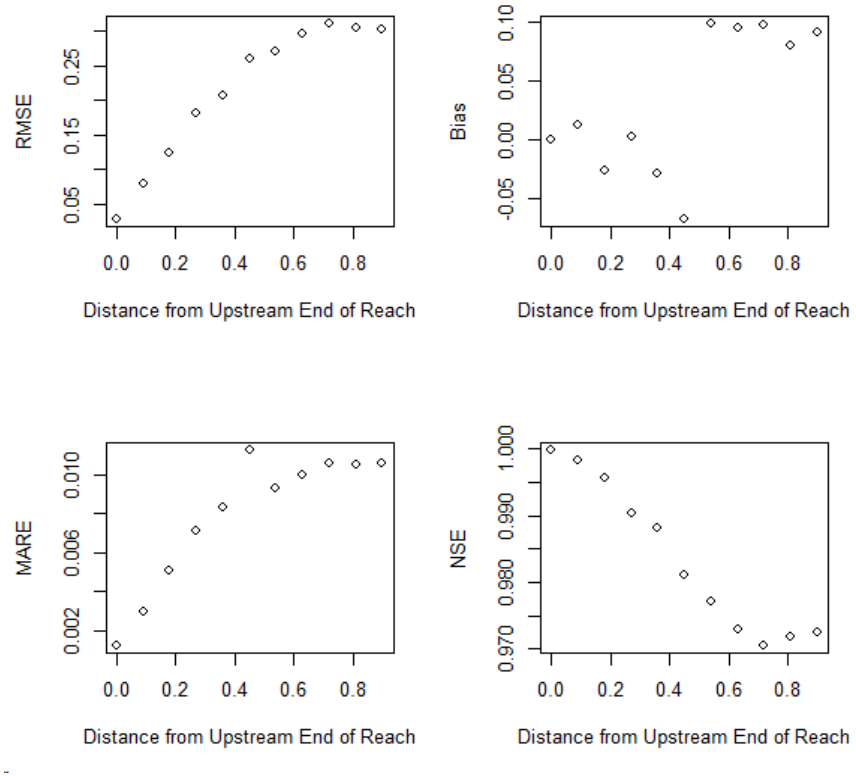

Figure 23. Four plots investigating Heat Source model performance by distance moving downstream (left to right), A) RMSE, B) Bias, C) MARE, and D) NSE, July 2012, Salmon River, CA, USA.

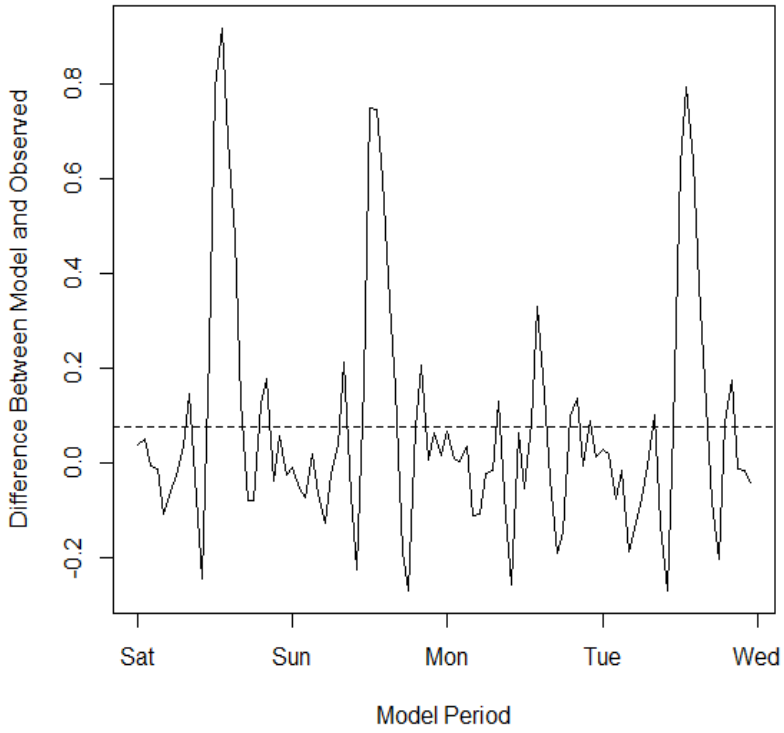

Figure 24. Plot of the periodic component of difference between Heat Source and DTS observations with mean bias (dashed line). Note how the model over-predicted during midday and under-predicted at night, July 2012, Salmon River, CA, USA.

Riparian Reforestation

Three scenarios were modeled in *Heat Source* to investigate the interactions between riparian vegetation and stream temperature. They included: 1) no forest, 2) partly forested, and 3) fully forested conditions. Effective shade calculated by *Heat Source* increased with increased vegetation height and density (Figure 24). Our results show that increasing riparian vegetation on barren areas around the stream reduces mean maximum temperature (Table 15, Figure 26, Figure 27). Cooling is similar between the scenarios, with forested conditions cooling slightly later most likely due to increased longwave radiation (discussed further below) (Figure 27).

Heat Source simulated energy flux diagrams were compared between the base model and reforested scenarios on July 22nd 2012 at model node 0.68 km to further investigate changes in heat flux within the system (Figure 28). Positive flux means the water column is being heated while negative flux means that heat is moving away from the water column (*e.g.* cooling such as evaporation and bed conduction). Overall, the energy flux diagrams look similar with solar radiation duration being shortened in the riparian reforestation scenarios, while peak radiation was the same between all three scenarios. There was no change in evaporation and air convection between the three scenarios. Variations in long wave (LW) radiation and bed conduction were detected. The daily range of LW radiation was dampened in the fully forested scenario resulting in less heat loss (*i.e.* less cooling) in the evening and more LW radiation during the day (Figure 30). Bed conduction, heat moving from the water column to the channel bed

substrate, was greater in the reforested scenarios during daily maximum temperatures.

This means that the bed stays cooler longer with greater shade from reforesting.

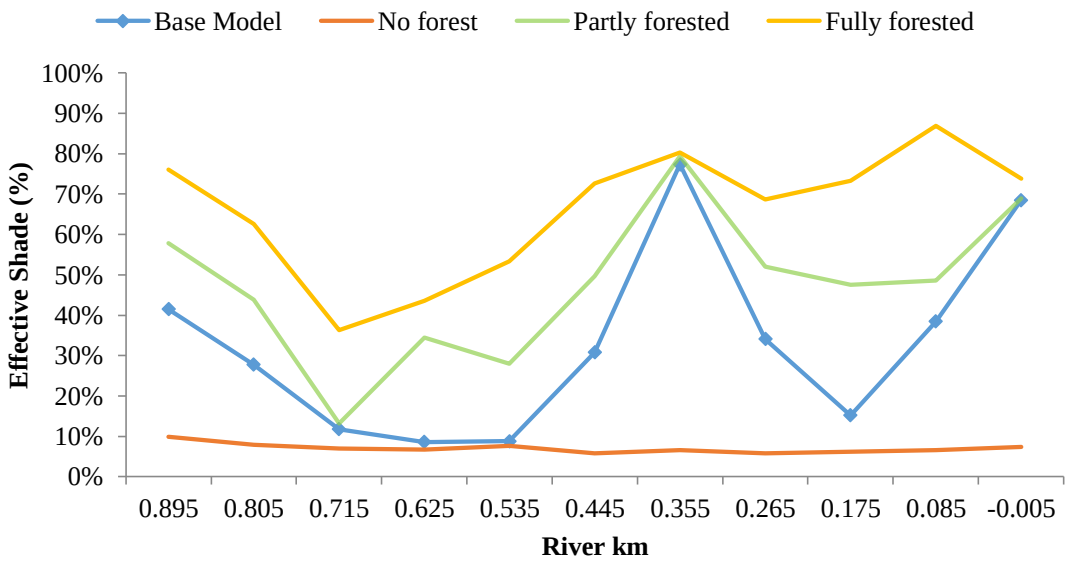

Figure 25. Effective shade calculated by *Heat Source* over the study reach for the base model, no forested condition, partly forested condition and fully forested condition, July 2012, Salmon River, CA, USA.

Table 15. Table of summary statistics of the three *Heat Source* forested scenarios compared to the base model.

Scenario	Mean Daily Max Temp. [ºC]	Mean Daily Min Temp. [ºC]	Mean Daily Duration above 21ºC [hr]
Base Model	21.57	16.09	3.8
No forest	22.21	16.14	4.4
Partly forested	21.18	16.07	2.4
Fully Forested	20.79	16.04	2.0

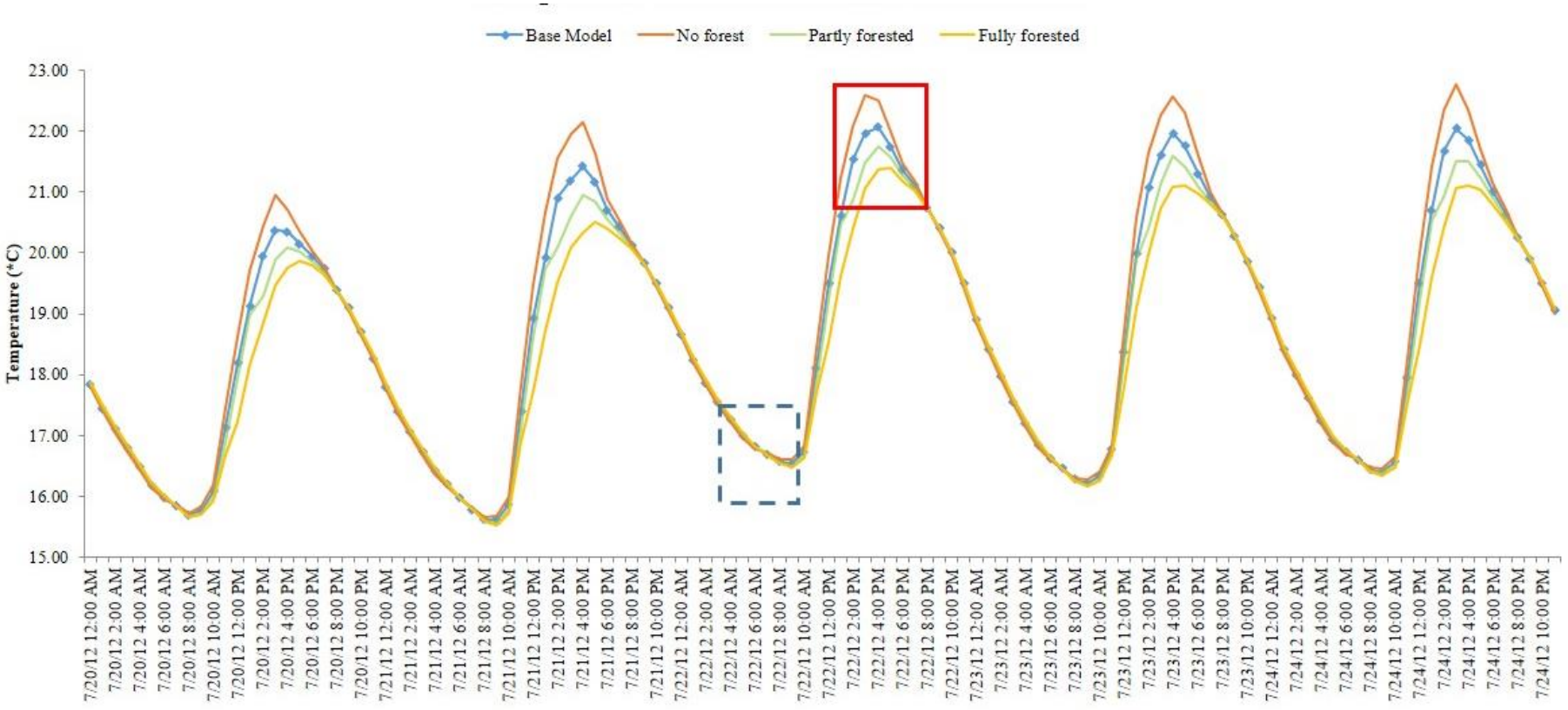

Figure 26. Thermal profile comparing reforestation scenarios at the bottom of the reach (i.e. most downstream (DS) node of *Heat Source*), using *Heat Source*, July 2012, Salmon River, CA, USA. Cooling inset (blue dashed box) and maximum temperature inset (red box) expanded in next figure.

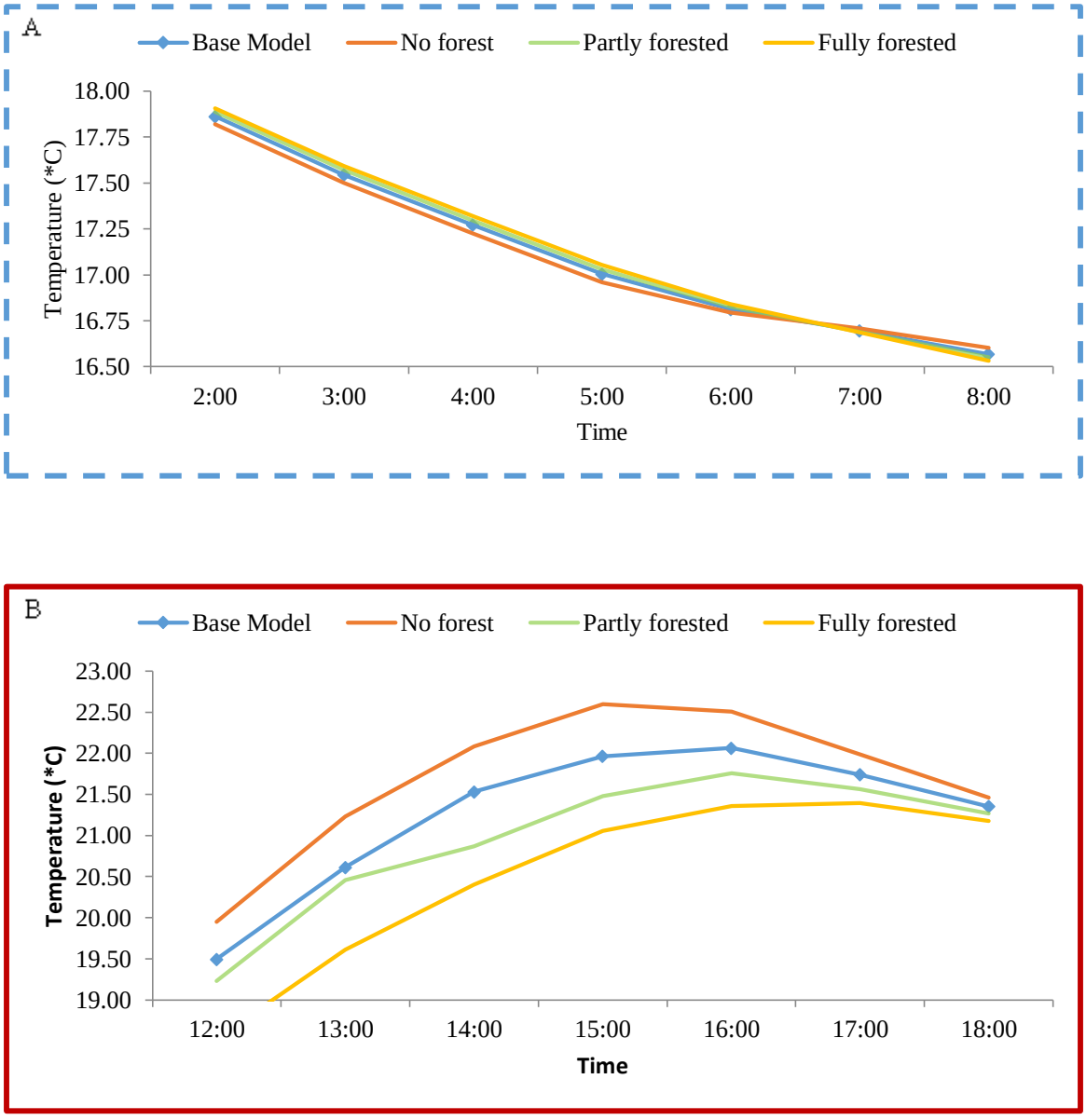

Figure 27. Thermal inset of Figure 26 comparing three forested scenarios to the base model in *Heat Source* during A) cooling between 2:00 and 8:00 and B) maximum temperature between 12:00 and 18:00 on July 22nd 2012, Salmon River, CA, USA.

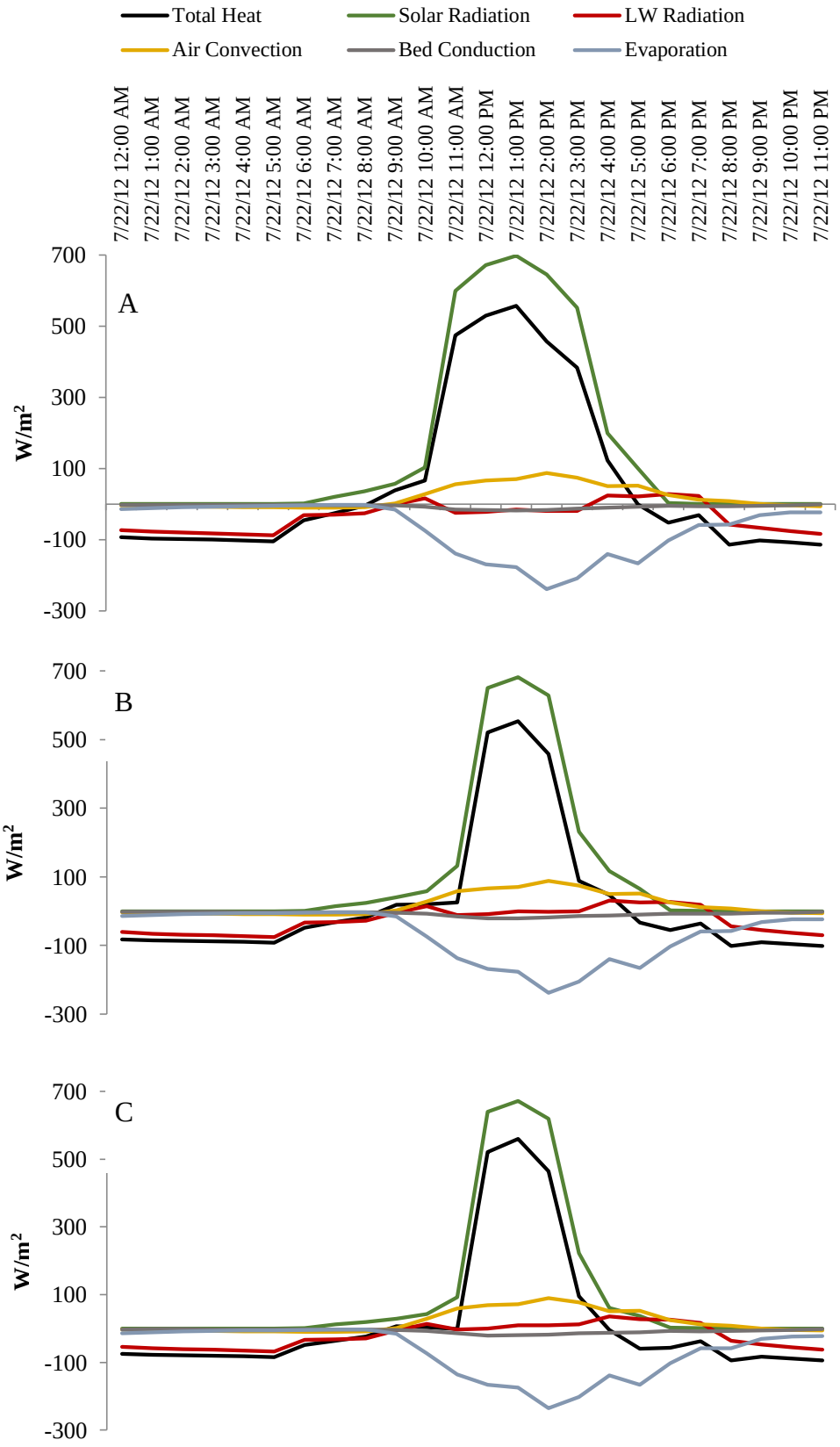

Figure 28: Energy flux diagrams created in *Heat Source* at model node 0.68 km of A) base model, B) partially forested, and C) fully forested on July 22nd 2012, Salmon River, CA, USA.

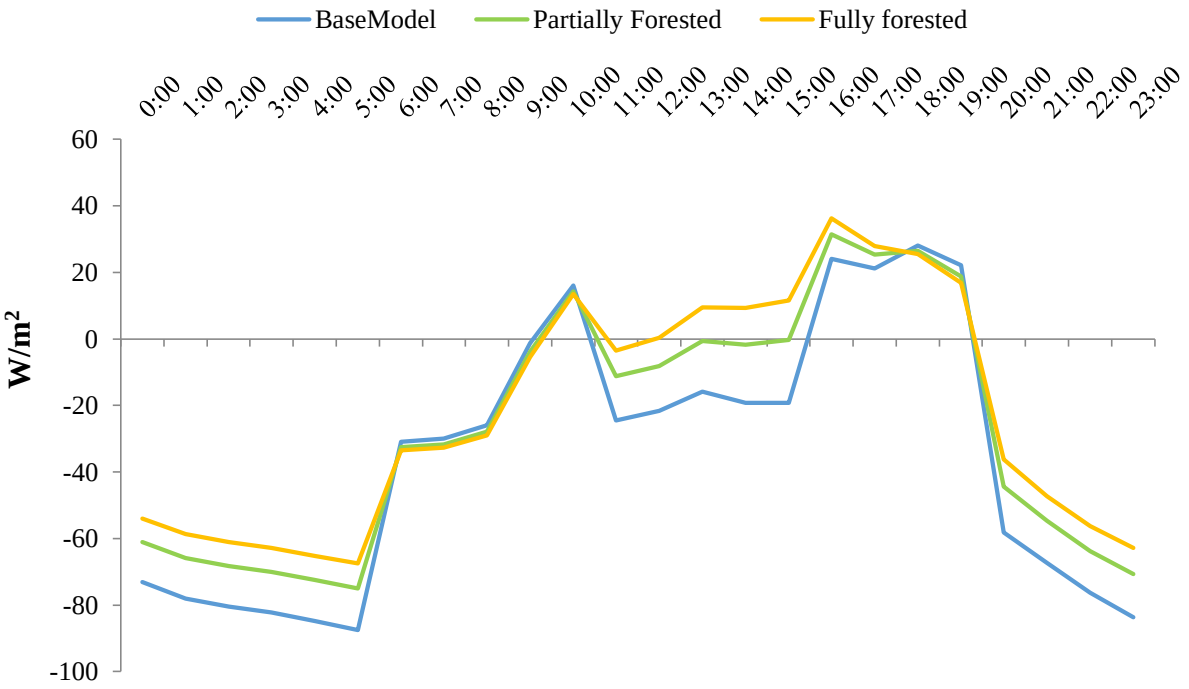

Figure 29. Temporal profile using *Heat Source* at model node 0.68 km of longwave radiation between the base model and reforestation scenarios on July 22nd 1012, Salmon River, CA, USA.

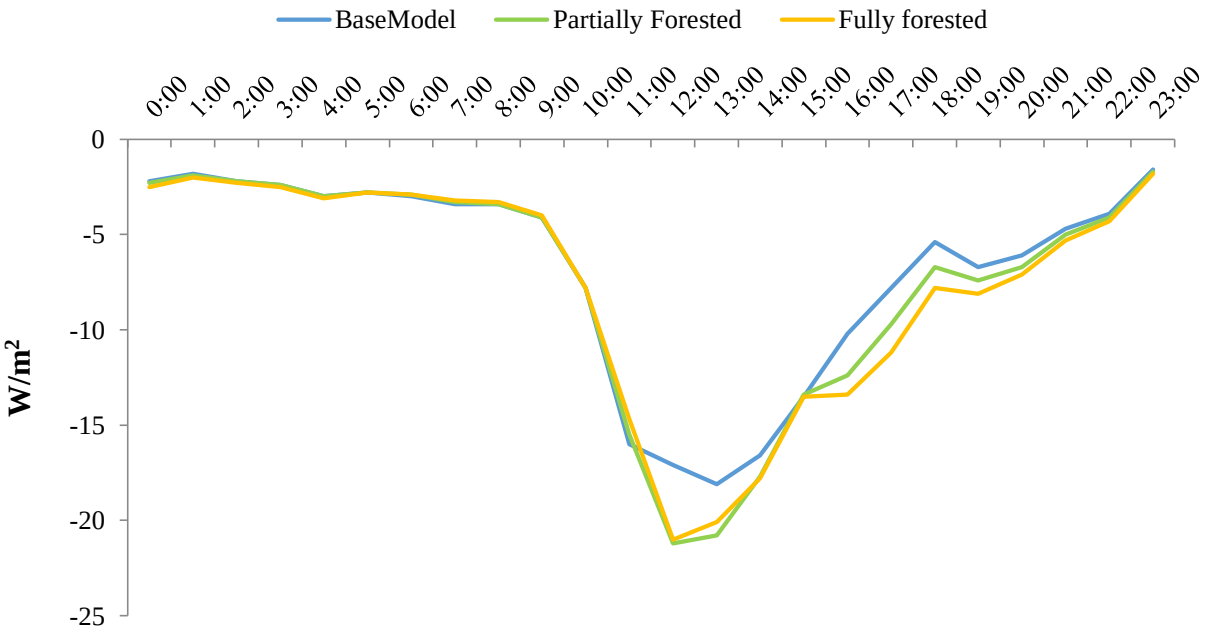

Figure 30. Temporal profile using *Heat Source* at model node 0.68 km of bed conduction between the base model and reforestation scenarios on July 22nd 1012, Salmon River, CA, USA.

Channel Geometry Restoration

The two scenarios reducing the channel bottom width of Run 1 from 32.5 m to 27 m and 20 m did not change stream temperature seen at the bottom of the reach (Figure 31). Reducing channel bottom width did however reduce the rate of heating in the treatment area by a mean 0.01 ºC/90 m and a maximum of 0.03 ºC/90 m over approximately 300 m in length (Figure 32). The maximum estimate is a relative reduction in the rate of heating by 34 %.

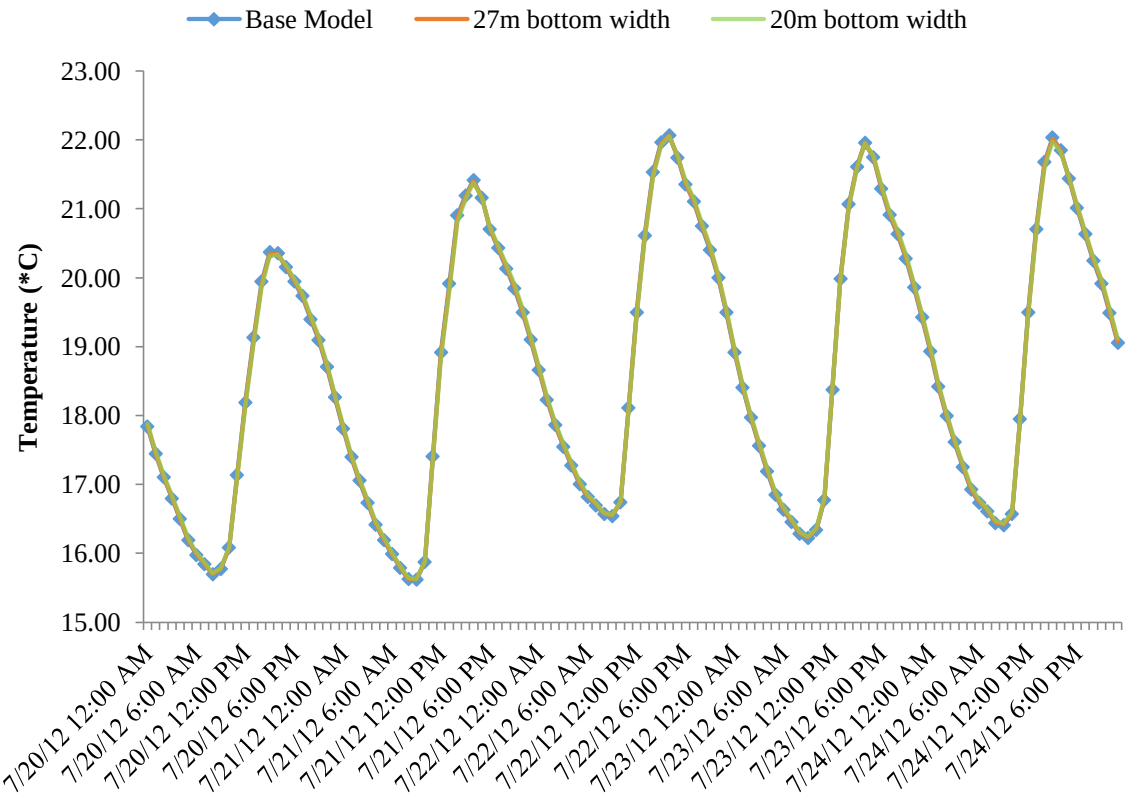

Figure 31. Thermal profile comparing channel restoration scenarios to the base model at the bottom of the reach, *Heat Source*, July 2012, Salmon River, CA, USA. Note there is no difference between the scenarios.

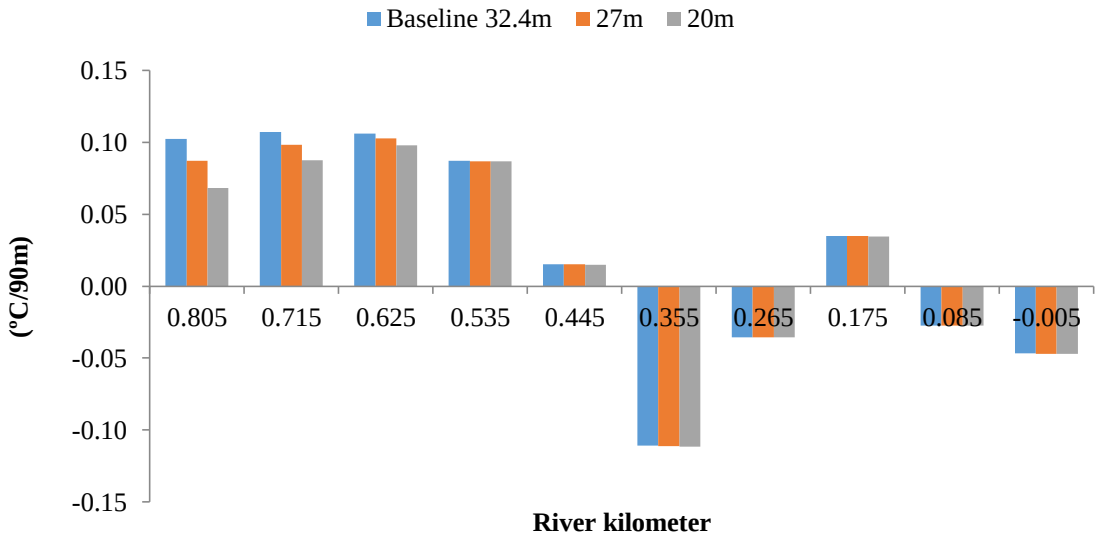

Figure 32. Rate of heating at daily maximum (14:00) July 22nd 2012 over the study reach, Salmon River, CA, USA. Flow is left to right. Note that river kilometers 0.805 and 0.715 vary in heating rate with a decrease in bottom width decreasing the rate of heating. Both river kilometer markers are within the treatment area. The downstream section of the reach is cooling (negative values) from other drivers (*e.g.* canyon shading). There is no difference in heating rates at the downstream end of the study reach.

Predicting Thermal Impacts from Climate Change

The three climate change scenarios simulating two, four, and six degree increases in air temperature reflected forecasted 2049 and 2099 conditions. Mean stream temperature increased by 0.09 ºC for every two degree rise in air temperature (Table 16). The overall thermal profile between climate scenarios does not show changes in overall shape (Figure 33). Mean maximum temperature increased with increasing air temperature while cooling rates were smaller in magnitude (Figure 34).

Table 16. Table of summary statistics of climate change scenarios compared to the base model.

Scenario	Mean Daily Max Temp. [ºC]	Mean Daily Min Temp. [ºC]	Mean Daily Duration above 21 ºC [hr]
Base Model	21.57	16.09	3.8
2 ºC	21.68	16.18	4.2
4 ºC	21.79	16.27	4.2
6 ºC	21.90	16.36	4.8

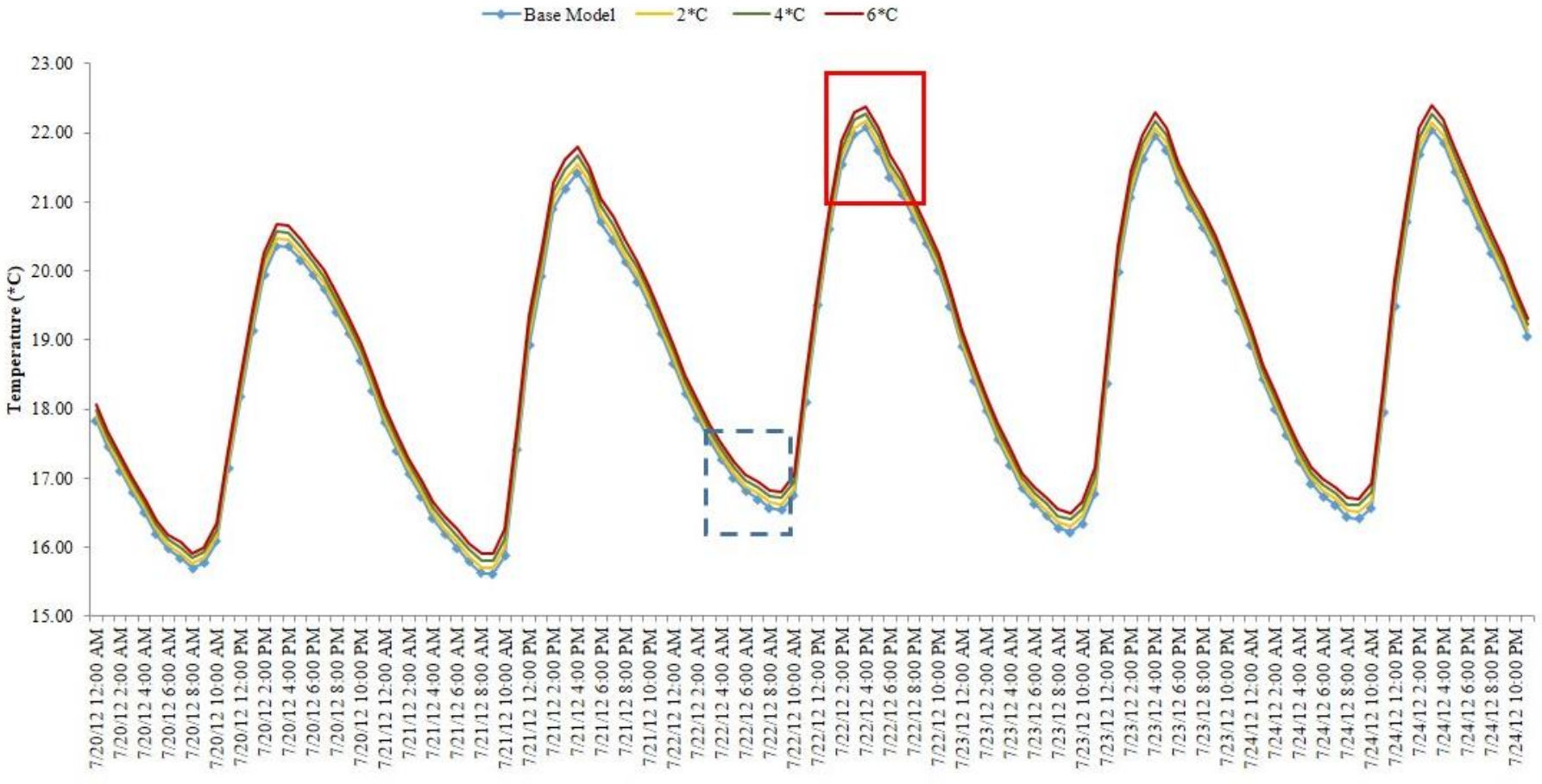

Figure 33. Thermal profile comparing climate scenarios at the bottom of the reach, using *Heat Source*, July 2012, Salmon River, CA, USA. Cooling inset (blue dashed box) and maximum temperature inset (red box) expanded in next figure.

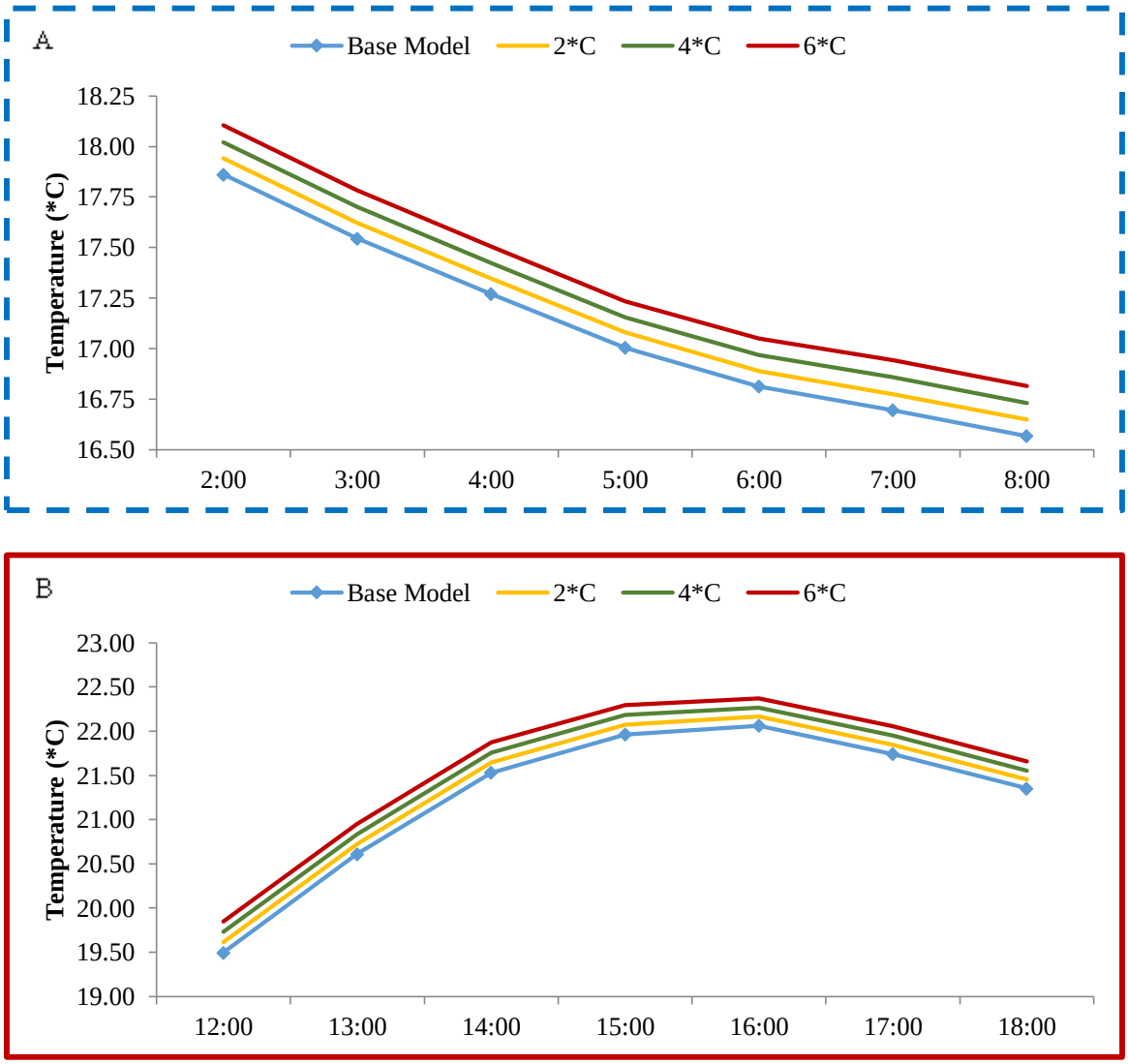

Figure 34. Thermal inset of Figure 33 comparing three climate scenarios to the base model in *Heat Source* during A) cooling between 2:00 and 8:00 and B) maximum temperature between 12:00 and 18:00 on July 22nd 2012 at the downstream end of the study reach, Salmon River, CA, USA.

Ameliorating Elevated Stream Temperature from Climate change.

Riparian reforestation appears to ameliorate forecasted climate change scenarios (Table 17). Mean stream temperature from climate warming was reduced by 0.11 ºC and

0.26 ºC for every 2 ºC air increase for partly and fully forested conditions respectively. The reduction is greater than heating caused by an increase in air temperature (0.09 ºC for every 2 ºC air increase). Our sensitivity analysis found no difference in the predictions of warming or buffering from reforestation when boundary stream temperature conditions were increased by 2 ºC.

Mean daily maximum temperature was reduced by 0.39 and 0.79 ºC for partly and fully forested conditions respectively, compared to baseline climate change scenarios (Table 18). Mean daily minimum temperatures are nearly uniform between all scenarios. Partly forested conditions reduced mean daily duration above the salmonid threshold by an hour and fully forested conditions reduced it by two hours compared to baseline climate scenarios.

Table 17. Table of summary statistics of climate change scenarios (with baseline forested conditions) compared to the base model (current condition) and partly and fully forested climate scenarios.

Scenario	Mean Daily Max Temp. [ºC]	Mean Daily Min Temp. [ºC]	Mean Daily Duration above 21 ºC [hr]
Base Model	21.57	16.09	3.8
2ºC Baseline	21.68	16.18	4.2
2ºC Partially forested	21.29	16.15	3.0
2ºC Fully forested	20.90	16.12	2.2
4ºC Baseline	21.79	16.27	4.2
4ºC Partially forested	21.40	16.24	3.6
4ºC Fully forested	21.00	16.20	2.4
6ºC Baseline	21.90	16.36	4.8
6ºC Partially forested	21.51	16.33	4.0
6ºC Fully forested	21.11	16.29	2.8

Table 18. Comparison of differences between climate change scenarios compared to partly and fully forested climate scenarios. A negative value means the forested condition scenario value was smaller than the climate scenario value.

Scenario	Difference Mean Max Temp. between scenarios [ºC]	Difference Mean Min Temp. between scenarios [ºC]	Difference Mean Daily Duration above 21 ºC [hr] between scenarios
2ºC Partly forested	-0.39	-0.03	-1.2
4ºC Partly forested	-0.39	-0.03	-0.6
6ºC Partly forested	-0.39	-0.03	-0.8
2ºC Fully forested	-0.78	-0.06	-2.0
4ºC Fully forested	-0.79	-0.07	-1.8
6ºC Fully forested	-0.80	-0.07	-2.0

The partly forested thermal profile shows the warming scenarios closely match current (base model) conditions (Figure 35). This is because they share the same boundary conditions. Cooling is also similar to the base model and may be slightly higher due to increased air temperature or increase long-wave radiation from the increased vegetation (Figure 36a). The fully forested thermal profile also shows that warming scenarios closely match current conditions (Figure 37). Cooling is still very close to the base model, and fully forested conditions show even more thermal buffering to daily maximum temperatures (Figure 38).

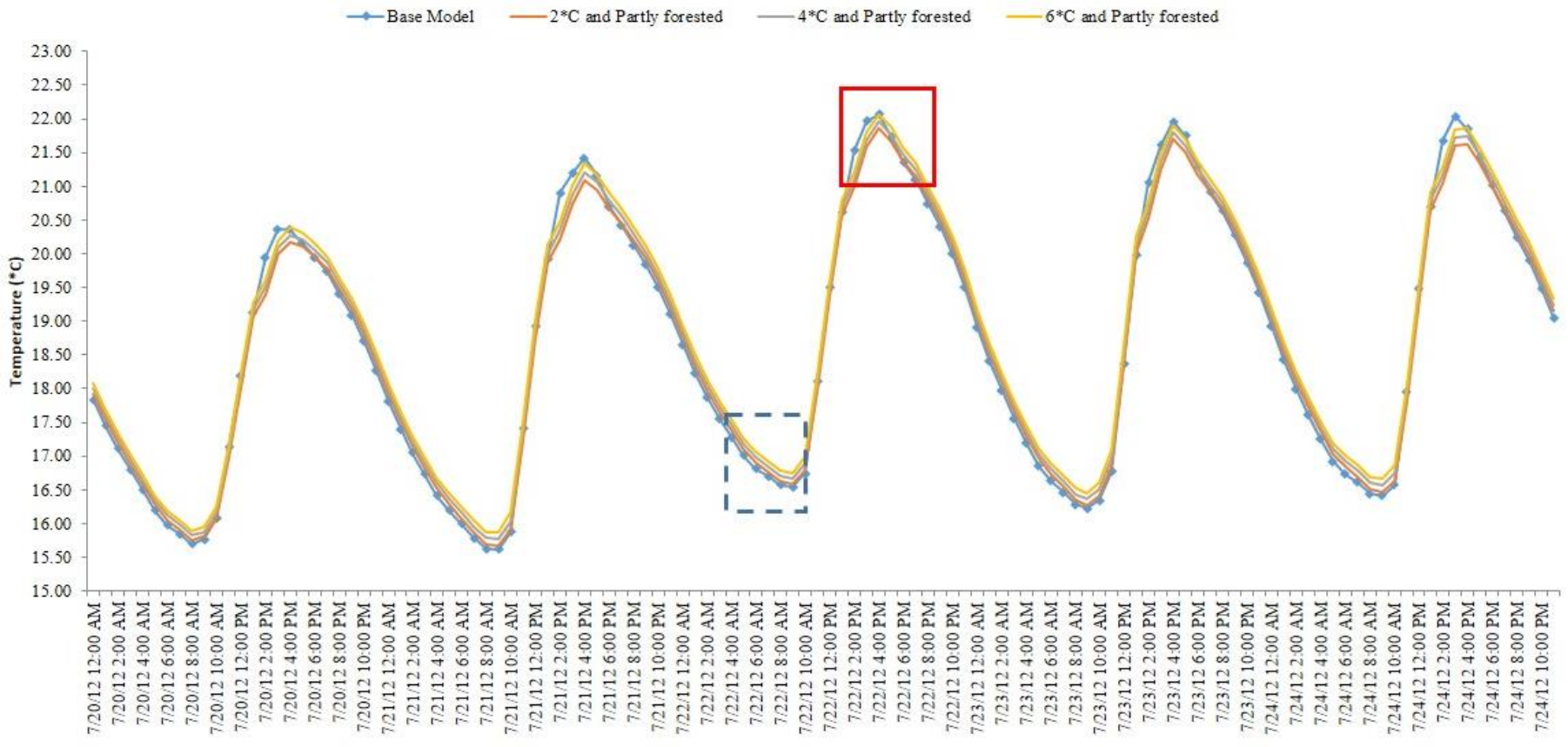

Figure 35. Thermal profile of climate amelioration with partly forested scenarios at the bottom of the reach, using *Heat Source*, July 2012, Salmon River, CA, USA. Cooling inset (blue dashed box) and maximum temperature inset (red box) expanded in next figure.

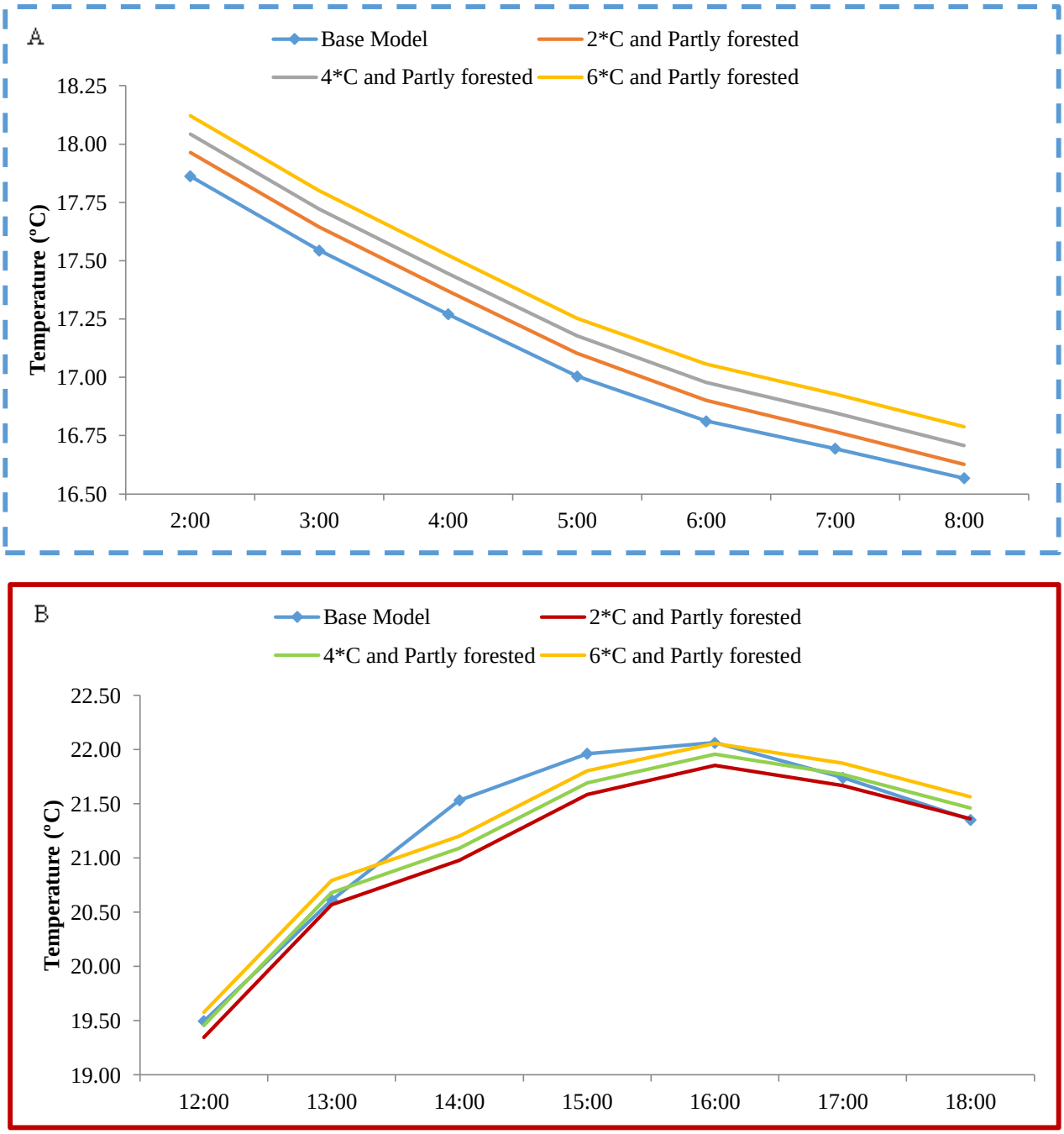

Figure 36. Thermal inset of Figure 35 comparing three climate ameliorating partly forested scenarios to the base model in *Heat Source* during A) cooling between 2:00 and 8:00 and B) maximum temperature between 12:00 and 18:00 on July 22nd 2012, Salmon River, CA, USA.

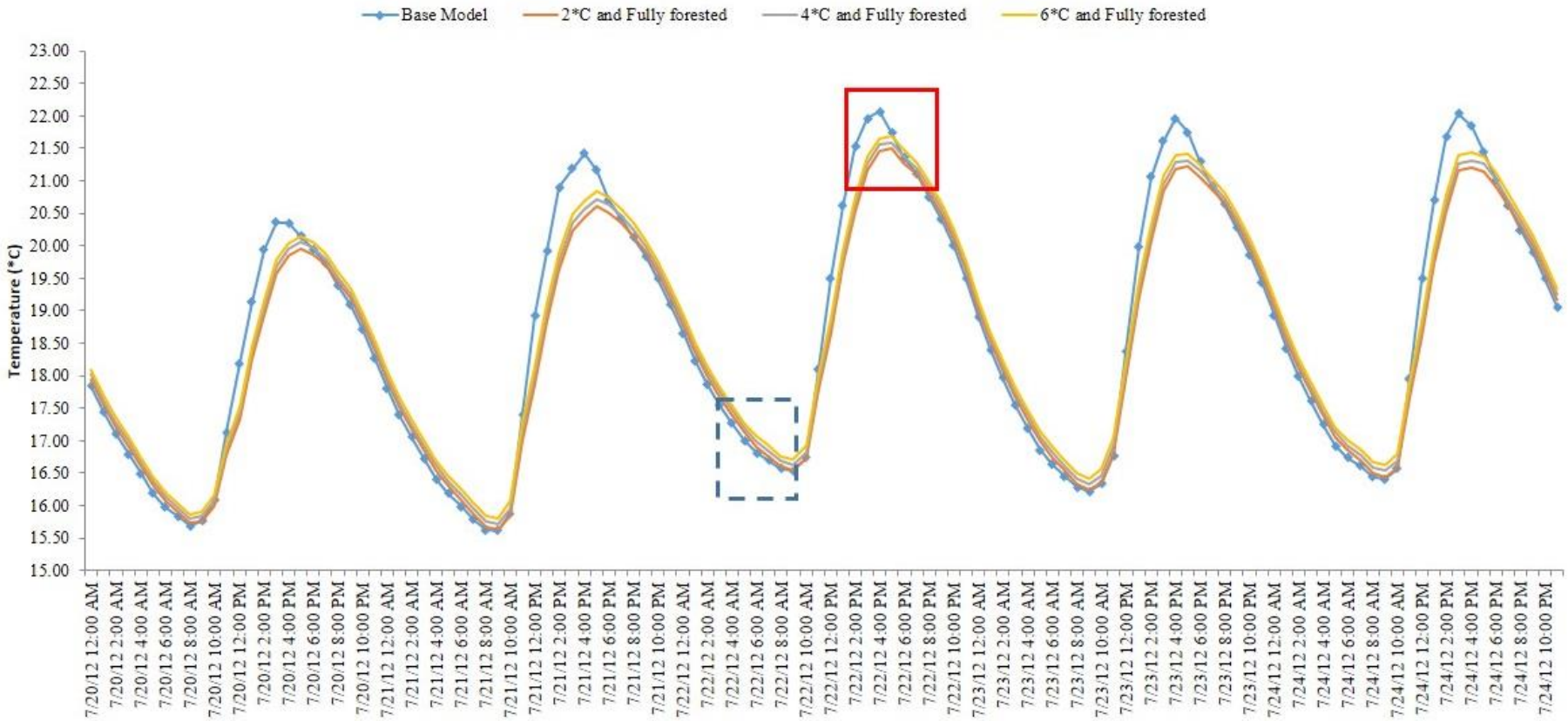

Figure 37. Thermal profile of climate amelioration with fully forested scenarios at the bottom of the reach, using *Heat Source*, July 2012, Salmon River, CA, USA. Cooling inset (blue dashed box) and maximum temperature inset (red box) expanded in next figure.

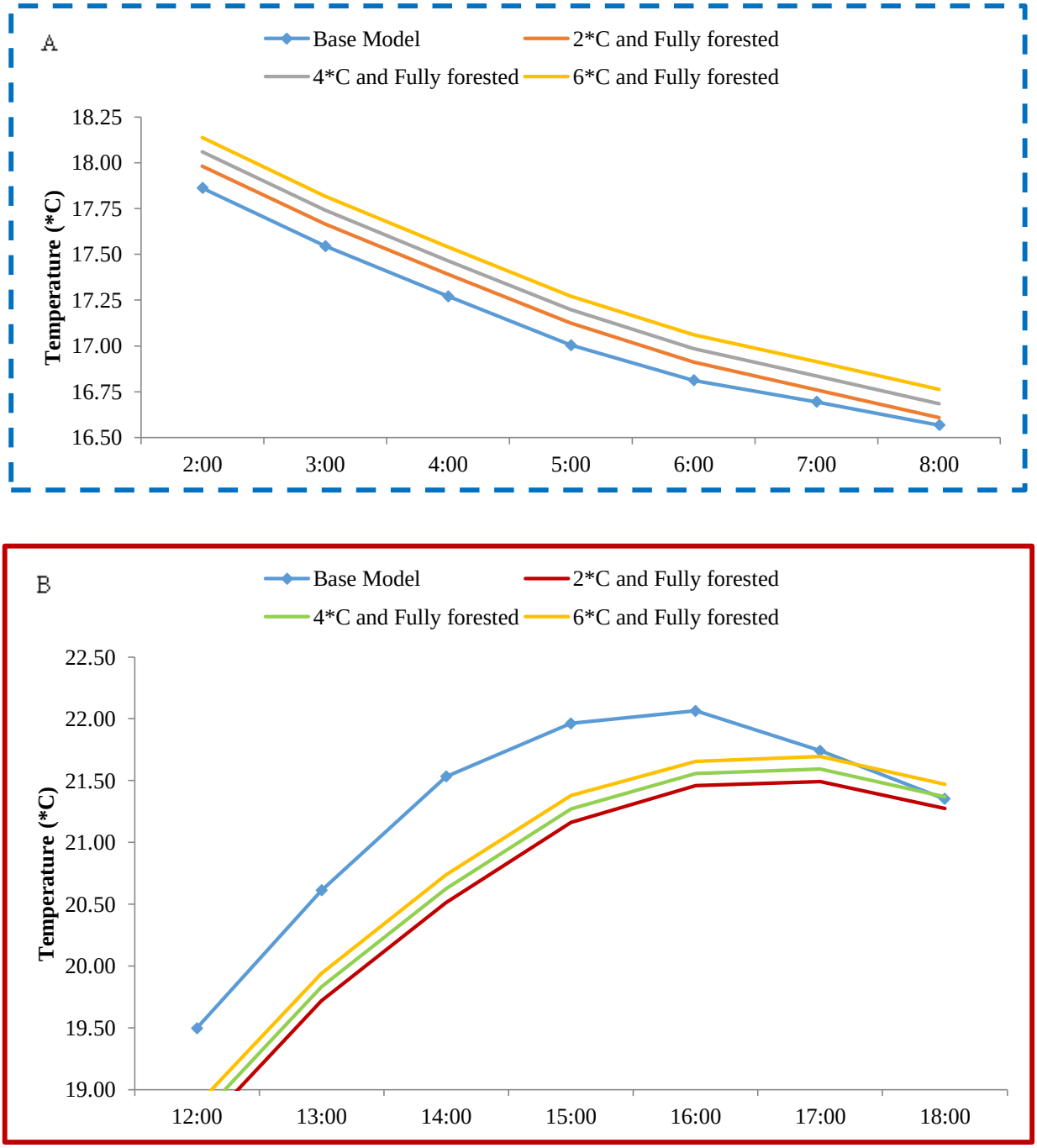

Figure 38. Thermal inset of Figure 37 comparing three climate ameliorating fully forested scenarios to the base model in *Heat Source* during A) cooling between 2:00 and 8:00 and B) maximum temperature between 12:00 and 18:00 on July 22nd 2012, Salmon River, CA, USA.

DISCUSSION

Physical Impacts on Salmonids

Salmonids typically spawn in the tributaries of the Klamath in the winter months. After emergence, coho rear in their natal stream for one year before outmigration in the spring. Juvenile rainbow trout (*i.e.* steelhead) and Chinook salmon also over-summer before outmigration. During the rearing period, juveniles are sensitive to chronically elevated summer stream temperatures because they typically stay in one place (Sutton and Soto 2010). Adult salmon and resident trout, on the other hand, actively seek thermal refugia during daily maximum temperatures. Over the study period no adult salmon were observed. This discussion will focus on juvenile exposure and rearing habitat quality. It is important to note that adult salmonid survival and success may be affected by daily maximum temperatures in the Salmon River and is a current topic of discussion.

Study Site Thermal Regime

Salmonids have evolved with a narrow range of stream temperature variability and are commonly identified as thermally stressed (Ebersole *et al.* 2001). "Thermally induced mortality" is a result of increased metabolic needs (*i.e.* growth, feeding, and reproduction) with inadequate food sources, protein heat shock (*i.e.* elevated temperatures change protein shape inhibiting molecular processes in the body), increased

exposure to pathogens, and increased competition with warm-water fishes (Feder and Hofmann 1999, Boyd and Kasper 2003).

In addition to physiological stresses, warm summer stream temperatures have fragmented cold-water habitat, resulting in isolated populations and restricted seasonal migration (Meisner 1990, Berman and Quinn 1991, Eaton and Scheller 1995). Previous research has illuminated the need for protection from thermal stress to improve salmonid population resilience (Mosley 1983). Landowners and managers are focusing their attention on the need for thermal protection of cold-water processes to relieve warm summer stream temperatures caused by land use and climate change (Meisner 1990, Matthews and Berg 1997, Ebersole *et al.* 2001 Boyd and Kasper 2003).

Numerous studies have investigated "optimal", "sub-optimal", "tolerable", and "lethal" temperature thresholds for salmonids. While laboratory experiments by Joblings (1981) found an upper acute lethal limit for salmonids ranging from 27 to 30 °C, field studies have found acute and long term thresholds at much cooler temperatures (Sullivan *et al.* 2000, Hardy *et al.* 2006, Sutton and Soto 2010). The DTS revealed nearly homogeneous warming over the study reach and a diel heating cycle of 5 °C with no major cooling inflows (Figure 14). This means that salmonids within the reach were subjected to uniform maximum temperatures regardless of where they were located. There were also no large detectable springs to provide thermal refugia against daily maximum temperatures.

The study observed a Maximum Weekly Maximum Temperature (MWMT) of 23.00 °C. While MWMT and MWAT estimates are typically averaged over a whole year

rather than just a week (like our study period), our estimates were similar to other thermally impaired streams in northern California (Welsh et al 2001, Madej *et al.* 2006). Furthermore, the observed MWMT exceeded salmon and trout protective temperature standards set by United States Environmental Protection Agency Region 10.

Mean temperature over the entire reach exceeded the critical salmonid temperature threshold of 21 ºC seven of the eight days monitored (Figure 13). After an extensive literature review, Stenhouse *et al.* (2012) defined water temperature above 21ºC in the Shasta Basin, California, as detrimental to juvenile salmonids. Above this temperature juveniles experience broad physiological stress. The temperature threshold in this study (also 21 ºC) was chosen as a benchmark of thermal stress, above which salmonids have reduced growth rates due to higher metabolic demand from increased temperature. Exceedance of 21 ºC on a nearly daily basis during summer conditions strongly indicates that over-summering juvenile salmonids are experiencing physiologically stressful temperatures in the Salmon River. The National Marine Fisheries Service temperature threshold standard for coho in the SONCC (Southern Oregon/Northern California Coasts coho salmon Evolutionary Significant Unit), including the Salmon River watershed, was 17 ºC which was exceeded all but the early morning hours every day of the study (NMFS 2012).

Groberg *et al.* (1978) and Elliot (1981) found that juvenile salmonids exposed to "sub-lethal" temperatures can inhibit growth and smoltification, reduce overwintering success, obstruct migration, and promote disease propagation. Previous research has found that Salmon River stream temperature has exceeded "upper growth requirements

for salmonid juveniles," which is consistent with our observations (Hardy *et al.* 2006). Hardy *et al.* (2006) credited summer stream temperatures to "natural climatic factors." Our research shows that regardless of the cause of increased water temperatures, salmonids are congregating in areas with greater depth and have poor rearing habitat to help buffer themselves from anthropogenic and climatic stream heating (discussed further below).

Salmonid Distribution

The distribution of juvenile salmon and trout revealed habitat preference during summer conditions. Statistical modeling of salmonid distribution found that both depth and temperature explained fish counts. Both total and salmon count had a positive relationship with depth while total count had an additional positive relationship with temperature. In regards to depth, previous studies have shown a positive correlation between salmonid numbers and depth (Torgersen *et al.* 1999, Ebersole *et al.* 2001, Sutton and Soto 2010). Considering that most of the stream is composed of relatively shallow fast-water habitat it is not surprising that salmonids are most concentrated in pool units - areas of greatest depth and presumably velocity refuges.

The AICc analysis of models explaining total count indicated the predictive ability was greater when temperature was added to the model already containing depth as a predictor (ΔAICc = 2.49, Table 6). DTS showed very little differences in temperature across habitat units at our chosen temporal and spatial scale. The positive response

between temperature and total count is most likely the result of small sample size. Though sampling of habitat units was random, four of the six transects in pool units were sampled in the afternoon (1500 and 1600). Sampling in the evening may have strengthened the temperature relationship. On the other hand, it may reveal behavioral preference of salmonids to congregate when thermally stressed. Torgersen *et al.* (1999) found that adult Chinook salmon in warm-water reaches in Oregon actively selected pool habitat to cope with higher metabolic energy demand (presumably from temperature) and flow refuge.

Salmonid Habitat

In addition to experiencing physiologically stressful temperatures, resident and juvenile salmonids in the study reach have poor habitat quality (Table 11). Pools are few and spread apart, leaving long stretches of fast water. Pools are an important refuge against velocity, temperature, and predation. Our longitudinal measurements indicate that the percentage of pools in the study reach is less than optimal conditions in the literature (McMahon 1983, Flosi *et al.* 2010). Furthermore, the fast-water to slow-water ratio is six times the optimal condition for salmonids indicating that juvenile and adult salmonids have few resting places when migrating through the study reach.

In-stream and cross-sectional measurements also indicate poor habitat quality. Mean bankfull width-to-depth ratio for the study reach is twice the optimal ratio standard set by the PACFISH / INFISH Riparian Management Objective (cited in Henderson *et al.*

2005). Likewise no instream course substrate cover, such as large woody debris (LWD), was observed in the study reach, further compounding the issues of homogenized habitat. LWD may have been swept downstream during hydraulic gold mining and has not recruited possibly due to logging in the 1960s around the study reach. Reduced complexity and lack of instream cover means that there are few resting spots for fish. Sutton and Soto (2010) found that juvenile coho on the mainstem Klamath seek out refuges that have low velocities and high instream cover.

Aerial cover (*i.e.* shade) by riparian vegetation is also low in the study reach. Mean percent total shade in the study was about 1/3 to 1/2 of optimal conditions for coho (McMahon 1983). Riparian shade provides a source of food, thermal buffering, and protection from aerial predictors. The lack of shade in the study reach compounds the issues of daily maximum temperatures which would normally be buffered with greater riparian vegetation. Overall, the observed channel metrics indicate a reduction in habitat complexity. No instream cover, little shade, and few pools has the potential to reduce juvenile success in the summer from daily maximum temperatures. Our measurements as well as other studies (NMFS 2012) also suggest that winter rearing habitat (*i.e.* the study site lacked any side-channel habitat) may also be affected and should be further investigated.

The reduction in channel complexity is most likely related to the historic hydraulic gold mining in the area. The majority of hydraulic gold mining in the Salmon River occurred between 1850s and 1940s. By the 1870s gold mining in Sawers Bar, CA was in full swing; the epicenter of gold mining activity on the North Fork Salmon River

(Stumpf 1979). While the Salmon River has had some time to recover from gold mining, many areas still show this lasting legacy as large denuded gravel bars. The study site is located approximately four and a half river kilometers downstream of Sawyers Bar, California. The Salmon River watershed had 1,376 known historic licensed mines operated in the sub-basin with 1,109 mines targeting gold. Two mines where within the study reach including hydraulic mining adjacent to Run 1 (Figure 39, Figure 40). Historic hydraulic mining sediment input in the entire river between 1870 and 1950 was estimated to be 12.1 million cubic meters (15.8 million cubic yards) (Elder *et al.* 2002).

The uniform warming captured by DTS is likely the result of two factors: one, the large wetted width-to-depth ratio (W:D), and two, the limited shade surrounding the channel margins. The wetted W:D indicated the water surface was greatly exposed to solar radiation compared to its depth. Shallow depth may have also permitted solar radiation to heat rock clasts on the channel bottom (*i.e.* streambed conduction), creating a thermal reservoir that extends warmer temperatures into the evening hours. Low riparian and total shade over the study reach (16% and 22% respectively), which would normally buffer streams from increased solar radiation, are relatively small further exacerbating increased streambed conduction from the channel geometry (Brown 1969, Brown 1970).

The sizable wetted W:D ratio in the study reach indicates possible channel aggradation, which is now reflected as an armored channel bottom. The study reach is similar to a C3 channel, which is expected to have a mean W:D ratio between 12 and 20 (Rosgen 1985, Rosgen 1994). While the bankfull ratio over the study reach is within the expected range, the wetted ratio of 41 is double the larger estimate. It is possible that the

W:D ratio is limiting channel incision which would otherwise "adjust" the channel from the current U-shape to pre-mining conditions, presumably a V-shape. Channel widening has also been seen in other northern California streams. For example, Redwood Creek widened 150-300% as the result of increased sediment supply from land use which was transported by the 1964 flood (Madej and Ozaki 1996). The sediment "slug" is still recognizable today.

Riparian vegetation recruitment may also be affected by legacy conditions. The study reach lacked topsoil, reducing nutrients and growing medium for vegetation. While areas uphill of Run 1 and the downstream section of the study reach do have vegetation, something is preventing recruitment on the denuded gravel bars. The bars may prevent vegetation from accessing water, and the large cobble pore size does not allow water to remain close to the surface for seedlings.

The study reach is shallow and exposed during summer conditions due to its current geometry. What is more troubling is that pools are spread far apart. This is consistent with previous research that speculated that mining tailings filled in pools along the Salmon River (Elder *et al.* 2002). Pool habitat became smaller and spread out, while the stream aggraded from increased sediment sources. Pools that remain in the study reach are maintained by meanders with bedrock margins, which scour the pools, removing additional sediment (*i.e.* "swing pools" (Lisle 1986)). Pool habitat characteristics such as depth, area, and complexity are positively associated with species diversity and abundance (Bjornn and Reiser 1991, Lamb 1996). Reduced pool frequency

in addition to peak summer temperature over the study reach may be limiting salmonid success and the larger aquatic community.

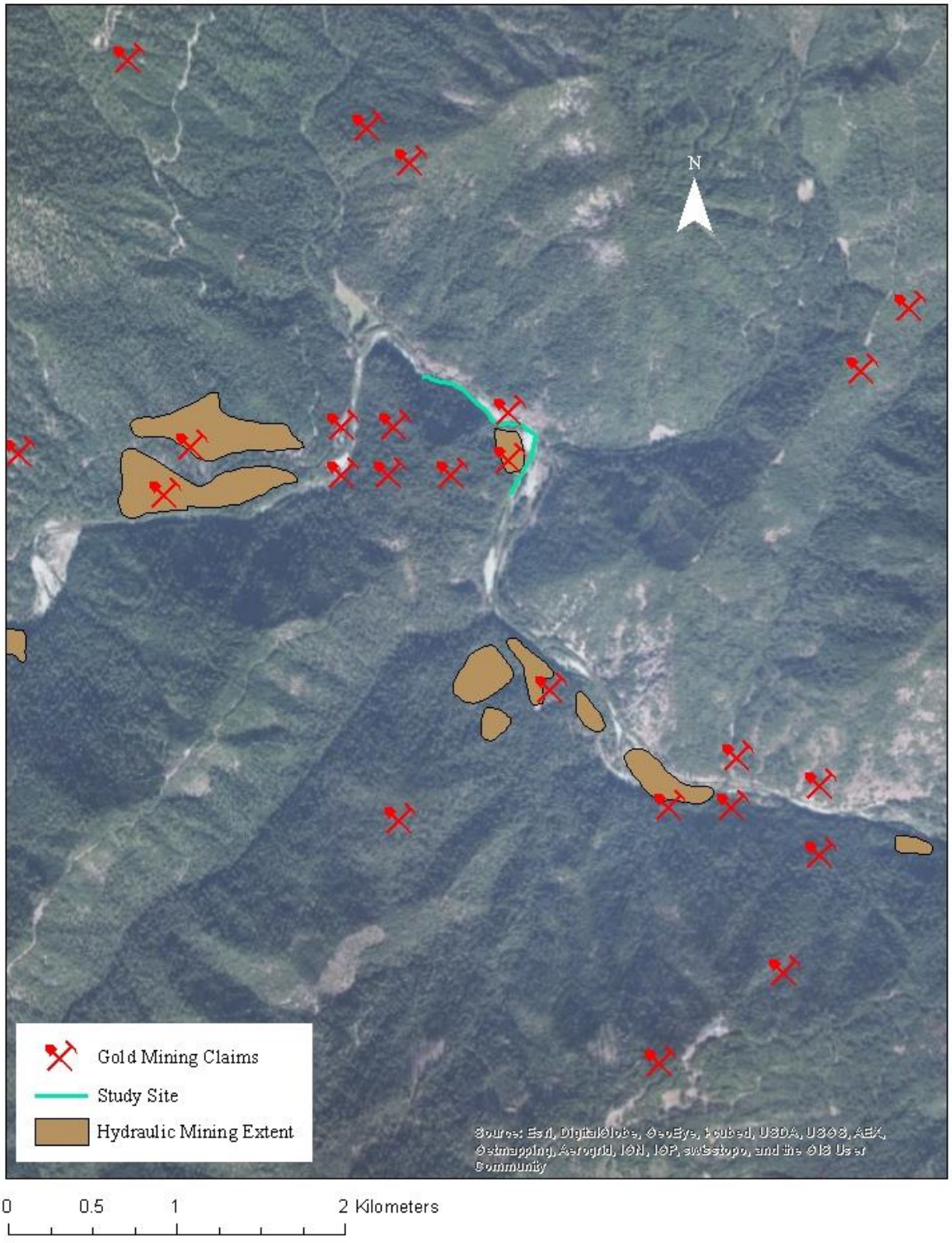

Figure 39. Map of licensed gold mining claims surrounding the study area along the North Fork Salmon River, CA, USA. The known extent of hydraulic mining is scattered along the mainstem and surrounds the left bank of the study area downstream of Run 1. Mining layer provided by the Salmon River Restoration Council.

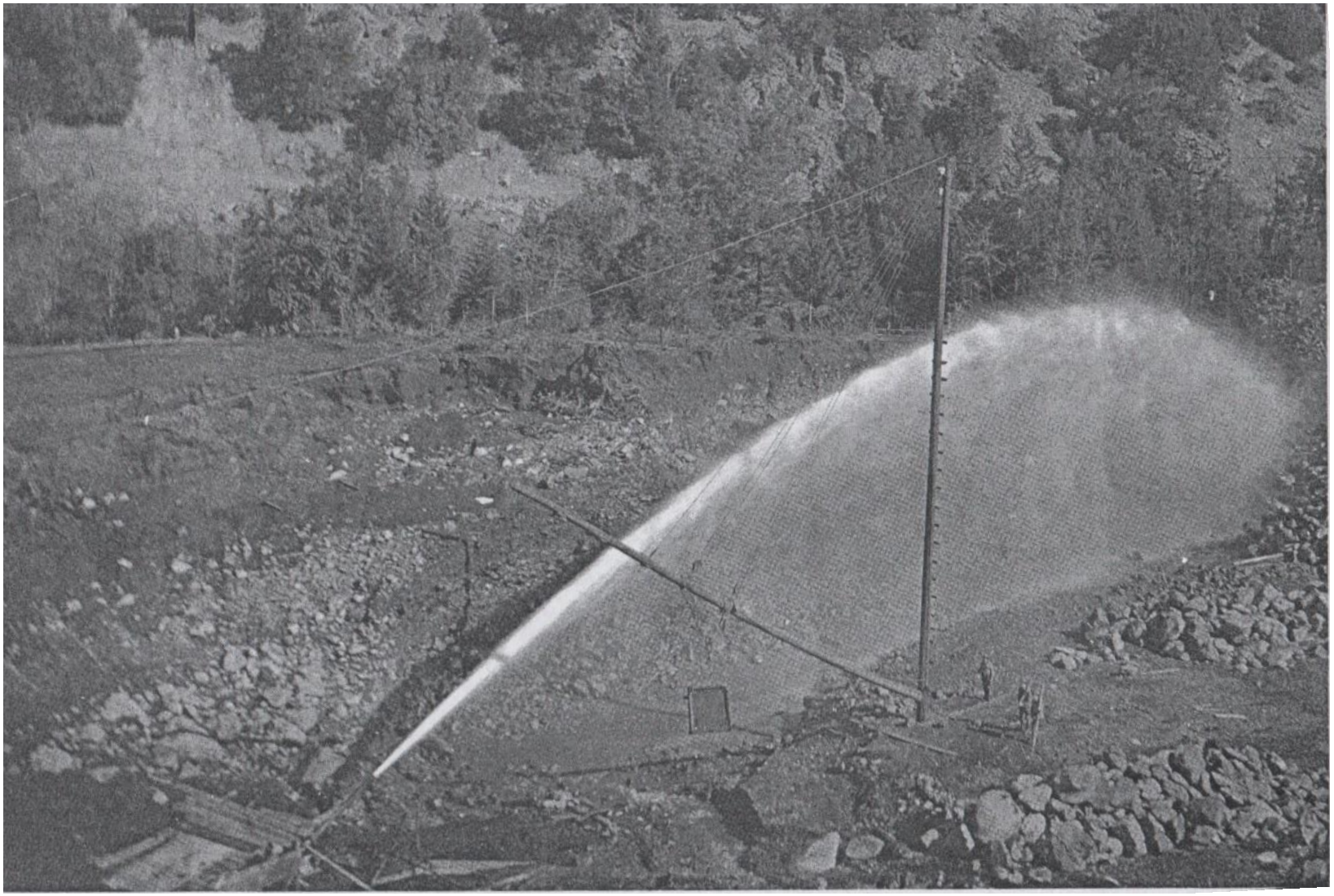

Figure 40. Photograph of Giant or Monitor (hydraulic pump) and derrick (crane structure), Slapjack Mine, circa 1894 near Sawyers Bar, CA, USA (Storms 1894).

Quantifying a Groundwater Spring

A spring was located below Pool 2 and quantified using DTS and the volumetric inflow calculation. The spring was located in what was a hydraulically mined area and may have been formed by a historic channel at the valley margin (Figure 18). Subsurface flow may be cooled along the valley margin, which is thickly forested, and then returns to the mainstem, circumventing the large exposed area (*i.e.* Run 1 and Riffle 1) above the mainstem's meander. The spring's inflow was in phase with mainstem temperatures, indicating that it was a groundwater spring (Collier 2008). Because this spring was about 7 % of mainstem flow, our results suggest that groundwater may be an important inflow in the Salmon River. Groundwater-deep alluvium interactions may be a source of cold water in low flow conditions. We did not observe any fish congregating around the spring confluence during the study period nor did we detect with DTS a distinct cold-water plume in the area.

Further study is needed to investigate if the spring has enough flow and thermal capacity to cool the mainstem by an ecologically significant amount (*i.e.* a few degrees Celsius) in lower flow conditions. Previous DTS applications have investigated springs in small streams (*i.e.* 1st order) with low flow (roughly 0.3 m^3s^{-1} (10 cfs)). We successfully applied the DTS spring identification methods to a large stream (*i.e.* mainstem channel) with greater flow (1.24 m^3s^{-1}) then previous applications. Additional seeps may be present in the study reach and were not captured by the DTS due to flow.

DTS is a valuable diagnostic tool because it is able to both identify where springs are located and then estimate flow in non-uniform (*i.e.* changing) conditions (Vogt *et al.* 2009). This is especially important in groundwater-dominated streams or areas with complex inflow patterns. Multiple studies have found that by using heat as a tracer in the stream system (*i.e.* like a dye or chemical solution tracer) (Stonestrom and Constantz 2003, Anderson 2005), DTS was able to measure seepage rates and identify losing and gaining reaches of the river (Tyler *et al.* 2008, Voget *et al.* 2009). While our study site was thermally homogeneous, the spring methods could be applied to other reaches of the Salmon River to investigate thermal refugia from tributary inflows or other thermally complex systems.

Heat Source Modeling

Stream temperature is a dynamic water-quality parameter that reflects both local and upstream conditions. Research has shown that stream temperature is directly related to land-use practices that alter flow conditions, such as damming and diversion, modify the quantity and quality of riparian vegetation, such as logging and livestock grazing; and modifying channel morphology and bank stability from a variety of compounding land uses. Previous stream temperature modeling approaches have tracked energy transfers and balances as well as conservation of mass (stream flow) within the stream (Brown 1970, Wunderlich 1972, Beschta and Weatherred 1984, Sinokrot and Stefan 1993, Boyd and Kasper 2003, Westhoff *et al.* 2007). Each attempt to accurately model stream temperature has expanded our understanding of hydrology as well as helped communities

identify areas of thermal concern in their watersheds. The aim of this study was to use *Heat Source*, developed by the Oregon Department of Environmental Quality (DEQ), to model instream temperatures for the study site. The calibrated model was then used to evaluate changes in stream temperature resulting from a variety of management actions and climate change.

Heat Source Accurately Predicts Stream Temperature

Stream temperature modeling falls into two categories: statistical models that typically relate parameters through linear regression (Flint and Flint 2004) and mechanistic models that take heat processes (*i.e.* thermodynamics) into account (Sinokrot and Stefan 1994). *Heat Source* is a mechanistic model which investigates stream temperature from geomorphic, meteorologic, and hydrologic conditions (Boyd and Kasper 2004). *Heat Source* was developed to help inform land managers on current and potential restoration conditions. The model has been employed by Oregon Department of Environmental Quantity to establish and enforce Total Maximum Daily Load (TMDL) stream temperature thresholds in Oregon, USA.

Models are inherently a simplification of reality and can vary in spatial and temporal predictions. The four measures of spatial model fit used in this analysis were comparable to previous *Heat Source* applications in Oregon (Table 19). The four basin averages presented in Table 19 cover larger watershed areas (*i.e.* sub-basins) and simulate conditions over longer periods of time. The RMSE values presented in the lower part of

Table 19 correspond to smaller drainages. Our study's MARE is much lower than previous applications most likely due to small sample size. This is also true of the study's high NSE. Our study's mean and maximum RMSE is similar to the RMSE's of the smaller drainages. For perspective, our study's maximum RMSE is 6 % of the diel fluctuation (5 ºC) over the study period.

The spatial pattern showing a decrease in fit in a downstream direction was most likely due to lack of continuous data at the downstream end of the study reach. Both stream flow and meteorological conditions (*i.e.* wind speed, air temperature, humidity, solar radiation) were measured only at the headwaters of the study reach. While *Heat Source* took the distance from the upstream continuous data node into account, additional meteorological stations at more locations would have increase model fit because the inputs at each spatial location would be more accurate than just using values measured at the upstream node. The temporal bias present in the model estimates was also a reflection of how models simplify reality. Observations over time are inherently correlated with previous observations. I found a first-order temporal autocorrelation in model-predicted errors. The magnitude and sign of the model error at a given time step was correlated with the magnitude and sign of the error at the previous time step. This means *Heat Source* over-predicted temperature during mid-day and under-predicted temperature at night (Figure 24). Mean temporal bias was 0.07 ºC which is very small (1.4%) compared to the diel fluctuation over the study period. It is important to note that the error does not systematically increase over time because observed meteorological conditions are updated hourly.

Our study focused on matching the entire daily cycle as best we could. Previous *Heat Source* TMDL applications have focused on matching daily maximum temperatures rather than both daily warming and cooling cycles. Overall, we believe we are within an acceptable range of error to use *Heat Source* to describe study period conditions. Future work could build on this study by applying *Heat Source* to larger areas in the Salmon River watershed and simulate conditions over the entire summer season.

Table 19. Summary of model performance measures from other *Heat Source* applications by sub-basin/drainage with literature source.

Sub-basin / Drainage	**Bias** [ºC] **(mean error)**	**RMSE** [ºC]	**MARE** [ºC] **(absolute mean error)**	**NSE** [ºC]	**Literature Source**
Rogue Basin Average	-0.08	0.8	0.63	0.86	Crown *et al.* (2008)
North Fork John Day Average	0.53	1.54	1.23	0.89	Crown (2010)
John Day Mainstem Average	0.04	1.36	1.07	0.68	Crown (2010)
Middle Fork John Day Average	0.53	1.54	1.23	0.90	Crown (2010)
Tumalo Creek		0.4			Watershed Sciences (2008)*
Umatilla River		1.3			ODEQ (2001)
Whychus Creek		0.7			Watershed Sciences (2008)*
Deschutes River		0.4 - 0.6			Watershed Sciences (2008)*
Upper Grande Ronde		0.8			ODEQ (2010)

* = Initial *Heat Source* calibration currently in review by ODEQ for final model calibration.

Riparian Reforestation

Simulated reforesting of exposed areas, denuded gravel bars from legacy mining and areas of low vegetation in the study reach, helped buffer daily maximum temperature. This is due to the shift in the timing of heating by solar radiation with reforestation (Figure 28). The absolute amount of solar radiation that reaches the stream is the same between the scenarios because the sun emits radiation at a relatively constant rate. The duration of heating is limited, but not eliminated, because of the channel configuration, meaning trees are shading the edges of the stream rather than the entire channel. Our results are consistent with those of Brown (1970), who found that riparian vegetation buffered streams from heating. The energy flux diagrams also showed that heat moving from the water column to the bed (*i.e.* bed conduction) was greater during daily maximum temperatures in the reforestation scenarios. This means that the bed stays cooler longer with greater shade, an additional benefit from reforesting. From a biological standpoint, it is important to note that effective shade for the fully forested scenario is within optimal conditions for salmonids (50-75%) over the entire study reach (McMahon 1983).

While the study reach daily mean maximum temperature in all scenarios is greater than the 21 ºC temperature threshold for salmonids, the relative mean hours per day over this threshold was reduced from 3.8 hours (current condition) to 2.4 and 2.0 hours for partly and fully reforested conditions, respectively. As previously discussed, salmonids are already thermally stressed; any increase in temperature value and/or duration increases this stress and has the potential to reduce salmonid success further. Catastrophic

wildfire simulated by “no forest” conditions increased daily mean maximum by nearly a degree Centigrade from the base model. The mean daily duration over the salmonid threshold was two hours longer and nearly 2.5 hours longer then partly forested and fully forested conditions, respectively. The wildfire scenario shows both the potential heating from having no vegetation, a worst case scenario, as well as indicate that the riparian vegetation that is currently present is buffering some heating from solar radiation which can be improved upon with greater riparian reforestation.

Daily minimum temperatures and cooling rates were similar between the four scenarios. Cooling rates in fully and partly forested areas were slightly smaller than the base model. This is most likely due to the dampening of long wave (LW) radiation resulting in less cooling in the evening in partly and fully forested scenarios (Figure 30). We maintained constant meteorological conditions in the input parameters for the reforesting simulations. Increasing vegetation height and density may change wind patterns changing evaporative cooling rates. Reforesting may also change flow quantity because there would be more roots up-taking water. Both of these assumptions in our simulations should be investigated further to reduce model prediction error.

Channel Geometry Restoration

Measuring the success of treatment effects are spatially sensitive, implying that it is the observational unit which dictates wither restoration efforts “worked” or not. Reducing the channel bottom width of Run 1 from 32.5 m to 27 m and 20 m reduced the

rate of heating at the daily maximum in the treatment area by 0.03 ºC/90 m, a 34 % reduction. It is unknown if the reduction in heating rate is ecologically significant. For biota in the treatment area it is possible that the reduction in heating rate helps reduce thermal physiological stresses. On the other hand, the channel scenarios did not appear to impact stream temperature seen at the bottom of the study reach; meaning by the time a packet of water reached the bottom of the study reach (~700 m), there was no difference in temperatures between the base model and channel restoration scenarios (Figure 31).

Perhaps a better strategy would be to vary the bottom width of entire reach rather than that of a small section. Increasing channel habitat complexity by including LWD structures may improve ecological structure more than simply re-channelizing the mainstem. Future research should investigate what pre-mining conditions could have looked like and use those estimates in *Heat Source* modeling. Modeling the creation of deep, forested side channel or braided habitat may also help land managers investigate possible restoration strategies.

Predicting Thermal Impacts from Climate Change

Previous studies investigating climate change have found consistently negative impacts on salmon habitat and productivity (Battin at al. 2007). Elevated stream temperatures are particularly harmful to salmonid spawning, incubation, and rearing life stages (Richter and Kolmes 2005). Research in the lower mainstem Klamath found that both air and stream temperature since the mid-twentieth century were warming.

Bartholow (2005) found that stream temperature increased at a rate of 0.50 ºC per decade between 1962 and 2001, an overall increase of 2 ºC. The study also found that air temperatures in the Klamath Basin increased at a rate of 0.33 ºC per decade during the same time period. This is particularly alarming when climate forecasts indicate continued increases in both stream and air temperature by the end of this century (2099).

Our research found that mean stream temperature increased by 0.09ºC for every two degree rise in air temperature. While this may be a small value, it may be important at the basin scale. If the rate of heating was constant between the study site and the confluence with the South Fork at Forks of Salmon, CA (17 kilometers downstream) stream temperature would increase by 1.53ºC. This is within the range of other basin estimates in California. Null *et al.* (2013) found an overall increase in stream temperature of 1.6ºC in California's west-slope Sierra Nevada using the same air temperature predictions. Such an increase could affect adult salmonid migration and juvenile rearing.

Null *et al.* (2013) found that viable cold water habitat moved to higher elevations with increased warming. Elevated stream temperatures from warming may prevent ocean up-migration from the mainstem Klamath to the Salmon River (Bartholow 2005) as well as to natal headwaters in the North Fork Salmon River. Our study site is between the North Fork headwaters and mainstem Salmon River confluence. Salmonids need to be able to migrate through the study reach to suitable spawning and rearing habitat at higher elevations. A sensitivity analysis was run to investigate how initial stream temperature boundary conditions affect model predictions and is discussed in detail in the following section.

Ameliorating Elevated Stream Temperature from Climate Change.

Riparian ecosystems are naturally resilient places and may provide an adaptive role in mitigating negative climate change impacts (Seavy *et al.* 2009). Our study shows that both partly and fully riparian reforestation scenarios improved stream temperature conditions compared to forecasted climate change scenarios (Table 17). Mean daily maximum temperature was reduced by reforesting while cooling conditions were relatively similar. The reduction (0.11 ºC and 0.26 ºC per 2 ºC air temperature increase for partial and fully forested respectfully) is within the same order of magnitude as simulated heating caused by climate change (0.09 ºC per 2 ºC air temperature increase). This means that reforesting denuded gravel bars and areas with little vegetation not only improves stream temperature related to current conditions but also buffer stream temperature to future warming conditions under constant boundary conditions. Our sensitivity analysis further showed the same magnitude of warming and warming offset between initial boundary conditions and when stream temperature boundary conditions were increased by 2 ºC. Our results are in contrast to Battin *et al.* (2007), who found that riparian vegetation in wide mainstem-rivers in the Snohomish Watershed (Washington, USA) has a "minor effect on water temperature."

Reforestation decreased mean daily maximum temperatures and shortened the mean daily duration above the 21 ºC salmonid threshold. From an ecological standpoint this is significant because salmonids are already thermally stressed in the summer and

any additional heating could continue to reduce salmonid survival rates in the watershed. It is further encouraging to note that land managers can focus initially on matching partially forested conditions for the near future (first half of the 21st century) and see immediate benefits. Fully forested conditions can further buffer stream temperature for the 2099 elevated air temperature scenario. Focusing restoration efforts on reforesting riparian area have additional ecological benefits such as linking aquatic and terrestrial systems, reduce the impacts of extreme flooding, and possibly create additional thermal refugia (Seavy *et al.* 2009).

Heat Source requires an hourly stream temperature boundary condition. Our study did not change this boundary stream temperature condition to reflect climate change though a sensitivity analysis on boundary conditions was run. Our investigation focused on the relative change in heating and timing through the study reach rather than the absolute change in temperature. Elevated air temperature is expected to change the initial condition of stream temperature. Our sensitivity analysis found no difference in warming or warming offset from reformation between the initial boundary conditions and a uniform 2ºC increase in stream temperature boundary conditions. It is currently unknown how we should adjusting boundary conditions to mimic prolonged climate warming but the sensitivity analysis shows that the relative magnitudes remain the same. Future study is needed to evaluate how additional meteorological factors: precipitation amount and form (*i.e.* snow vs. rain), stream flow, and "adjusted" stream temperature will be altered by climate change and then model these resultant impacts on stream temperature.

CONCLUSIONS

The primary objective of this research was to quantify the thermal regime of a one-kilometer reach on the North Fork Salmon River and investigate sources of heat flux. The research aimed to: 1) investigate the geomorphic and thermal condition of the study reach and their impact on native salmonids; 2) spatially identify groundwater seeps and quantify their contribution to the stream's thermal regime; and 3) employ and calibrate *Heat Source* to predict stream temperatures resulting from riparian reforestation, channel modification, and climate change scenarios. This section presents the ten hypotheses investigated in this study. Each hypothesis is followed by a true or false statement and the evidence found in the study.

1.1 Over-summering juvenile salmonids are experiencing physiologically stressful temperatures in the Salmon River.

True - DTS observations revealed homogeneous warming over the study reach and a diel heating cycle of 5 °C, with no major cooling inflows (Figure 14). This means that salmonids within the reach were subjected to high maximum temperatures regardless of where they were located. Mean temperature over the entire reach exceeded the critical salmonid temperature threshold of 21 ºC seven of the eight days monitored (Figure 13). The study found a Maximum Weekly Average Temperature (MWMT) of 23.00 °C, which exceeds salmon and trout protective temperature standards set by United States Environmental Protection Agency Region 10.

1.2 Temperature is driving the distribution of juvenile and resident salmon and trout at the reach scale.

False - Statistical modeling of salmonid distribution found that both depth and temperature informed counts. Both total and salmon count had a positive relationship with depth while total count had an additional positive relationship with temperature. Depth is the most important parameter driving fish distribution in our study reach. The positive response between temperature and total count is most likely the result of small sample size.

1.3 Channel geometry is outside the range of suggested literature values for providing salmonid habitat in the Salmon River.

True - Most habitat characteristics in the study reach were dramatically different from optimal conditions cited in the literature (Table 11). The study reach consisted primarily of fast-water habitat, six times the recommended fast-to-slow water ratio. Our metrics indicate reduced habitat complexity and few pools to help buffer salmonids from daily maximum temperature and mainstem velocity. No instream cover or large woody debris was observed in the study reach. Current channel geometry is most likely the legacy of historic hydraulic gold mining in the area, which substantially changed sediment transport processes and filled in pool habitat.

2.1 Groundwater springs are detectable and quantifiable using Distributed Temperature Sensing fiber-optics.

True - A spring was located below Pool 2 and quantified using DTS using the volumetric inflow calculation during larger flow conditions (1.24 m^3s^{-1}) then previous DTS studies. Spring flow was calculated as 0.08 ± 0.01 m^3s^{-1} (2.63 cfs); 7.30 % ± 1.16 % of mainstem flow. Our results suggest that groundwater may be an important inflow in the Salmon River. Groundwater - deep alluvium interactions may be a source of cold-water in low-flow conditions. We did not observe any fish congregating around the spring confluence nor detect a plume of cold-water over the study period.

3.1 The energy budget model *Heat Source* correctly predicts summer stream temperature for the study reach in the Salmon River.

Four measures of model performance, Bias, RMSE, MARE, and NSE, were all within the range of previous *Heat Source* applications (Table 19). The spatial component of model performance decrease in fit in the downstream direction (Figure 23). This is in part due to meteorological observations being tied to the most upstream part of the study reach. Temporal bias was calculated as 0.075. A first-order autocorrelation was found, meaning when the model over predicted an observation it was likely to overpredict the next observation. A plot of the periodic component of the differences between *Heat Source* and DTS observations revealed that *Heat Source* over-predicted observations during midday and under-predicted observations at night (Figure 24). Overall, we believe

we were within an acceptable range of error to use *Heat Source* to describe study period conditions and forecasted scenarios.

3.2 Riparian reforestation can buffer maximum daily summer stream temperatures.

True - Simulated reforesting of exposed areas, denuded gravel bars from legacy mining and areas of low vegetation in the study reach, helped buffer daily maximum temperature (Table 15, Figure 27b). The duration of solar radiation hitting the water column was reduced with reforestation (Figure 28). While the study reach daily mean maximum temperature in all scenarios is greater than the 21 ºC temperature threshold for salmonids, the mean hours per day over this threshold was reduced from 3.8 hours (current condition) to 2.4 and 2.0 hours for partly and fully reforested conditions, respectively. Cooling was similar between the scenarios, with forested conditions cooling slightly later in the day most likely due to increased longwave radiation (Figure 27a, Figure 30).

3.3 Reducing the channel bottom width of the most upstream run in the study reach (*i.e.* Run 1) will buffer current summer stream temperatures.

False - Reducing the channel bottom width of Run 1 from 32.5m to 27 and 20m did reduce the rate of heating in the treatment by a maximum of 34 % (Figure 32) but does not appear to result in an ecologically significant change in stream temperature 200 m or further downstream from the treatment area (Figure 31). Future research should

investigate what pre-hydraulic mining conditions could have looked like and use those estimates in *Heat Source* modeling.

3.4 Increased air temperature from climate change will increase mean summer stream temperatures.

True - Our research found that mean stream temperature increased by 0.09 ºC for every two degree rise in air temperature. While this may be a small value, it may by important at the basin scale. If the rate of heating was constant between the study site and the confluence with the South Fork at Forks of Salmon, CA (17 kilometers downstream), stream temperature would increase by 1.53 ºC. The overall thermal profile between climate scenarios does not show changes in overall shape (Figure 33). Cooling rates were similar between climate scenarios while mean maximum temperature increased with increasing air temperature (Figure 34).

3.5 Riparian reforestation can ameliorate elevated stream temperature from climate change.

True - By modeling climate and restoration scenarios land managers can be more informed about not only the magnitude of expected warming but also the magnitude of offsetting this warming with management actions. Both partial and full riparian reforestation scenarios improved stream temperature conditions compared to forecasted climate change scenarios (Table 17). The reduction (0.11 ºC and 0.26 ºC per 2 ºC air temperature increase for partial and fully forested respectfully) is within the same order

of magnitude as simulated heating caused by climate change (0.09 ºC per 2 ºC air temperature increase). A sensitivity analysis of boundary stream temperatures the magnitude of warming and warming offset were the same as initial boundary conditions. This means that reforesting denuded gravel bars from legacy mining and areas with little vegetation not only improves stream temperature related to current conditions but also buffers stream temperature to future warming conditions.

Lessons Learned: Future DTS Recommendations

The Center for Transformative Environmental Monitoring Programs was instrumental in making the DTS technology accessible for this research. I highly recommend anyone interested in conducting research with DTS to visit and help other DTS studies before embarking on their own adventure. This will give you an idea of the full scope of the technology. Also, a field crew of 12 people was barely enough to unspool and place the kilometer long cable in the stream. I recommend practicing with the crew beforehand with rope and a clear communication strategy to relay messages among crewmembers. We had three "waterproof" walky-talkies which broke during the cable placement process. If you have access to reliable and "waterproof" walky-talkies, having one placed every four people will make your communication run more smoothly.

REFERENCES

AFL Telecommunications. 2007. Fiber Optic Cable Specification Sheet. http://www.aflglobal.com/Products/Fiber-Optic-Cable/ADSS/Drop-Cable/Flat_Drop_Cable.aspx. accessed: 1/22/13.

Anderson MP. 2005. Heat as a Ground Water Tracer. Ground Water 43:951-968.

Ando CJ, Irwin WP, Jones DL, Saleeby JB. 1983. The ophiolitic North Fork terrane in the Salmon River region, central Klamath Mountains, California. Geological Society of America Bulletin 94: 236.

Arik AD. 2011. A study of stream temperature using distributed temperature sensing fiber optics technology in Big Boulder Creek, a tributary to the Middle Fork John Day River in eastern Oregon. Master's thesis. Water Resources, Oregon State University, Corvallis, Oregon.

Armour CL, Duff DA, and W Elmore. 1991. The effects of livestock grazing on riparian and stream ecosystems. Fisheries 16: 7-11.

Battin J, Wiley MW, Ruckelshaus MH, Palmer RN, Korb E, Bartz KK, and H Imaki. 2007. Projected impacts of climate change on salmon habitat restoration. Proceedings of the National Academy of Sciences 104:6720–6725.

Berman CH and TP Quinn. 1991. Behavioural thermoregulation and homing by spring chinook salmon, Oncorhynchus tshawytscha (Walbaum), in the Yakima River. Journal of Fish Biology 39: 301-312.

Boderie P and L Dardengo. 2003. Warmtelozing in oppervlaktewater en uitwisseling met de atmosfeer, Report Q3315, Delft Hydraulics.

Bolker BM. 2008. Ecological Models and Data in R. Princeton University Press. Princeton, New Jersey.

Bjornn,TC and DW Reiser. 1991. Habitat requirements of salmonids in streams. American Fisheries Society Special Publication 19: 83-138.

Boyd M. 1996. Heat Source: Steam Temperature Prediction Model. Master's Thesis. Departments of Civil and Bioresource Engineering, Oregon State University, Corvallis, Oregon.

Boyd M and B Kasper. 2003. Analytical methods for dynamic open channel heat and mass transfer: methodology for the Heat Source Model Version 7.0, Watershed Sciences Inc., Portland, Oregon. found at: http://www.heatsource.info/Heat Source v 7.0.

Brown GW. 1969. Predicting temperatures of small streams. Water Resources Research 5: 68.

Brown GW. 1970. Predicting the effect of clearcutting on stream temperature. Journal of Soil and Water Conservation 25: 11-13.

Brown GW and JT Krygier. 1970. Effects of clear-cutting on stream temperature. Water Resources Research 6: 1133-1139.

Burnham KP and DR Anderson. 2004. Multimode inference: understanding AIC and BIC in model selection. Sociological Methods and Research 33: 261-304.

Caissie D, Satish MG, and N El-Jabi. 2005. Predicting river water temperatures using the equilibrium temperature concept with application on Miramichi River catchments (New Brunswick, Canada). Hydrological Processes 19: 2137–2159.

Caissie D. 2006. The thermal regime of rivers: a review. Freshwater Biology 51: 1389-1406.

California. Division of Mines, & California State Mining Bureau. 1916. *Mines and Mineral Resources of Siskiyou County* (Report XIV). State of California, Department of Natural Resources, Division of Mines. Biennial Period 1913-1914.

California Environmental Protection Agency (CA EPA). 2002. Section 303(d) List Fact Sheet for California.

Collier MW. 2008. Demonstration of fiber optic distributed temperature sensing to differentiate cold water refuge between ground water inflows and hyporheic exchange. Master's Thesis. Departments of Civil and Bioresource Engineering, Oregon State University, Corvallis, Oregon.

Crown J, Meyers B, Turgaw H, and D Turner. 2008. Rogue River Basin Total Maximum Daily Load (TMDL): Appendix A, Temperature Calibration. Technical Report. Oregon Department of Environmental Quality, Portland, Oregon.

Crown J. 2010. John Day River Basin Total Maximum Daily Load (TMDL) and Water Quality Management Plan (WQMP) Technical Report: Appendix A: Temperature Model Calibration Report. Technical Report. Oregon Department of Environmental Quality, Portland, Oregon.

Dettinger MD. 2005. From climate-change spaghetti to climate-change distributions for 21st Century California. San Francisco Estuary and Watershed Science 3.

Dolloff A, J Kershner, and R Thurow. 1996. Underwater Observation. Pages 533-554 *in* BR Murphy and DW Willis, editors. Fisheries techniques, 2nd edition. American Fisheries Society, Bethesda, Maryland.

Dong J, Chen J, Brosofske K, and R. Naiman. 1998. Modeling air temperature gradients across managed small streams in western Washington. Journal of Environmental Management 53: 309–321.

Eaton JG and RM Scheller. 1996. Effects of climate warming on fish thermal habitat in streams of the United States. Freshwater Ecosystems and Climate change in North America 41: 1109-1115.

Ebersole JL, Liss WJ, and CA Frissell. 2001. Relationship between stream temperature, thermal refugia and rainbow trout Oncorhynchus mykiss abundance in arid-land streams in the northwestern United States. Ecology of Freshwater Fish 10: 1-10.

Elder D, Olson B, Olson A, Villeponteaux J, and P Brucker. 2002. Salmon River Subbasin Restoration Strategy: Steps to Recovery and Conservation of Aquatic Resources. U.S. Fish & Wildlife Service, The Klamath River Basin Fisheries Restoration Task Force (Interagency Agreement 14-48-11333-98-H019).

Environmental Protection Agency (EPA). 2006. EMAP Western Pilot Study Operations Manual for Wadeable Streams, Peck, DV, Lazorchak JM, and DJ Klemm, editors. Washington, D.C.

Evans EC, McGregor GR, and GE Petts. 1998. River energy budgets with special reference to river bed processes. Hydrological Processes, 12: 575–595.

Fagan WF. 2002. Connectivity, fragmentation, and extinction risk in dendric metapopulations. Ecology 83: 3243-3249.

Environmental Systems Research Institute (ESRI). 2011. World Imagery Basemap website: http://www.arcgis.com/home/item.html?id=10df2279f9684e4a9f6a7f08febac2a9.

Feder ME and GE Hofmann. 1999. Heat-shock proteins, molecular chaperones, and the stress response: evolutionary and ecological physiology. Annual Review of Physiology 6: 243-282.

Federal Register. 1997. Endangered and Threatened Species: Threatened status for coho salmon in the Southern Oregon/ Northern California Evolutionary Significant Unit in California. Federal Register, Washington D.C. 62: 24588 - 24609.

Fleischner, TL. 1994. Ecological costs of livestock grazing in western North America. Conservation Biology 8: 629-644.

Flint LE and AL Flint. 2008. A basin-scale approach to estimating stream temperatures of tributaries to the lower Klamath River, California. Journal of Environmental Quality 37: 57–68.

Flosi G, Downie S, Bird M, Corey R, and B Collins. 2010. California salmonid stream habitat restoration manual. California Department of Fish and Game Resources Agency. Sacramento, CA

Freeze RA and JA Cherry. 1979. Groundwater. Prentice-Hall, Englewood Cliffs, NJ.

Gilbert, GK. 1917. Hydraulic-mining debris in the Sierra Nevada. US Geologic Survey, Professional Paper 105. Washington, D.C..

Gregory JS, Beesley SS, and RW Van Kirk. 2000. Effect of springtime water temperature on the time of emergence and size of Pteronarcys californica in the Henry's Fork catchment, Idaho, U.S.A.. Freshwater Biology 45: 75-83.

Groberg WJ, McCoy RH, Pilcher KS, and JL Fryer. 1978. Relation of Water Temperature to Infections of Coho Salmon (Oncorhynchus kisutch), Chinook Salmon (O. tshawytscha), and Steelhead Trout (Salmo gairdneri) with Aeromonas salmonicida and A. hydrophila. Journal of the Fisheries Research Board of Canada 35: 1-7.

Hamilton JB, Curtis GL, Snedaker SM, and DK White. 2005. Distribution of Anadromous Fishes in the Upper Klamath River Watershed Prior to Hydropower Dams—A Synthesis of the Historical Evidence. Fisheries 30: 10-20.

Hardy TB, Addley RC, and E Saraeva . 2006. Evaluation of instream flow needs in the lower Klamath River – Phase II Final Report. Institute for Natural Systems Engineering, Utah Water Research Laboratory, Utah State University, Logan, Utah. Report Number 84322-4110.

Hausner MB, Suárez F, Glander KE, van de Giesen N, Selker JS, and SW Tyler. 2011. Calibrating single-ended fiber-optic raman spectra distributed temperature sensing data. Sensors 11: 10859-10879.

Hayhoe K, Cayan D, Field C, Frumhoff P, Maurer E, Miller N, Moser S, Schnider S, Nicholas Cahill K, Cleland E, Dale L, Drapek R, Hanemann M, Kalkstein L, Lenihan J, Lunch C, Nielson R, Sheridan S, and J Verville. 2004. Emissions pathways, climate change, and impacts on California. Proceedings of the National Academy of Sciences 101: 12422-12427.

Heller NE and ES Zavaleta. 2009. Biodiversity management in the face of climate change: a review of 22 years of recommendations. Biological conservation 142: 14-32.

Henderson RC, Archer EK, Bouwes BA, Coles-Ritchie MS, and JL Kershner. 2005. PACFISH/INFISH Biological Opinion (PIBO): Effectiveness Monitoring Program seven-year status report 1998 through 2004. Gen. Tech. Rep. RMRS-GTR-162. U.S. Department of Agriculture, Forest Service, Rocky Mountain Research Station, Fort Collins, CO.

Huff JA. 2009. Monitoring river restoration using fiber optic temperature measurements in a modeling framework. Master's Thesis. Oregon State University, Corvallis, Oregon.

International Panel on Climate change (IPCC). 2007. Climate change 2007: The Physical Science Basis. Contribution of Working Group I to the Fourth Assessment Report of the Intergovernmental Panel on Climate change [Solomon, S., D. Qin, M. Manning, Z. Chen, M. Marquis, K.B. Averyt, M. Tignor and H.L. Miller (eds.)]. Cambridge University Press, Cambridge, United Kingdom and New York, NY, USA.

James LA. 1993. Sustained reworking of hydraulic mining sediment in California: Gilbert's sediment wave model reconsidered. Z. Geomorphol. N.F: Suppl.-Bd. 88: 49-66.

James LA. 1997. Channel Incision on the Lower American River, California, from Stream-flow Gage Records. Water Resources Research 33: 485-490.

James LA, Singer MB, Ghoshal S, and M Megison. (2009). Historical channel changes in the lower Yuba and Feather Rivers, California: Long-term effects of contrasting river management strategies. *in* Management and Restoration of Fluvial Systems with Broad Historical Changes and Human Impacts. Geological Society of America Special Publication 451: 57-81.

Johnson SL. 2003. Stream temperature: scaling of observations and issues for modeling. Hydrologic Processes 17: 497–499.

Kelley RL.1954. Forgotten giant: The hydraulic gold mining industry in California. Pacific Historical Review 23: 343-356.

Knighton D. 1998. Fluvial forms and processes: a new perspective. Hodder Arnold Publication. London, UK.

Lamb AW. 1996. Geomorphic conditions in salmonid-supporting streams, Umatilla National Forest, northeast Oregon and southeast Washington. Master's Thesis. Department of Geography, University of Oregon, Eugene, Oregon.

Lisle TE. 1986. Stabilization of a gravel channel by large streamside obstructions and bedrock bends, Jacoby Creek, northwestern California. Geological Society of America America Bulletin 97: 999-1011.

Loheide SP and SM Gorelick. 2006. Quantifying Stream−Aquifer Interactions through the Analysis of Remotely Sensed Thermographic Profiles and In Situ Temperature Histories. Environmental Science & Technology 40: 3336–3341.

Lowney CL. 2000. Stream temperature variation in regulated rivers: Evidence for a spatial pattern in daily minimum and maximum magnitudes. Water Resources Research, 36: 2947-2955.

Madej MA and V Ozaki. 1996. Channel response to sediment wave propagation and movement, Redwood Creek, California, USA. Earth Surface Processes and Landforms 21: 911-927.

Madej MA, Currens C, Ozaki V, Yee J, and DG Anderson. 2006. Assessing possible thermal rearing restrictions for juvenile coho salmon (Oncorhynchus kisutch) through thermal infrared imaging and in-stream monitoring, Redwood Creek, California. Canadian Journal of Fisheries and Aquatic Sciences 63: 1384-1396.

Markarian RK. 1980. A study of the relationship between aquatic insect growth and water temperature in a small stream. Hydrobiologia 75: 81-95.

Matheswaran K, Blemmer, M, Mortensen, J, Rosbjerg, D, and E Boegh. 2011. Investigating the effect of surface water-groundwater interactions on stream temperature using Distributed temperature sensing and instream temperature model. *in* Conceptual and Modelling Studies of Integrated Groundwater, Surface Water, and Ecological Systems, Proceedings of Symposium H01 held during IUGG2011 in Melbourne, Australia.

Matthews KR and NH Berg. 1997. Rainbow trout responses to water temperature and dissolved oxygen stress in two southern California stream pools. Journal of Fish Biology 50: 50–67.

McMahon TE. 1983. Habitat suitability index models: Coho salmon. US Department of Interior, Fish and Wildlife Service. FWS/OBS-82/10.49.

Meisner JD. 1990. Effect of climatic warming on the southern margins of the native range of brook trout, Salvelinus fontinalis. Canadian Journal of Fisheries and Aquatic Sciences 47: 1065-1070.

Millar CI, Stephenson N L, and SL Stephens. 2007. Climate change and forests of the future: managing in the face of uncertainty. Ecological Applications 17: 2145-2151.

Moffett KB, Tyler SW, Torgersen T, Menon M, Selker SJ, and SM Gorelick. 2008. Processes controlling the thermal regime of saltmarsh channel beds, Environmental Science Technology 42: 671–676.

Mohseni O, Heinz S, and J Eaton. 2003. Global Warming and Potential Changes in Fish Habitat in U.S. Streams. Climatic Change 59: 389 - 409.

Mosley MP. 1983. Variability of water temperatures in the braided Ashley and Rakaia rivers. New Zealand Journal of Marine and Freshwater Research 17:331-342.

National Marine Fisheries Service. 2012. Public Draft Recovery Plan for Southern Oregon/Northern California Coast Coho Salmon (Oncorhynchus kisutch). National Marine Fisheries Service Arcata, California.

National Research Council. 2004. Endangered and threatened fishes in the Klamath River Basin: causes of decline and strategies for recovery. Technical Report.

Neilson BT, Hatch CE, Ban H, and SW Tyler. 2010. Solar radiative heating of fiber-optic cables used to monitor temperatures in water. Water Resources Research 46.

North Coast Regional Water Quality Control Board (NCRWQCB). 2005. Salmon River, Siskiyou County, California Total Maximum Daily Load for Temperature and Implementation Plan. State Water Resources Control Board, Resolution No. R1-2005-0058, Sacramento, California.

Null SE, Viers JH, Deas ML, Tanaka SK, and JF Mount. 2013. Stream Temperature Sensitivity to Climate Warming in California's Sierra Nevada: Impacts to Coldwater Habitat. Climatic Change 116: 149–170.

Oregon Department of Environmental Quality (ODEQ). 2001. UmatillaRiver Basin Total Maximum Daily Load (TMDL) and Water Quality Management Plan (WQMP): Appendix A-4: Temperature Technical Analysis. Technical Report, Oregon Department of Environmental Quality.

ODEQ. 2010. Upper Grande Ronde Sub-Basin TMDL. Appendix A Temperature Analysis: Thermal Patterns, Source Assessment and Analytical Framework. Technical Report, Oregon Department of Environmental Quality.

ODEQ. 2012. *Heat Source* version 8.0.8, http://www.deq.state.or.us/wq/tmdls/tools.htm.

Poole GC and CH Berman. 2001. An Ecological Perspective on In-Stream Temperature: Natural Heat Dynamics and Mechanisms of Human-Caused Thermal Degradation. Environmental Management 27: 787-802.

Reiser DW and TC Bjornn. 1979. Habitat requirements of anadromous salmonids. in W.R. Veehan, ed. Influence of forest and range and management on anadromous fish habitat in western North America. J.S. For. Serv. Gen. Tech. Rep. PNW-96. Pacific Northwest Forest and Range Experiment Station, Portland, OR.

Rosgen DL. 1985. A stream classification system. *in* Riparian ecosystems and their management: reconciling conflicting uses. First North American Riparian Conference, Arizona.

Rosgen DL. 1994. A classification of natural rivers. Catena 22: 169-199.

Roth TR, Westhoff MC, Huwald H, Huff JA, Rubin JF, Barrenetxea G, Vetterli M, Parriaux A, Selker JS, and MB Parlange. 2010. Stream Temperature Response to Three Riparian Vegetation Scenarios by Use of a Distributed Temperature Validated Model. Environmental Science & Technology 44: 2072-2078.

Salmon River Restoration Council (SRRC) Salmon River Spring Chinook Voluntary Recovery Work Group. 2004. Spring Chinook Limiting Factors Analysis. Salmon River Restoration Council Publication. Sawyers Bar, California.

Sawyer L, Deady MP, and E Woodruff. (Woodruff v. Bloomfield). 1884. *Opinions of Lorenzo Sawyer, Circuit Judge, and Matthew P. Deady, District Judge, Delivered January 7, 1884, in the Case of Edwards Woodruff, Complainant, Vs. North Bloomfield Gravel Mining Co.*, Et al., Defendants: With Note and Index.

Sayde C, Gregory C, Gil-Rodriguez M, Tufillaro N, Tyler S, van de Giesen N, English M, Cuenca R, and JS Selker. 2010. Feasibility of soil moisture monitoring with heated fiber optics. Water Resources Research W06201.

Seavy NE, Gardali T, Golet GH, Griggs TF, Howell CA, Kelsey R, Small SL, Viers JH, and JF Weigand. 2009. Why climate change makes riparian restoration more important

than ever: recommendations for practice and research. Ecological Restoration 27: 330-338.

Selker JS, Thévenaz L, Huwald H, Mallet A, Luxemburg W, van de Giesen N, Stejskal M, Zeman J, Westhoff M, and MB Parlange. 2006a. Distributed fiber-optic temperature sensing for hydrologic systems. Water Resources Research WR005326.

Selker J, van de Giesen N, Westhoff M, Luxemburg W, and MB Parlange. 2006b. Fiber optics opens window on stream dynamics. Geophysical Research Letters GL027979.

Sinokrot BA and HG Stefan. 1994. Stream water temperature sensitivity to weather and bed parameters, Journal of Hydraulic Engineering 120: 722-736.

Smith K. 1972. River water temperatures: an environmental review, Scottish Geographic Magazine 88: 211-220.

Steele-Dunne SC, Rutten MM, Krzeminska DM, Hausner M, Tyler SW, Selker J, Bogaard TA, and NC van de Giesen. 2010. Feasibility of soil moisture estimation using passive distributed temperature sensing. Water Resources Research WR008272.

Stenhouse SA, CE Bean, WR Chesney, and MS Pisano. 2012. Water temperature thresholds for coho salmon in a spring-fed river, Siskiyou County, California. California Fish and Game 98: 19-37.

Stonestrom DA and J Constantz (eds.). 2003. Heat as a tool for studying the movement of groundwater near streams. U.S. Geologic Survey Circulation 1260.

Storms WH. 1894. Methods of Mine Timbering. Bulletin No. 2, California State Mining Bureau, Sacramento, Claifornia.

Stumpf GD.1979. Gold Mining in Siskiyou County, 1850-1900. No. 2. Siskiyou County Historical Society, Yreak, California.

Sutton R and T Soto. 2010. Juvenile coho salmon behavioural characteristics in Klamath river summer thermal refugia. River Research and Applications 28: 338–346.

Thurow RF. 1994. Underwater methods for study of salmonids in the Intermountain West. Gen. Tech. Rep. INT-GTR-307. U.S. Department of Agriculture, Forest Service, Intermountain Research Station, Ogden, Utah.

Torgersen CE, Price DM, Li HW, and BA McIntosh. 1999. Multiscale thermal refugia and stream habitat associations of chinook salmon in northeastern Oregon. Ecological Applications 9: 301–319.

Tyler SW, Burak SA, McNamara JP, Lamontagne A, Selker JS, and J Dozier. 2008. Spatially distributed temperatures at the base of two mountain snowpacks measured with fiber optics sensors, Journal of Glaciology 54: 673–679.

Tyler SW, Selker JS, Hausner MB, Hatch CE, Torgersen T, Thodal CE, Schladow SG. 2009. Environmental temperature sensing using Raman spectra DTS fiber-optic methods. Water Resources Research WR007052.

U.S. Department of Agriculture (USDA), Forest Service. 2006. Region 6 Stream Inventory Handbook, Level II, Version 2.6.

Watershed Sciences. 2008. Deschutes River, Whychus Creek, and Tumalo Creek Temperature Modeling. Technical Report prepared for Oregon Department of Environmental Quality, Bend, OR.

Watershed Sciences. 2009. Airborne Thermal Infrared Remote Sensing Salmon River Basin, California. Salmon River Restoration Council, Sawyers Bar, CA.

Welsh H, Hodgson G, Harvey B, and M Roche. 2001. Distribution of Juvenile Coho Salmon in Relation to Water Temperatures in Tributaries of the Mattole River, California. North American Journal of Fisheries Management 21: 464-470.

Westhoff M, Savenije H, Luxemburg W, Stelling G, Van De Giesen N, Selker J, Pfister L, and S Uhlenbrook. 2007. A distributed stream temperature model using high resolution temperature observations. Hydrology and Earth System Sciences 11: 1469–1480.

Westhoff MC, Gooseff MN, Bogaard TA, Savenije HHG. 2011. Quantifying hyporheic exchange at high spatial resolution using natural temperature variations along a first-order stream. Water Resources Research WR009767.

Wolman MG, 1954. A method of sampling coarse river-bedmaterial. Transactions of the American Geophysical Union 35 951– 956.